International Science Group
ISG-KONF.COM

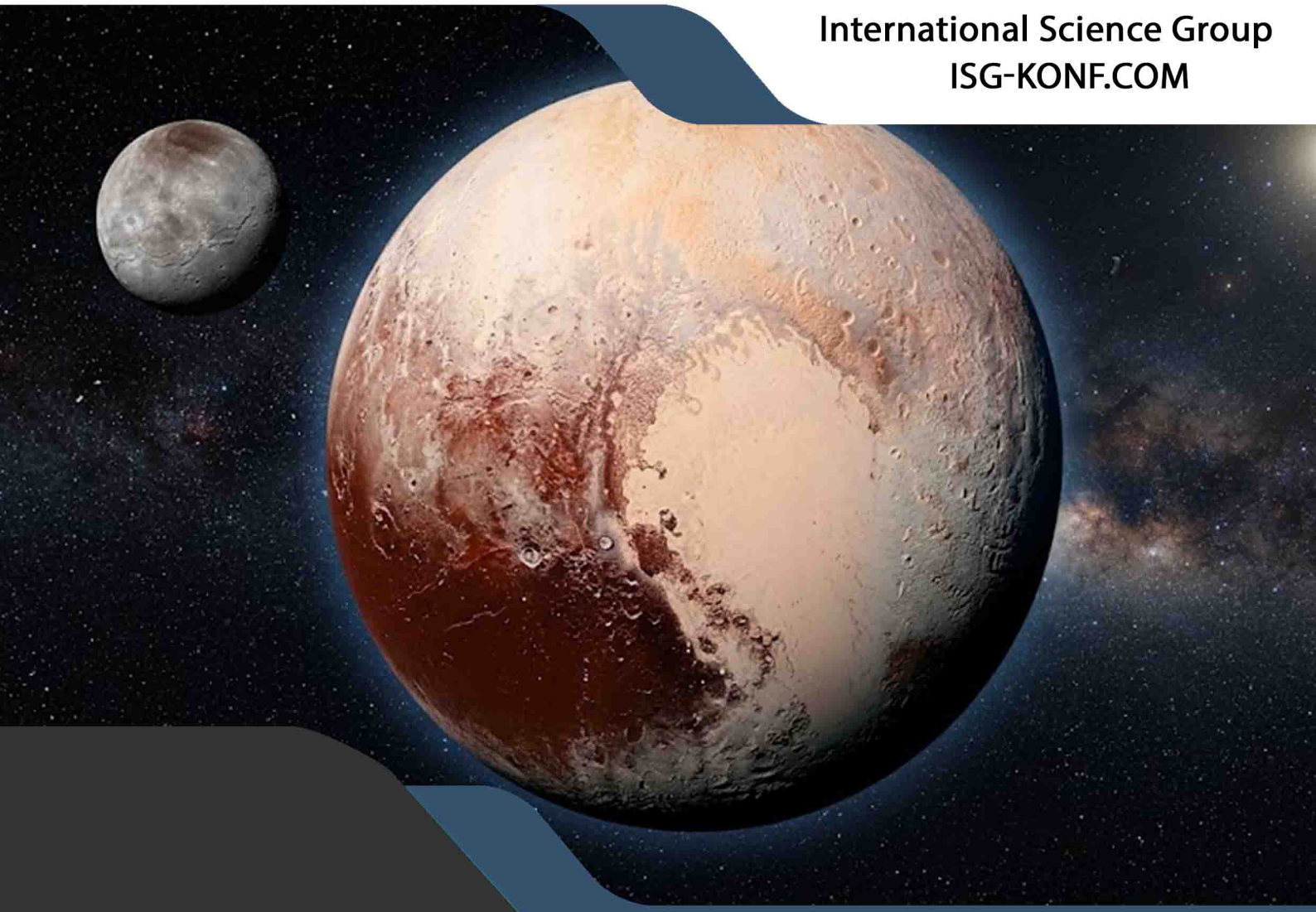

VIDMACHENKO A. P.

PHYSICAL PARAMETERS OF PLUTO AND OTHER DWARF PLANETS

ISBN 979-8-90383-424-2
DOI 10.46299/979-8-90383-424-2

Vidmachenko A. P.

PHYSICAL PARAMETERS OF PLUTO AND OTHER DWARF PLANETS

Monograph

Boston 2026

UDC 523.4

Author:
Vidmachenko A. P.

Editor:
Vidmachenko Anatoliy Petrovych, Doctor Phys.-Math. Sci., Professor, Professor of Department of Physics, National University of Life and Environmental Sciences of Ukraine; Chief Researcher of the Department for Physics of Sub-stellar and Planetary Systems, Main Astronomical Observatory of National Academy of Sciences of Ukraine; Kyiv, Ukraine. ORCID 0000-0002-0523-5234

Reviewers:
B.O. Grudynin – Doctor of Pedagogical Sciences, Associate Professor of the National University of Life Resources and Environmental Management of Ukraine, ORCID 0000-0001-8084-653X
O.V. Mozghovyi – Candidate of Technical Sciences, Associate Professor of the Vinnytsia State Pedagogical University named after M. Kotsiubynskyi, ORCID 0000-0002-0797-8779

Vidmachenko A. P. Physical parameters of Pluto and other dwarf planets. Monograph. – International Science Group. Primedia eLaunch, Boston, USA, 2026. – 172 p.

Library of Congress Cataloging-in-Publication Data

ISBN – 979-8-90383-424-2
DOI – 10.46299/ 979-8-90383-424-2

UDC 523.4

ISBN – 979-8-90383-424-2

ABSTRACT

In the Solar System, eight classical planets, several recently discovered dwarf planets, and hundreds of thousands of small planets or asteroids orbit the Sun; many of these have their own satellites; and there are also comets, meteoroids, and countless small meteorite particles and dust.

Since 2006, dwarf planets have included until recently such a “large” planet as Pluto, as well as the previously largest asteroid of the Main Asteroid Belt, Ceres, and the largest bodies in the Kuiper Belt and, probably, the largest bodies in the Oort Cloud; some of the dwarf planets have a multiple structure.

It is believed that, like many Kuiper Belt bodies, Pluto consists of ice mixed with rocky rocks. In 1978, D. Christie discovered an asymmetric appearance in the image of Pluto, which gave reason to talk about the presence of a satellite, which was soon found. It was called Charon. It has a diameter of 1186 km, a mass of ~1/30 of Pluto's mass, a distance from the center of Pluto of ~20,000 km and a synchronous rotation period of 6.39 Earth days. Pluto and Charon are considered a double dwarf planet.

Somewhat later, two more satellites of Pluto were found in images from the Hubble Space Telescope, which were given the names Nix and Hydra. On 06/28/2011, using the same images, another satellite of Pluto with a diameter of 13-34 km was discovered. It was called Kerberos. It rotates between the satellites Nix and Hydra in 32.167 Earth days.

On 06/11/2012, the fifth satellite of Pluto was discovered. It turned out to be the smallest of Pluto's five known moons at the time. Its dimensions were refined to 16×9×8 km in a single image from the New Horizons space probe in July 2015. It orbits between the moons Charon and Nix with a period of about 20.16 Earth days at a distance of about 42,656 km from the barycenter of the Pluto-Charon system. It was named Styx.

Pluto is the best-known dwarf planet in the Solar System and the largest trans-Neptunian object to date. It is currently the ninth largest and tenth most massive celestial body orbiting the Sun (excluding several planetary satellites). Pluto's surface

is very heterogeneous. Studies have shown that this body is the second most contrasting body in the Solar System after Iapetus. The albedo of individual areas on its surface varies from 10% to almost 70%. Such heterogeneity leads to periodic changes in Pluto's brightness, sometimes reaching 0.35m, as it rotates. Also, its spectrum changes significantly as Pluto rotates.

Spectral observational data have shown that water ice is also present on Pluto's surface. Although most of the surface is covered with other more volatile ices; mainly - more than 95% - it is nitrogen ice. In addition, spectral observations have indicated the presence of frozen methane, carbon monoxide, and - in small quantities - some other compounds, which may well be formed from methane and nitrogen under the influence of hard radiation.

These may include more complex hydrocarbons and nitrites, as well as the so-called tholins, which give the surfaces of Pluto and some other bodies located far from the Sun a brown color. The most noticeable geological detail on the visible part of Pluto's surface is the Sputnik Plain. This depression with dimensions of more than 1000 km occupies about 5% of its entire surface.

Pluto's atmosphere was discovered only in 1985 during observations of its occultation of the star. When Pluto is at aphelion, most of the atmosphere should freeze and fall to the surface. Currently, Pluto's atmosphere is a relatively thin gas shell. It consists mainly of nitrogen, as well as methane and carbon monoxide. The presence of such an atmosphere is maintained due to constant evaporation from the surface ice layer. The interaction of the surface layers with the atmosphere also affects the temperature of Pluto's surface.

Calculations show that the atmosphere, despite the very low pressure near the surface, is able to significantly smooth out daily temperature fluctuations. However, there are still temperature variations of about 20 degrees. This may be because the areas of the surface from which nitrogen ice evaporates are significantly cooled. Due to the elongated orbit, Pluto receives 2.8 times more heat at perihelion than at aphelion. This causes strong changes in its atmosphere.

TABLE OF CONTENTS

Introduction

As is known, in the Solar System, eight large (or classical) planets, several recently discovered dwarf planets (Fig. 1), as well as hundreds of thousands of small planets or asteroids, and many of the above with their satellites, revolve around the central star – the Sun; as well as comets, meteoroids and countless small meteorite particles and dust. The mass of all large planets is 743 times less than the mass of the Sun; and the mass of the remaining objects is more than 100,000 times less.

Fig. 1. The largest bodies in the Solar System [240].

According to the recent definition, **a planet was considered to be a body that was in orbit around a central star, was not its companion, and must have a mass large enough to assume a spherical shape during formation**. These conditions are met by bodies with a mass of more than $5 \cdot 10^{20}$ kg and a diameter of more than 800 km. Since more than a dozen other cosmic bodies meet these requirements, it was necessary to set a number of additional conditions to clarify the definition of **a planet**.

In early 1930, K. Tombaugh discovered an object on the plates he received that was moving among the stars at a very low speed. This fact showed that this celestial body was further from the orbit of the then farthest planet, Neptune. And in mid-March 1930, on Lovell's birthday and on the anniversary of the discovery of Uranus, the director of the Lovell Observatory, Slipher, announced the discovery of the ninth planet in our Solar System at that time.

In 2005, another trans-Neptunian object (TNO) comparable in size to Pluto was discovered, Eris [160]. Therefore, the question arose, what should be called **a planet**? The International Astronomical Union, at its General Assembly in 2006, held in Prague, approved a list of basic characteristics according to which a planet should differ from a non-planet. And one of these characteristics was the requirement that a true planet should be able to "clear" its orbit of other large bodies. Pluto could not cope with this task and on August 24, 2006, it became the founder of a new class of planetary bodies – a dwarf planet.

Thus, starting from 2006, a new type of fairly large bodies was introduced in the Solar System, which became **dwarf planets**. These now include the recently "large" planet Pluto, as well as the then largest asteroid in the Main Belt, Ceres, the largest bodies in the Kuiper Belt (Fig. 2) and probably the largest bodies in the Oort Cloud; some of the dwarf planets have a multiple structure.

Fig. 2. New trans-Neptunian objects of larger sizes shown in comparison to Earth [237a].

1. Historical background on the cosmogony of the gas-dust cloud and the discovery of small and dwarf planets

In a gas-dust cloud that revolved around the central star, under the influence of gravity, dust particles gradually descended to the central plane and formed a dust disk. When a certain critical value of the average density was reached, due to gravitational instability, this disk disintegrated into a huge number of dust condensations. Subsequent collisions of these dust condensations led to their unification; their subsequent compression led to the formation of some compact bodies with asteroid dimensions. After that, larger planetary bodies could already be formed from the swarm of such bodies of relatively small size, their fragments and remnants of the primary dust disk.

The gravitational interaction of bodies of intermediate sizes intensified as they increased, could gradually change their orbits, eccentricities and inclinations to the plane of the dust disk. Those bodies that increased the fastest became the central nuclei of future planetary bodies. The largest planets absorbed not only solids, but also gases. Thus, the largest of the modern asteroids with a diameter of more than 100 km were formed during the formation of the planetary system; and medium and smaller asteroids are mostly fragments of large asteroids that were crushed during collisions. It is due to the collisions of asteroid bodies that the supply of dusty matter in interplanetary space is continuously replenished. Another source of small solid particles is the disintegration of comets when flying near the Sun.

The interior of the primary large asteroids could obviously be heated to almost 1000 K. And this affected the composition and structure of their matter.

All bodies of the Solar System, the mass of which exceeds a certain value, are in a state close to hydrostatic equilibrium. Due to the plasticity of matter, they should have acquired an almost spherical shape, and their level surface would be the surface of the planet. However, in reality this is not the case, which indicates a deviation of the actual conditions from the state of hydrostatic equilibrium. Special terms have been

introduced to denote a level surface. For example, according to Listing [118], the equipotential surface of our Earth is called the geoid.

While compiling catalogs of the positions of stars in the sky, on 1.01.1801 G. Piazzi noted that one of the stars had changed its position relative to the previous night. Continuation of observations the next night showed that this celestial body was not a distant star, but belonged to the Solar System. At that time, K. Gauss had developed a method for calculating the orbit of a celestial body using only three coordinates on different nights, and from the observational data obtained, he was able to calculate that the found body was located between the orbits of Mars and Jupiter in a practically circular orbit at only 2.8 AU from the Sun.

According to the calculated coordinates during observations on 1.01.1802, G. Piazzi was able to detect a luminous object in the predicted place. In honor of the goddess – the patron saint of the island of Sicily, Piazzi named it Ceres. Already on 28.03.1802, the German amateur astronomer Olbers discovered an object of about 9m near Ceres, also between the orbits of Mars and Jupiter, which was named Pallas. On 1.09.1804, another German astronomer K. Harding managed to detect Juno, and on 29.03.1807, G. Olbers again was able to detect Vesta.

Since these bodies during observations with telescopes did not show the presence of visible disks in them, they were called **asteroids**; that is, **"star-like" objects**; a little later they began to be named **minor planets**.

Their number began to increase again only in December 1845, when the postman from the city of Dresden K. Henke was able to discover the 5th minor planet with a magnitude of 9.5m, which was called Astraea. And on July 1, 1847, Gauss discovered the sixth minor planet, which was proposed to be called Hebe. In the same year, J. Hind discovered Iris and Flora.

In the future, several asteroid bodies were discovered almost every year. And their number in 1891 reached 322. For most of them, their orbits were between the orbits of the large planets Mars and Jupiter. And therefore, the name **Main asteroid belt** was chosen for this place in the Solar system. In 1891, M. Wolf introduced a method of photographing the starry sky. This method significantly accelerated the pace of

discovery of new asteroid bodies. In 1915, P. Lovell published "A Treatise on a Trans-Neptunian Planet," in which he summarized the results of the search for the so-called "Planet X" that he had begun in 1905. And in April 1929, the program for searching for trans-Neptunian objects was resumed at the short-focus refractor at Lovell Observatory. There, an exposure of one hour allowed stars up to 17.5^m to be recorded. And these searches ended on February 18, 1930, when K. Tombaugh discovered a new object beyond the orbit of Neptune. It was named after the Greek god of darkness, Pluto. In 1930, the International Astronomical Union officially granted it the status of the ninth planet, and it remained in this rank until August 21, 2006, when the XXVI Assembly of the IAU satisfied the recommendation of its nomenclature commission and decided that Pluto is one of the representatives of the dwarf planets. At the same time, in 2006, by decision of the IAU, the asteroid Ceres and another Kuiper belt object – Makemake – were attributed to a new type of astronomical body – **dwarf planets**.

At one time, F. Leonard [115] expressed the opinion about the possible existence of trans-Neptunian bodies, one of the representatives of which is Pluto, and which C. Edgeworth [72] and J. Kuiper [105A] transformed into a hypothesis about the existence of a large number of bodies that form the modern **Kuiper belt**. However, a long search for these bodies was crowned with success only in 1992, when the 2.2-m telescope at the University of Hawaii managed to discover the object 1992 QB1 [99], the semi-major axis of which orbit was 44.5 AU.

The creation of increasingly powerful ground-based telescopes and the use of the Hubble Space Telescope also contributed to the discovery of many small objects on the outskirts of the Solar System. Starting from 1999 to 2003, almost 800 previously unknown TNOs were discovered. Among them was the relatively bright celestial object 2003 UB313 [189] with a semi-orbital axis of 67.89 AU, an eccentricity of 0.4378, and an inclination of its orbit to the ecliptic plane of 43.993° [26]. In 2003, this object was located near aphelion at a distance of about 97.5 AU from the Sun; it will be at perihelion at a distance of 38.2 AU in 2257 [40].

In 2005, a minor planet 2004 XR190 (Buffy) was discovered with a diameter in the range of 500–1000 km. This TNO is characterized by a nearly circular orbit (at

perihelion the distance is 52 AU, at aphelion – 62 AU) and this distinguished it from the so-called **scattered objects** in this belt, which have rather elongated orbits; Buffy's orbit is inclined to the ecliptic plane at an angle of 47° (Fig. 3).

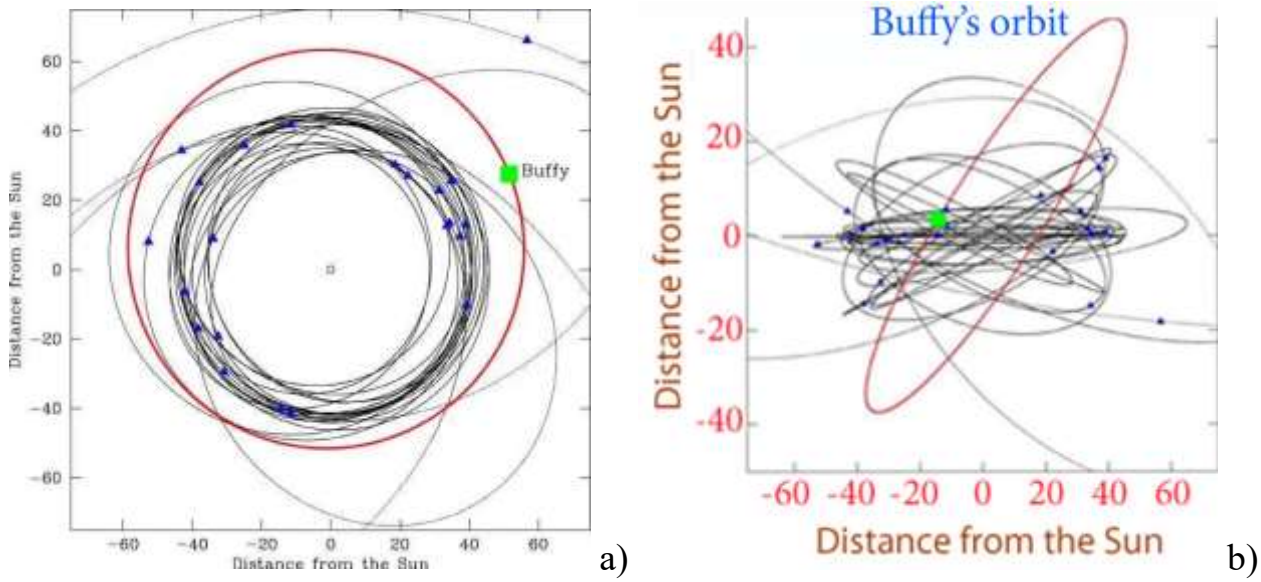

a) b)

Fig. 3. Diagram of Buffy's orbit in two mutually perpendicular planes. Heliocentric distances are plotted on the axes (a - https://images.newscientist.com/wp-content/uploads/2005/12/dn8455-2_539.jpg, b - https://images.newscientist.com/wp-content/uploads/2005/12/dn8455-1_539.jpg?width=800).

More than 90% of the newly discovered TNOs move in close to circular orbits at distances from the Sun from 30 to almost 50 AU. A significant number of orbital planes of these icy bodies are highly inclined to the ecliptic plane: for 20 of them the inclination exceeds 40°, and sometimes reaches 90°.

Estimation of the sizes of trans-Neptunian bodies assuming the value of their geometric albedo A_g=0.09 showed that at the beginning of 2025 the catalog of trans-Neptunian objects contains 5256 cosmic bodies (Table 1). It is also known that 12 of these bodies have semi-axial orbits of more than 150 AU and perihelion distances of about 30 AU. Therefore, they are called extreme trans-Neptunian objects. It is believed that there may be about 500,000 bodies in the Kuiper Belt with a size of more than 30 km.

Table 1. The largest known TNOs with calculated size

№	Name (designation)	Size (km)
(136199)	Eris (scattered disc TNO)	2400 km
(134340)	Pluto (2:3 resonance with Neptune, plutinum)	2320 km
(90377)	Sedna (Oort belt object?)	<1500 km
(136472)	Makemake (classical TNO)	1500 km
(136108)	2003 EL61, Haumea (scattered disc TNO)	1200 km
(84522)	2002 TC302 (2:5 resonance with Neptune)	1150 km
(50000)	Quaoar (classical TNO)	1200 km
Charon	(satellite of Pluto, plutinum)	1212 km
(90482)	Orcus (2:3 resonance with Neptune)	910 km
(19308)	1996 TO66 (classical TNO)	900 km
2007	UK126 (scattered disc TNO)	880 km?
(174567)	2003 MW12 (classical TNO)	840 km?
2005 UQ513	(cubivano)	840 km?
2005 QU182	(scattered disc TNO)	800 km?
(20000)	Varuna (classical TNO)	800 km
(55565)	2002 AW197 (classical TNO)	770 km
2006 QH181	(scattered disc TNO)	760 km?
(19521)	Chaos (classical TNO)	740 km
(145452)	2005 RN43 (classical TNO?)	730 km?
(28978)	Ixion (2:3 resonance with Neptune)	730 km
2002 MS4	(classical TNO)	730 km
(84922)	2003 VS2 (2:3 resonance with Neptune)	720 km
(55636)	2002 TX300 (classical TNO)	710 km
(24835)	1995 SM55 (classical TNO)	700 km
(145453)	2005 RR43 (classical TNO?)	700 km?
2003 AZ84	(2:3 resonance with Neptune)	690 km
(90568)	2004 GV9 (classical TNO)	680 km
(120178)	2003 OP32 (classical TNO)	670 km?
(55637)	2002 UX25 (classical TNO)	650 km
(42301)	2001 UR163 (scattered disc TNO)	640 km?
2003 UZ413	(2:3 resonance with Neptune?)	610 km?
(15874)	1996 TL66 (scattered disc TNO)	600 km

Currently, the following classes of TNOs are distinguished in the Kuiper belt:

Classical bodies, which include most of the known TNOs;

Resonant bodies that are in resonance with the planet Neptune;

The most saturated is the 3:2 resonance with a semi-major axis of 39.4 AU; since Pluto is in the same resonance, bodies of this class are also called **plutons**.

Scattered disk bodies, which are distinguished by elongated orbits with high inclination and eccentricity. The population of these bodies extends much further than 50 AU.

Isolated trans-Neptunian bodies, which include bodies with very elongated orbits and perihelion distances in AU [10] close to 40 AU (for example, 2000 CR105 and 90377 Sedna).

M. Brown and colleagues announced on March 5, 2004, that during observations in November 2003 at the high-altitude Palomar Observatory they were able to discover the most distant object in the Solar System (~100 AU). This object indicated the possibility of the existence of the **Oort-Epic cloud**.

This body was located at distances significantly greater than the currently generally accepted value for the outer boundary of the so-called planetary zone of 50 AU in the Solar System (Fig. 4). It received the temporary designation for a minor planet under the number 2003 VB12.

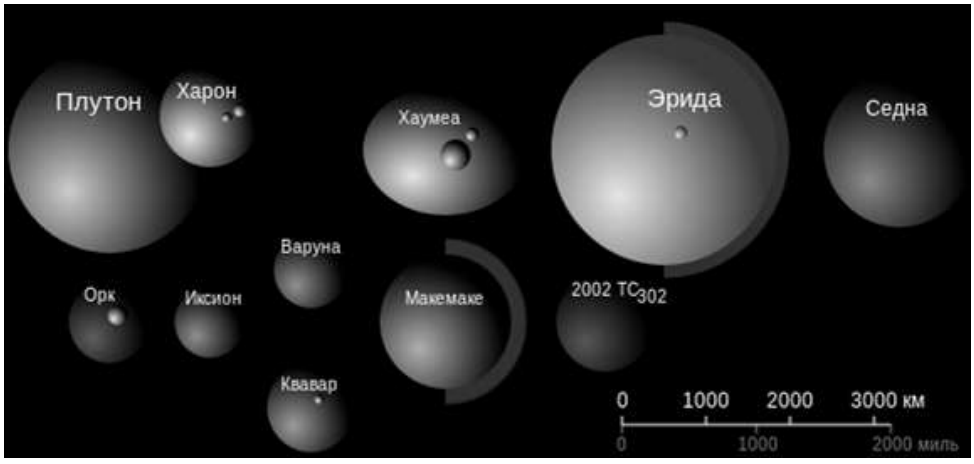

Fig. 4. Comparative sizes of the largest objects in the Kuiper belt [39].

This body was later named after the Eskimo sea goddess Sedna; according to Eskimo myths, she lives in the dark depths of the very cold Arctic Ocean. The semi-major axis of its orbit was 480±40 AU, the minimum distance from the Sun was 76 AU, the inclination of the orbit to the ecliptic plane was 11.9°, and the period of rotation around the Sun was about 10,500 years. Sedna's orbit resembles the orbits of scattered objects in the Kuiper belt. However, it differs significantly in that its perihelion is so

far away that the formation of such an orbit cannot be explained by gravitational scattering on the currently known planets in the Solar System. The only possible mechanism for placing Sedna in such an elongated orbit requires, if not a gravitational perturbation from a yet-to-be-discovered very distant planetary body, then from the action on Sedna from outside our Solar System during a close flyby of another star while it was still forming in the star cluster of our Solar System. Some preliminary estimates indicate the possibility of the existence of up to 500 more objects with geometric and brightness characteristics similar to Sedna.

Observations of Sedna from the Spitzer Space Infrared Telescope have allowed us to estimate that the upper limit of its diameter does not exceed 1,700 km. The mystery is the unusually red color of Sedna's surface, which, according to [42]. It has also been found that Sedna is one of the reddest objects in the Solar System. And the obtained light curves indicated a very slow rotation of this body: the day there is not measured in hours, as is typical for most asteroids of the Main Belt or in the Kuiper Belt, but lasts more than 20 Earth days. For known bodies in the Solar System, slow daily rotation is almost always caused by the action of the tidal force from the side of a nearby massive satellite. An example is the Pluto and Charon system.

In 2006, another object, 2006 SQ372, was found, which was a kind of analogue of Sedna with a diameter of 50-100 km. Its orbit also turned out to be extremely elongated with an eccentricity e=0.967 and a semi-major axis of about 1600 AU; the period of rotation around the Sun was as much as 22,500 years.

In 2010, three such objects were discovered that were dynamically associated with the part of the Oort Cloud closer to the Sun. The first two were joined by the object 87269 2000 OO67. All of them have a very red surface color. Such material may be associated with the presence of a significant amount of organic matter on the surface of these objects, which are located at a great distance from the Sun [156]. It is believed that due to the very low temperature in this region distant from the Sun, the composition of the asteroid bodies in the Kuiper belt should consist mainly of nitrogen, water, methane, methanol, carbon dioxide, ammonia and other ices. Careful studies of the large object 2003 EL61, as well as four slightly smaller objects, from different points

in the Earth's orbit have indicated noticeable changes in its brightness. This allowed us to propose a hypothesis according to which their surface should be covered with a fairly fresh and loose ice layer with an age of less than 100 million years. After all, the presence of bright ice on the surfaces of large objects can be explained, for example, by traces of the atmosphere; however, such an explanation is unlikely to be applicable to small TNOs, on which an atmosphere of noticeable size can hardly form, which could seasonally crystallize and fall as snow or frost on their surface. Therefore, it was necessary to distinguish a class of dwarf planets from large planets, to which Pluto, Ceres and several larger bodies from the Kuiper belt were attributed. Below we will consider the main characteristics of some of the representatives of this class, obtained from the results of remote observations. The characteristics of the largest of the dwarf planets are presented in Table. 2.

Table 2. Characteristics of some dwarf planets

Characteristics	**Ceres**	**Pluto**	**Eris**	**Haumea**	**Makemake**
Semi-major axis of the orbit, AU	2.77	39.439	97.56	51.544	53.075
Eccentricity	0.08	0.25	0.446	0.195	0.159
Periodical period around the Sun, years	4.6	247.7	557	283.28	309.88
Periodical period around its own axis, days	0.378	6.39	>0.33	0.125	0.937
Inclinations of the orbital planes to the ecliptic	10.6°	122.5°	44.0231°	28.22°	28.96°
Inclination of the orbital plane to the equator	4-5°	17.2°	?	?	?
Radius, km	487	1194	≈1350	980×759×498	750
Mass, 10^{22} kg	0.00943	1.79	1.67 ± 0.02	0.4	0.4
Density, g·cm^3	2.44	1.7	1.20 ± 0.03	2.78	2
Geometric albedo	0.06	≈0.6	0.86 ± 0.07	0.65-0.93	
Temperature, K	111-242	60	25	<50	30-35
Number of satellites	0	4	1	2	?

2. Methods for determining the characteristics of distant bodies

2.1. Direct methods.

For sufficiently large bodies in the Solar System, their linear dimensions can be determined from direct measurements of the angular dimensions of their images obtained in the focal planes of even relatively small telescopes. Thus, the minimum measurable dimensions of planetary bodies must be limited by the angular resolution of a particular telescope; this is determined using Rayleigh's law by the formula

$$\Delta\psi = 1{,}22(\lambda/D) \text{ radian}, \quad (1)$$

and turbulent blurring of a particular image by the Earth's atmosphere. For each such image, the intensity distribution can be written as a Gaussian

$$F(r) = \int_{-\infty}^{+\infty} f(r-x)\exp\left(-x^2/2(\bar{r})^2\right)dx, \quad (2)$$

here D – is the diameter of the mirror of the telescope used, r is the half-width of the turbulent contour under study (Fig. 5) [6]. For example, if the value of the diffraction spatial resolution for a 1-meter telescope is about 0.13″, then the half-width of the Gaussian (2) will very rarely be 0.2″ even in astronomical observatories with the best astroclimatic conditions.

Recall that in recent years, the negative impact of the Earth's atmosphere has begun to be minimized using adaptive optics and speckle interferometry methods [106]. For example, the use of adaptive optics systems allows you to determine the degree of distortion of the light wave under study in almost real time, and restore its original appearance quite accurately. This allows you to achieve a spatial resolution very close to the capabilities of a particular telescope (1). The speckle interferometry technique is based on the study of the effect of turbulent blurring of a specific image. Its use for observations of asteroid bodies was proposed in [106]. For example, having obtained an image of an almost point distant celestial body with a very short exposure (0.01 s) using a long-focus telescope (over a hundred meters), instead of a single image in the focal plane we will have many randomly arranged images.

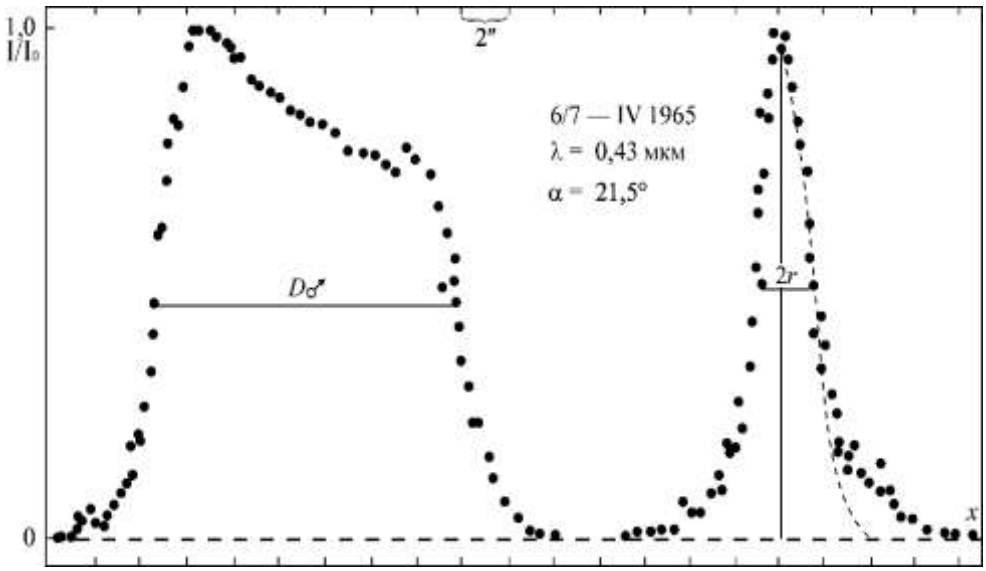

Fig. 5. On the left is a photoelectric scan of images of the planet Mars, obtained with an aperture of about 0.3″. On the right is a scan of a star with a slit of 0.2″×100″. The dots show the results of the observations, and the dashed line shows the Gaussian approximation (2) [6].

In this case, the sizes of the smallest of the images will correspond almost to the diffraction limit of the resolution of the telescope used. Moreover, this method will be much more effective in astropoints with worse astroclimate. After all, in places with high image quality, the obtained speckles will overlap. The spatial distribution of the obtained images is called speckle structures; and each individual image is called speckle. In the case when the apparent diameter of the selected celestial body has a finite size, the dimensions for each of the individual speckle images will have somewhat larger dimensions and will practically be determined by the form of expression (2), in which r will be the value of the half-width of the diffraction resolution of the telescope used. Mathematical processing of the resulting set of images allows us to determine the dimensions of the observed celestial bodies.

We can also mention the use of the capabilities of traditional interferometry methods. A. Dollfuss [69] described the first use of this method by H. Hami to obtain the diameter of the asteroid Vesta in 1899. To determine the dimensions, two telescopes were used, separated by a certain distance, which could vary. This method is also widely used in radio astronomy when determining the sizes of stars. The

following method allows us to determine not only the dimensions, but also the shape of asteroids. It is based on observations of the phenomenon of covering stars with asteroid bodies. It was first successfully applied in 1975 during observations of the eclipse of the star κ Geminorum by the asteroid Eros [140]. When the star is eclipsed, the asteroid casts a shadow to the Earth with the same size as its diameter.

Therefore, by determining the time Δt from the beginning to the end of the eclipse during observations, it is possible to determine the size of the asteroid quite accurately. If the observations are carried out by a group of observers located at different observation points along the calculated eclipse strip, then the results obtained at different chords of the shadow from the asteroid [167] allow, if there are two chords, to determine the size of a particular asteroid, assuming that it has a spherical shape. And if the observational data were obtained for three or more chords along the shadow on the Earth's surface, then the size and shape of a particular asteroid can also be obtained.

2.2. Indirect methods.

An approximate value of the radius R of a planetary body can be obtained using the value of its absolute magnitude at a known spectral albedo A(α,λ) according to the following expression:

$$m(\alpha,\lambda) = -\ln[R^2 A(\alpha,\lambda)\cdot E_0(\lambda)], \quad (3)$$

here E0(λ) – is the spectral value of the solar constant.

D. Alen [8] after the start of active observations in the thermal part of the spectrum, proposed to use the radiation, or thermal method for finding the sizes of planetary bodies.

This method is based on observational data obtained on the stellar magnitudes of asteroid bodies in the visible and thermal parts of the spectrum. For the thermal part, it is best to use effective wavelengths of 10 and 20 microns. Minor improvements to this method allowed to determine both the sizes of such bodies and the bolometric albedo of asteroids [145]. The essence of this method is that the stellar magnitude of an asteroid in the thermal part of the spectrum can be found from the expression

$$m(\alpha,\lambda) = -\ln[R^2\, B(T,\lambda)\, \delta'(\lambda)], \quad (4)$$

where B(T, λ) is the Planck function for the so-called blackbody radiation; the form of this function for solids in the Solar System (at hν << kT) corresponds to the well-known Rayleigh-Jeans approximation

$$B_\nu(T) = \frac{2\nu^2 n_\nu^2 kT}{c^2}; \quad (5)$$

here n_ν is the refractive index at frequency ν, c is the speed of light, *k* is the Boltzmann constant, *h* is the Planck constant; and $\delta'(\lambda) = 1 - R_o$ is the emissivity, or a measure of the "grayness" of a given "cold" body; it is calculated from the value of the effective temperature of this body [6, 238, 240].

For atmosphereless bodies, all the energy of the Sun reaches its surface. Therefore, the value of the effective temperature is determined only by the values of the reflectivity of the latter and the height of the Sun above the visible horizon. It is clear that the effective temperature will be greater for darker areas of the disk and will decrease with increasing zenith distance of the luminary. For this reason, during the day the surface will heat up quite quickly, while at night it will cool down.

The rates of heating and cooling are determined by such properties of the soil as its thermal conductivity and heat capacity. The value of bolometric albedo is usually taken to be equal to the spherical albedo in B filters, or V for the Johnson system.

$$A_s = qA_g. \quad (6)$$

Value for phase integral

$$q = 2\int_0^\pi F(\alpha) \sin\alpha\, d\alpha\,. \quad (7)$$

is taken as the same as for the Moon [238, 240]. More details on the methodology of the corresponding calculations can be found in [6, 137]. Another indirect method is the polarimetric method. It is based on the relationship obtained empirically in laboratory studies between the values of the reflectivity of the surface layer and the slope of the branch of the so-called positive polarization relative to the phase angle coordinate [6], or between the value of the reflectivity and the largest value for negative polarization [263].

However, it must be taken into account that when using the above-mentioned methods, one can encounter quite significant errors, the values of which can have a coefficient of 2 to 4. A weak point for using the thermal method is also the fact that for transitions between spherical A_s and geometric albedo A_g, it is necessary to determine the value of the phase integral q. And its value for atmospheric-free bodies can vary by 2-2.5 times.

2.3. Methods for determining some celestial mechanical characteristics for distant bodies and the Solar System.

The methods used to determine individual celestial mechanical characteristics for distant bodies in the Solar System are based on separate provisions of the work [4].

The rotation period P of asteroid bodies, similar to the methods used in the study of large planets, is determined from observational data on the change in their brightness with time, which are attributed to differences in the shape of a particular body, or to optical inhomogeneities on the surface of the visible disk. Although it is clear that the most likely model for the observational changes will be the simultaneous action of both of these factors. In addition to this graphical approach, in the work [92] it was proposed to approximate the observed light curve using a Fourier series in the following form:

$$m(\alpha,t)=m(\alpha+\sum[A_i\sin(2\pi i/P)(t-t_0)+B_i\cos(2\pi i/P)(t-t_0)], \quad (8)$$

here $m(\alpha)$ is the average value of the stellar magnitude of the celestial body at the phase angle α; t_0 is a kind of zero point of time, taken close to the middle of the full observation interval; and A_i and B_i are Fourier coefficients.

The direction of rotation of an asteroid can be determined from the results of observations of the times of the same positive and negative extrema on the obtained light curves, which are recorded at different values of the ecliptic longitude during several oppositions with a well-known value of the rotation period P around the axis [191]. The essence of this method is that when the position of the asteroid relative to the Earth changes at the times of observations at different oppositions during the time interval Δt, the number of N cycles will be inserted between observations of a specific known photometric detail on the light curve; and this number will differ by the value

ΔL/360 from an integer; ΔL – here will be the angle that characterizes the change in the directions of the ray of sight between each of the observations, and it will be equal to the change in the value of the Earth's longitude in the coordinate system for this asteroid; and therefore, it will be approximately equal to the difference between the ecliptic longitudes Δλ of the asteroid at two adjacent moments of observations, at which the axis of rotation of this asteroid will not differ significantly from the perpendicular to the plane of the ecliptic. Under such conditions, the sign in the correction Δλ/360 for the expression

$$(\Delta t/P_{sid}) = N \pm (\Delta\lambda/360) \quad (9)$$

will determine the direction of the asteroid's motion. The "plus" sign will correspond to direct motion, while the "minus" sign will correspond to reverse motion.

In this expression, Psid is the sidereal period of rotation of the asteroid body. After finding the value Δλ/360 and determining the direct and reverse motions, two values can be determined for the number of cycles between adjacent moments of observation. For the actual direction of rotation, the value N will correspond, which will be close to some integer. And since Δt/N is the apparent, or so-called synodic period in the time interval Δt, then the transitions from sidereal to synodic period can be carried out according to the following expression

$$P_{syn} = P_{sid}\,[1 \pm (\Delta\lambda/\Delta t)(P_{sid}/360)]4 \quad (10)$$

here the plus and minus signs will determine the directions of motion.

The direction of rotation can also be determined from data from radar observations [238, 240]. Methods for determining the orientation of the axis of rotation of an asteroid body are also based on the difference between the light curves obtained at different times of observation (the so-called epochs). An example can be the data given in Fig. 6. It shows the results of processing by the epoch method of observational data obtained in 2001 during a long observational “window” for the asteroid body 5587 SB. This asteroid belongs to the so-called Amur class (a=2.39 AU, e=0.55).

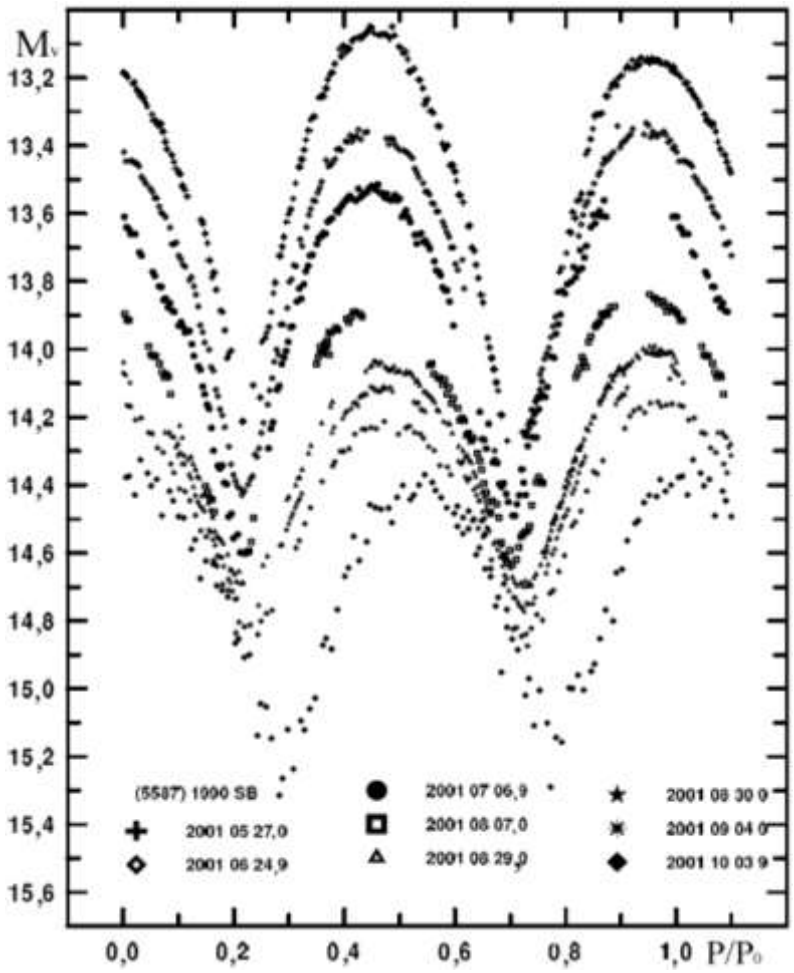

Fig. 6. Normalized light curves for asteroid (5587) 1990 SB from observations in 2001 [82].

The data from this figure show that the geometry of the asteroid's location changed significantly, causing changes in the amplitude of its brightness in the range from 0.7 to 1.25^m. The average value of its rotation period was 5.0494^h. This method began to be developed in the 1930s; now two of its varieties are mainly used. One of them is the method of "photometric astrometry", or E-method [84, 180] and the method of "amplitude – stellar magnitude", or AM-method [4, 128]. The first of them allows you to simultaneously obtain the coordinates of the pole and determine the direction of rotation. Its main equation has the following form:

$$(\Delta t_c/P_{sid}) - N - q\ \{(\Delta L_B/360) + \Delta n] = 0, \qquad (11)$$

where Δt_c is the time interval between adjacent epochs of the same extremum on the light curve; N is the integer number of synodic rotation periods in a given interval; ΔLB is the change in longitude of a point located under the bisector of the phase angle

value of the studied asteroid in the planetographic coordinate system; Δn is the correction for the number of cycles during complete revolutions of the asteroid around the Sun during the time interval Δt_c; q = +1 and -1, respectively, for forward and reverse rotation of the asteroid body.

Since the true value of the period Psid should not depend on the time interval at which it is determined, then for the chosen direction of rotation it is necessary to find such coordinates of the poles at which the spread of the values of the period Psid for different time intervals Δt_c will be the smallest. The advantage of this method is that when using it, neither the shape of the asteroid body nor the optical inhomogeneity of the visible disk are of decisive importance.

In the AM method [262], an analysis of changes in the amplitude values for the light curves A and the magnitude of the asteroid body at its maximum are used, with a change in the angle between its axis of rotation and the line of sight ψ; this angle is determined from the expression

$$\cos\psi = \sin\beta\sin\beta_0 + \cos\beta\cos\beta_0\cos(\lambda - \lambda_0). \quad (12)$$

It is believed that the asteroid disk should be optically homogeneous and have a shape close to an ellipsoid. For example, for this type of asteroid with semi-axes a > b > c, the amplitude for the light curve is given by:

$$A(\psi) = 1{,}25\lg\{[(b/c)^2\cos^2\psi + \sin^2\psi] / [(b/c)2\cos^2\psi + (b/a)2\sin2\psi]\} = \beta_A\alpha, \quad (13)$$

here β_A is the change in amplitude when the phase angle α changes by 1°. The amplitude reaches its maximum value at the angle ψ = 90° with the axis ratio given by the expression

$$A(90^o) = A_{max} = -2{,}5\lg(b/a). \quad (14)$$

The difference in stellar magnitudes when observed from the polar region ψ = 90° and from the equator ψ = 0° can be found according to the expression

$$V_0(90°) - V_0(0°) = -2{,}5\lg(c / b). \quad (15).$$

These last two expressions allow us to determine the ratio of the semi-axes and the coordinates of the pole by minimizing the calculated deviations.

3. Physical characteristics of dwarf planets according to remote sensing data

3.1. Pluto

Due to its large eccentricity, Pluto is sometimes closer to the Sun than Neptune. It is believed that, like many Kuiper belt bodies, it consists of ice mixed with rocks.

In 1978, D. Christie [56] discovered an asymmetric image of Pluto, which gave reason to talk about the presence of a satellite, which was found a few months later (Fig. 7) and named Charon (according to Greek mythology, this is the name of the carrier of souls to the kingdom of Pluto across the river Styx). Its diameter is 1186 km, mass ~ 1/30 of Pluto's mass, distance from the center of Pluto ~20,000 km, rotation period 6.39 Earth days. Pluto and Charon rotate synchronously and therefore they are considered a double dwarf planet.

Fig. 7. One of the first images of Pluto and Charon, obtained with the Mauna Kea Observatory telescope [176].

Somewhat later, on the KTH images, a group of researchers led by A. Stern found two more satellites of Pluto (S/2005 P2 and S/2005 P1, Fig. 8), by which decision the IAU approved the mythical names Nix and Hydra. Their luminosity is 5000 times lower (23^m) than that of Pluto. This value, depending on the surface albedo, gives an estimate of their size in the range of 45-167 km. On 20.07.2011, the discovery of another satellite S/2011P1 with a size of 13-34 km was announced. The two new moons are located at distances of 49,400 ± 600 and 64,700 ± 850 km from Pluto, with orbital

periods of 25 and 38 days, and with the orbital planes of all three moons coinciding. This is evidence that they were formed simultaneously during a collision of Pluto with another Kuiper belt object, which occurred about 4 billion years ago after the moons' orbits were pulled away from Pluto by the gravitational pull of Charon.

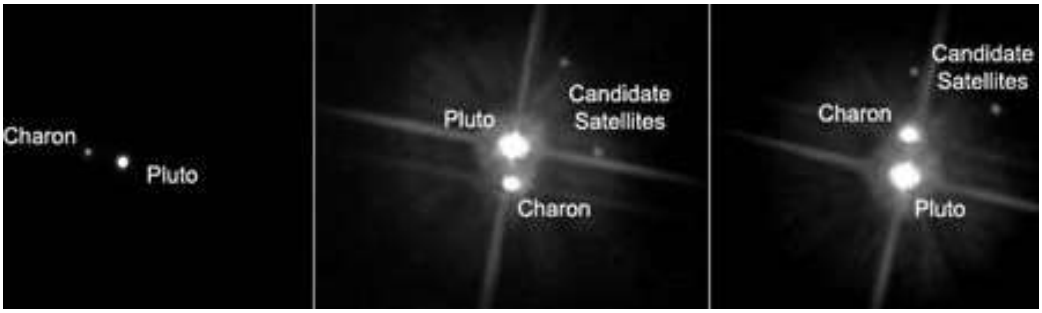

Fig. 8. Images of Pluto and its moons taken by the Hubble Space Telescope at different dates [46].

The choice of names for the new moons is due to the fact that Hydra, until she was killed by Hercules, guarded the entrance to the underworld, and Nyx is the goddess of darkness and night, who lives in the underworld. It is also symbolic that the first letters of the names of the new moons "H" and "G" are associated with the first letters of the spacecraft "New Horizons", which went to Pluto on 19.01.2006. Since the name Nyx was already involved in the system of astronomical names, it was decided to change the English transcription of the goddess "Nyx" to the name of the moon "Nix". According to modern estimates, at least 20% of the Kuiper belt objects also have satellites (one or more). Data on Pluto's magnetic field are still missing, but from the theory of the baroelectric effect its magnetic moment may be an order of magnitude smaller than the Earth's.

Photometric, polarization and thermal properties. The first photoelectric measurements of Pluto's brightness in the UBV filter system revealed a change in time and determined the color indices $B - V = 0.79^m$ and $U - B = 0.26^m$ [1, 2, 5, 11, 29, 30, 50, 80, 123] confirmed the reality of such changes (Fig. 9) and revealed the dependence of brightness on the longitude of the central meridian (Fig. 10) with an amplitude of up to 0.22^m. If the amplitude of the brightness change in different periods of observations

was different, then the color index remained practically unchanged: B - V = 0.82 ± 0.03^m. The longitudinal dependence of the brightness is due to the asymmetry of the number of details along the equator with different reflectivities, the change in time is due to the asymmetry of the location of the polar caps [17, 49, 260], the inclination of which relative to the direction to the Earth changes as the planet moves in orbit. The trailing hemisphere of the planet in the visible part of the spectrum is 25-30% darker than the leading one and 4% redder in the B and R filters [48, 124]. Analysis of the brightness curves of the Pluto-Charon system (Fig. 10) showed that on the surface of Pluto there are two twice as dark spots of a round shape at 23° N. lat. with a size of 46° and 28°, separated by 134° in longitude. Regarding age-related changes, an assumption is made about the presence of a dark strip crossing the planet's equator, or bright polar caps [116]. Observations of the effects of the Pluto-Charon system eclipse are also used to study the optical heterogeneity of Pluto's disk [28, 48, 49]. The period of age changes is believed to be 124 years, half the orbital period [29]. Near perihelion, the temperature regime was critical for the condensation conditions of methane and nitrogen. Therefore, observations during that period were very important.

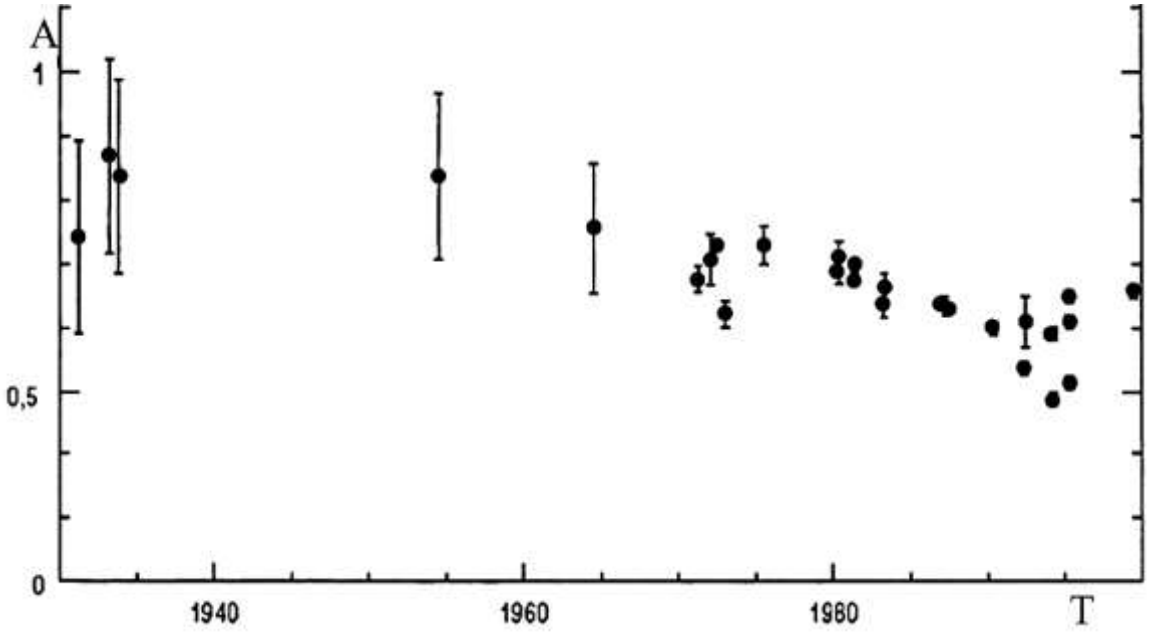

Fig. 9. Relative changes in the geometric albedo (A) of Pluto in visual rays with time (T) [46].

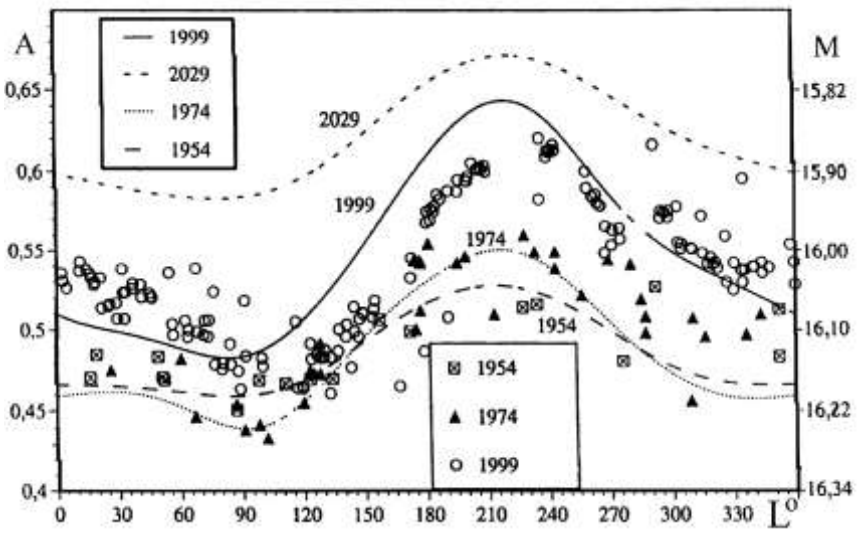

Fig. 10. Comparison of calculated brightness curves (geometric albedo A and stellar magnitude M in filter V) with Pluto longitude (L) from observations of the Pluto-Charon system for the time interval 1954-1999 [50].

Based on the reflectivity map of the surface of Pluto (Fig. 11) and Charon, model brightness curves were calculated at $\alpha = 0°$ for their mutual configurations in 1954, 1974, 1999 and a forecast of changes in the longitudinal dependence of brightness for 2029 and the brightness itself from 1954 to 2029 was made (Fig. 10) [50]. According to ground-based observations, Pluto's brightness within the phase angles of 0-2° linearly depends on α with a phase coefficient of ~ 0.05^m/deg [12, 30].

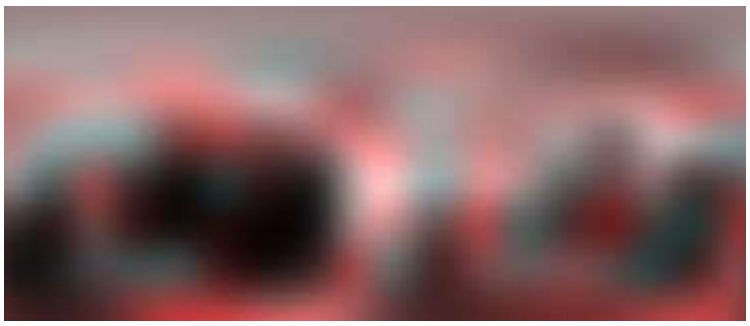

Fig. 11. Map of the distribution of various components on the surface: dark areas indicate contaminated water ice, light areas indicate frozen nitrogen, red areas indicate methane ice and other organic matter. The brightest spot in the center is frozen carbon monoxide [47].

Few works have been devoted to the study of the polarization properties of Pluto. In [111], it was found that at $\alpha = 0.8°$ the degree of polarization is $P = 0.27 \pm 0.02\%$, the orientation of the polarization plane is $\psi = 156 \pm 2°$. The data of works [2, 36] confirmed that $P = 0.26 \pm 0.02\%$, $\psi = 121.9 \pm 22°$ at $\alpha = 0.82°$ and $P = 0.29 \pm 0.02\%$ at $0.8° \leq \alpha \leq 1.8°$. Such values of the position of the polarization plane and the practical independence of the polarization degree P from α are compatible with the assumption of the manifestation of the effect of multiple scattering of limb points in the presence of a clearly pronounced asymmetry in the location of optically inhomogeneous details of the invisible disk of the planet.

Spectrophotometry and conclusions about the nature of the surface layer. According to the first IR photometry in standard JHK and two narrow-band ($\lambda = 1.55$ and 1.73 μm) filters [62], it was concluded that the surface layer of Pluto is covered with frost. Further observations in a wide range of wavelengths [13, 15, 25, 33, 45, 63, 70, 80, 109, 125, 144] revealed absorption bands at $\lambda > 600$ nm (Fig. 12). The band at $\lambda = 2.14$ μm belongs to nitrogen N_2 (at a temperature of 40 ± 2 K), at $\lambda = 2.35$ μm to CO, and the others to pure methane CH_4 and its mixture with nitrogen N_2. Quantitative estimates show that the concentration of CO and CH_4 on the surface of Pluto is 5 times higher than on Triton. The search for other components of the atmosphere (Fig. 13) was carried out by comparing the observed spectrum of the planet with the calculated synthetic spectra at $\lambda = 2.9$-3.9 μm, taking into account the absorption of certain non-methane hydrocarbons with the addition of methane CH_4 [153], liquid methane with solid molecular nitrogen with the addition of C_2H_6 and C_2H_2, etc. It is believed that since the formation of the Pluto-Charon system, a nitrogen layer over 500 m thick may have evaporated from Pluto's surface.

Especially informative were observations during eclipses in the Pluto-Charon system [70, 79, 154], which revealed the spectral dependences of the albedo of Pluto [149] and its satellite Charon. Since frozen methane should quickly darken under the influence of solar radiation and charged particles, the relatively high values of geometric albedo indicate the presence on the surface of Pluto of a layer of methane frost, which is renewed due to the sublimation and condensation of volatiles in the

atmosphere during its movement in orbit. This explains the long-term change in Pluto's brightness. Charon's low albedo is associated with the absence of volatiles there [176].

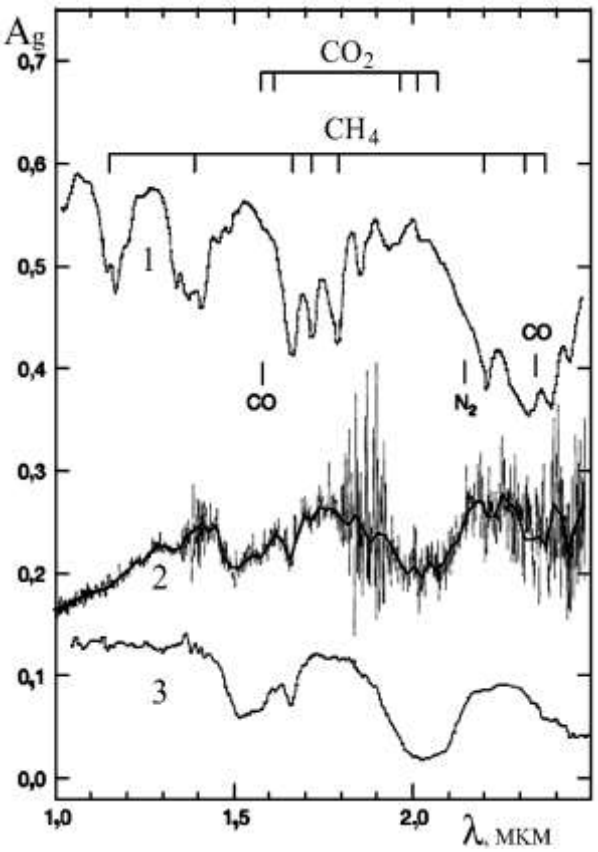

Fig. 12. Manifestations of methane, nitrogen, CO_2 and CO in the spectral value of the geometric albedo of Pluto (1), Quaoar (2) and Charon (3) [155].

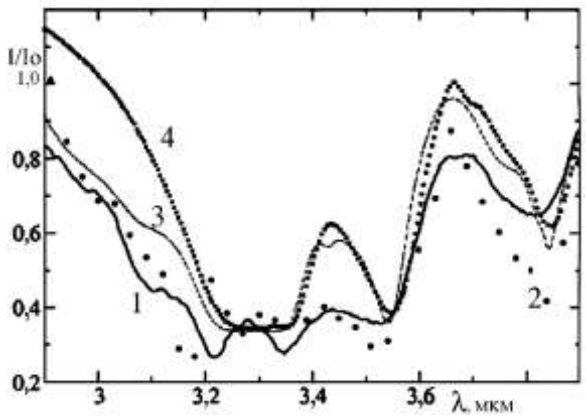

Fig. 13. Spectral reflectance of Pluto (solid line 1 and points 2 [87]); synthetic spectra of the N_2-CH_4-CO mixture with a mass ratio of 1:0.01:0.002 – dashed line 3; spectrum of pure methane – curve from points 4. All data are normalized to the value at $\lambda = 3.58$ μm [153].

Pluto's atmosphere. Pluto is approximately 40 times further from the Sun than the Earth, and therefore at an average temperature of T ≈ 45 K (which can drop to 33 K in winter and rise to over 55 K at midday in summer), only neon does not liquefy in its atmosphere; although as early as 1974 it was believed that its atmosphere may contain minor admixtures of argon and nitrogen [92]. The low temperature was indicated by IRAS measurements at λ = 25, 60, 100 μm, according to which T = 45 K at an emissivity of 0.9 [14], and radio astronomy observations at λ = 1.2 mm (T = 39 ± 4 K) [10]. Based on these data, G. Golitsyn estimated that the atmospheric pressure of a possible atmosphere does not exceed a few tenths of a bar [3]. The detection of methane absorption bands in the spectrum of Pluto made it possible to suspect the existence of gaseous methane there [45, 63,144], the amount of which in the line of sight is from 3 m-atm at p = 0.01 bar to 27 ± 7 m-atm at p = 0.00015 bar.

Fundamentally new data on the atmosphere of Pluto were obtained from observations of the phenomenon of a stellar eclipse on June 9, 1988 using a high-speed photometer on the 90-cm telescope of the Kuiper Observatory [74]. Comparison of calculations [77] with observational data gave the best agreement for a two-layer atmosphere with a strongly absorbing lower layer with an optical thickness of 0.19 and a height scale of H = 33.4 ± 6.9 km, extending to a height of 46 km, and a purely methane atmosphere above it. If we take into account the temperature regime of Pluto, then most likely there are significant changes in the methane component of the atmosphere over time, which contributed to the detection of its manifestations in the phenomena of coverage in the 1980s [34, 74, 77, 98].

Calculations of the isothermal upper atmosphere model showed that the atmospheric pressure increased by a factor of 2 from 1988 to 2002, and in 2002-2007. pressure stabilization occurred [73, 75, 162]. Below 1215 km from the planet's center, a strong increase in absorption was observed, which was attributed to absorption by stratospheric haze. In model calculations, it was assumed that Pluto's atmosphere consists mainly of nitrogen N_2. Methane has been reliably detected in spectroscopic observations [255] and its total amount has been estimated at 1.2 cm-am with a correction factor of 4 [75, 110, 162]. High-quality spectral observations of gaseous

methane and analysis of photometric data of Pluto's coverage of stars have yielded a new estimate of the amount of methane, new constraints on the structure of Pluto's lower atmosphere, the pressure near the surface, and the equivalent temperature of methane. Experimental confirmation of the presence of gaseous methane in Pluto's atmosphere was provided by its spectrum (Fig. 14), obtained on the 8.2 m telescope with a cryogenic IR spectrograph [102] with a spectral resolution of 60,000 [76].

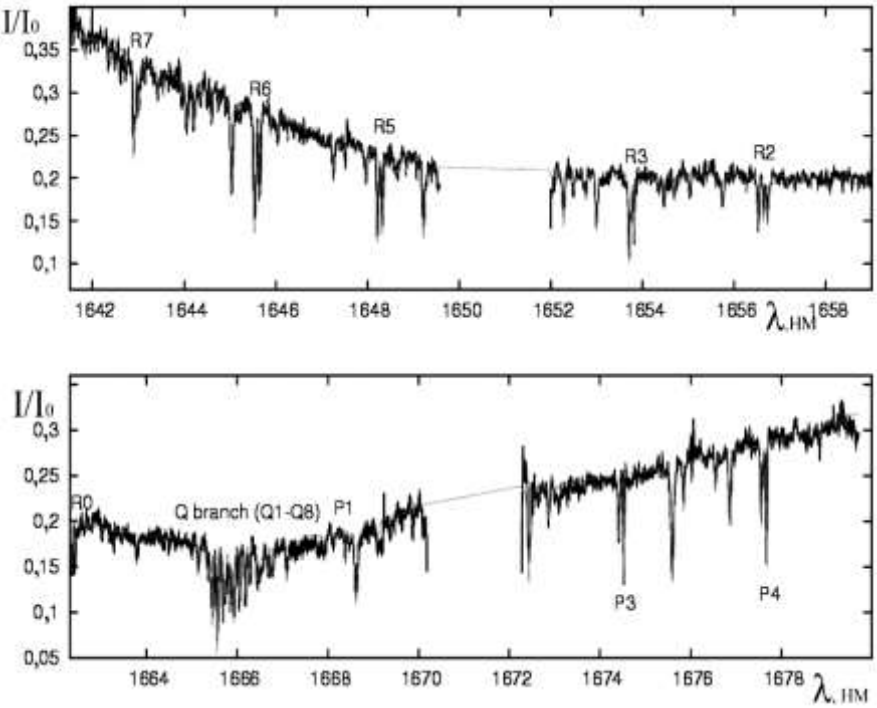

Fig. 14. Pluto's spectrum superimposed on an isothermal model (lighter curve) of a methane atmosphere with a power of 0.75 cm-am at a temperature of T = 90 K. It is believed that the overall "sag" of the continuum is caused by absorption by solid methane [70].

From the modeling, it was obtained that the amount of methane should be 0.33-0.105 cm-am at T = 80-90 K. From the analysis of the effects of the coating, the temperature gradient in the stratosphere was estimated (3-15 K/km) and it was found that the tropopause is quite cold (< 38 K) and has a small height.

To reconcile the temperature of the troposphere with the estimates of the rotational temperature, a model was proposed according to which the source of methane is on the

surface, and a significant fraction of the gaseous methane is in the upper atmosphere of the planet.

As a result, it was obtained that the maximum value of the height of the troposphere does not exceed 17 km, and the maximum estimate of the pressure on the surface is 24 microbars. Taking into account all inaccuracies, the atmospheric pressure on the surface of Pluto in 2008 should have been within 6.5-24 microbars, and the amount of methane - 0.65-1.3 cm-am.

3.2. Ceres

Recall that immediately after its discovery in 1801, Ceres was classified as a major planet. After the discovery of other similar bodies, it headed the list of minor planets (asteroids) at number 1. UV images from the CTC revealed a dark spot on its surface, which was named after Ceres' discoverer, Piazzi, and a mysterious white spot (Fig. 15) [145].

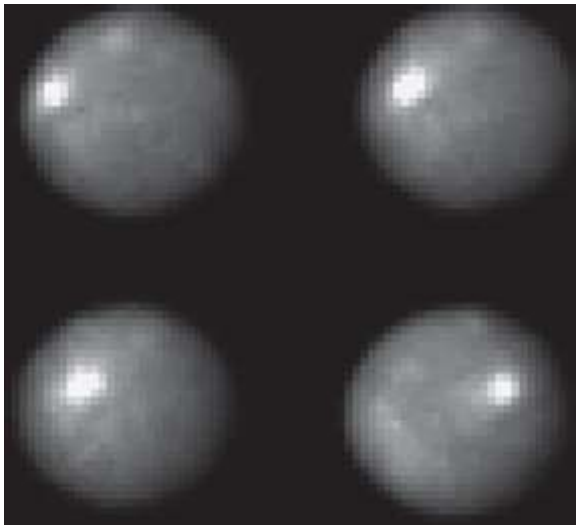

Fig. 15. Change in the position of the bright spot on the surface of Ceres due to a rotation around the axis by 93° [185].

Based on observations with the Keck telescope after 2005 in the IR region of the spectrum using adaptive optics, the first albedo maps of the surface of Ceres were constructed (Fig. 16), which cover 80% of the surface.

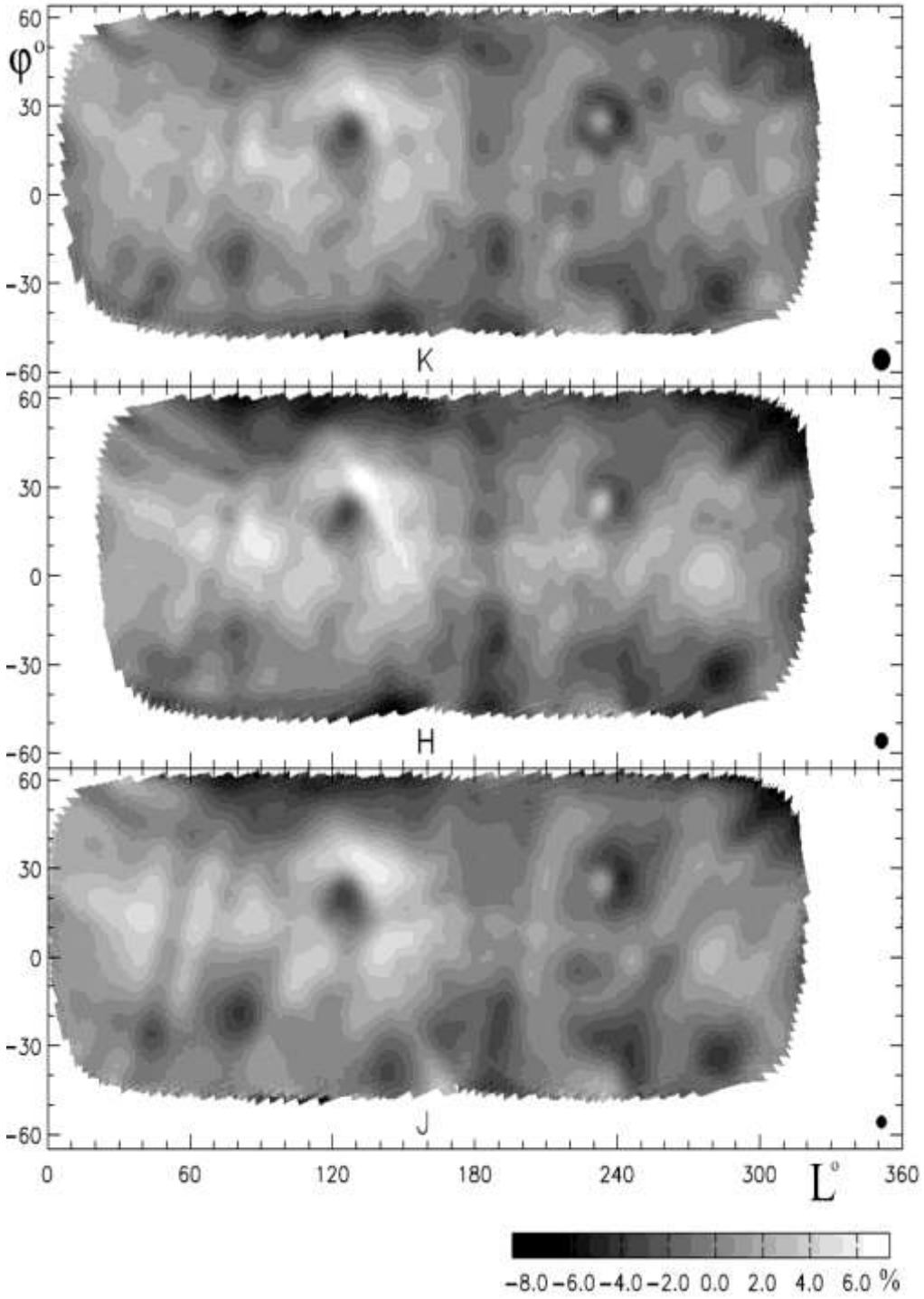

Fig. 16. Albedo maps of Ceres' surface in filters J, H and K [52].

Albedo variations relative to the mean are ± 6% (with an error of ≈ 2.5%). The dark feature with a bright spot in the center with coordinates (234°, +23°) is called the "A" region; the dark spot with coordinates (125°, +20°) is called the Piazzi (region "B"); two more dark features are visible in the southern hemisphere with coordinates (80°, -20°) and (285°, -35°). There are also a number of dark bands that run from pole

to pole. It is believed that Ceres has a rocky core located under an icy mantle, and above it is a crust. The icy mantle is estimated to be 60 to 120 km thick and may contain up to 200 million km3 of water, more than the amount of fresh water on Earth [53]. There is a belief [126] that Ceres is a planetary embryo that has stopped developing due to the influence of Jupiter's powerful gravitational field, which did not allow it to accumulate the necessary amount of material to turn into a full-fledged planet. This is supported by the fact that, even taking into account the obstacles created by Jupiter, Ceres managed to grow to almost 1000 km in diameter and accumulate a mass that is almost a quarter of the total mass of debris that makes up the main asteroid belt located between Mars and Jupiter. However, it should be noted that even if Ceres managed to collect all the building material of the belt, it would still be 4-5 times lighter than even Pluto. Photometric, polarization and spectrophotometric observations showed the following.

1. On the phase dependences there is an effect of brightness opposition (Fig. 17) and a rather deep branch of negative polarization (Fig. 18).

2. The longitudinal dependence of brightness in visual rays has a very small amplitude (< 0.03m) on which, in addition to the main minimum and maximum, respectively at longitudes 230° and 100°, there are also secondary ones – at 30° and 0° [54], the secondary maximum coincides with a bright spot on the surface (Fig. 15, 16). At the same time, at $\lambda = 3.7$ and 3.9 μm the amplitude is larger, especially at longitudes 205-215° where it reaches 27% (Fig. 19).

3. Ceres has an extremely small geometric albedo, which has a specific spectral dependence (Fig. 20): the smallest value (~ 0.03) falls on $\lambda \sim 300$ nm, increases sharply in the far UV and at higher λ, reaching 0.08 at $\lambda = 400$ nm; at $400 > \lambda > 800$ nm it varies within 0.08-0.09 variations; in the far IR region there are molecular absorption bands. In general, the spectrum of Ceres resembles carbonaceous chondrites and C-type asteroids with absorption in $\lambda \approx 3$ μm, due to hydrates or hydroxyls of various minerals and characteristic of some C-type asteroids, but absent in meteorites, the spectra of which can be found in the ASTER spectral library (http://speclib.jpl.nasa.gov).

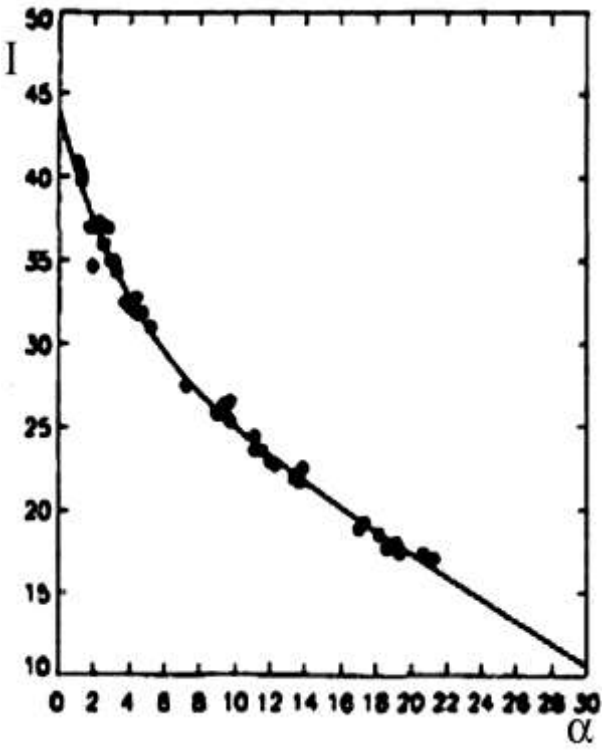

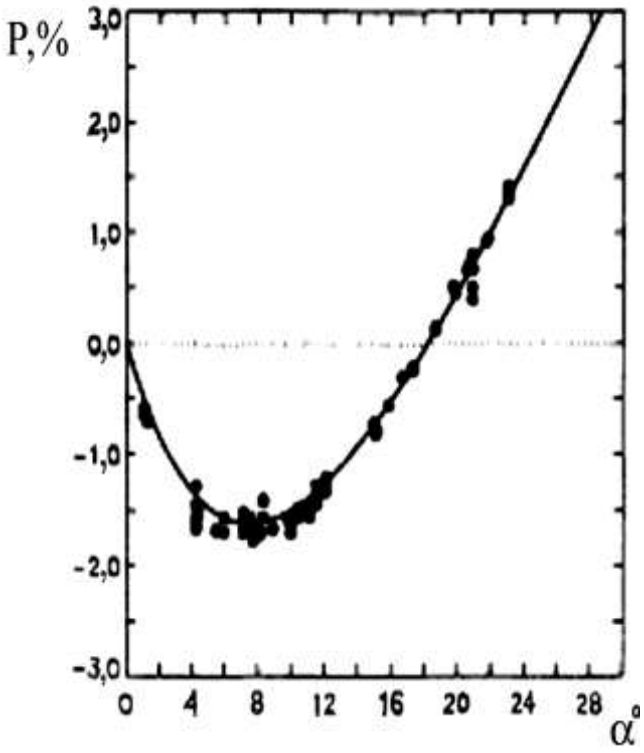

Fig. 17. Phase dependence of the brightness of Ceres [138].

Fig. 18. Phase dependence of the degree of polarization of Ceres [138].

4. As can be seen from Fig. 21, at visible λ there is a rather large value of negative polarization, which weakly depends on λ. Observations at λ = 10 μm revealed that P = 0.22 ± 0.03%, ψ = 165 ± 5° and 0.60 ± 0.12%, ψ = 137 ± 7°, respectively, at α = 3.7° and 13° [24].

5. Observations in the thermal part of the spectrum indicated a decrease in the brightness temperature with increasing λ (Table 3), according to the data at λ = 3.3 mm and 29 cm, it was concluded that the dielectric properties of the upper layer with a thickness of ≈ 3 cm correspond to dry clay [247].

6. According to radar data at λ = 12.6 cm, the cross-section was estimated to be $(0.04 \pm 0.01)\cdot\pi R^2$ (for R = 510 km), which was smaller than that of any other celestial body and which also varied with rotation. From the shape of the power spectrum, it was concluded that on a wavelength scale, the roughness of the surface layer of Ceres is greater than that of the Moon and the inner planets, but less than that of the three outer Galilean satellites [237, 239].

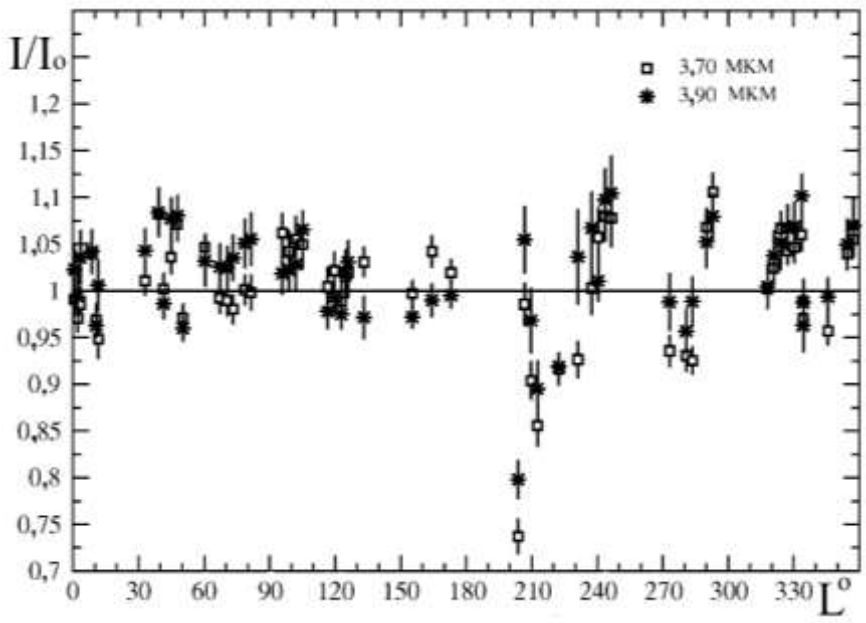

Fig. 19. Longitudinal dependence of Ceres albedo at λ = 3.7 and 3.9 μm [152].

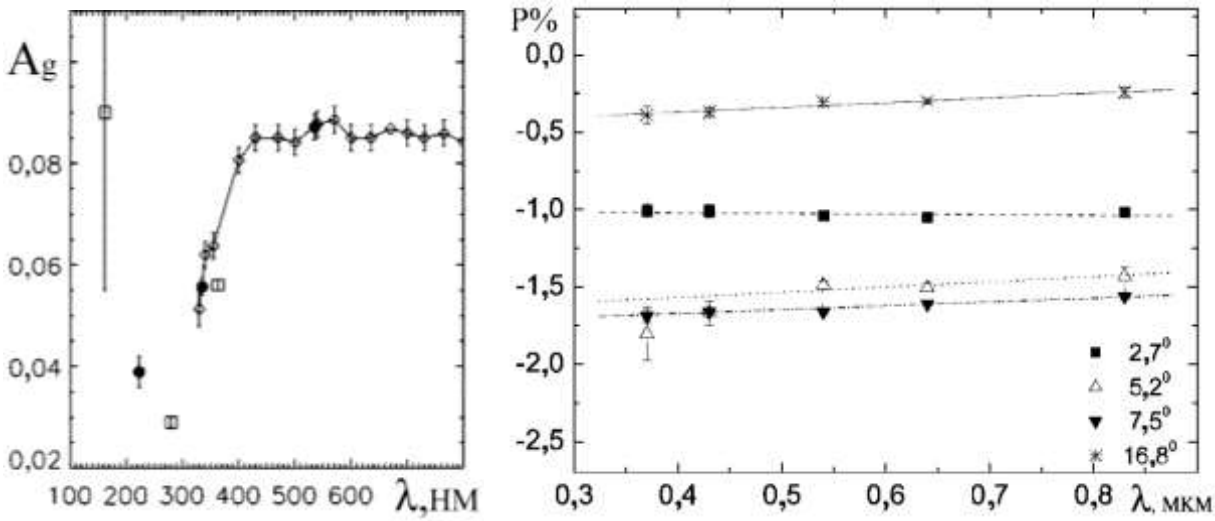

Fig. 20. Spectral geometric albedo of Ceres according to different observations. Error about 2%, 3% and 8% at λ = 535, 335 223 nm [107].

Fig. 21. Spectral dependence of the degree of polarization of Ceres [24].

Table 3. Bright-axis temperature of Ceres

Wavelength	T, K
8-13 microns	242 ± 1
3.33 mm	137 ± 25
3.5 cm	160 ± 53
2 and 6 cm	111 ± 35

3.3. Other large bodies in the Kuiper Belt

TNO **Eris (2003 UB313, 136199, Xena or Xena)** discovered on 10/21/2003 and after establishing its large size (diameter 2400-3000 km, mass $(1.67 \pm 0.02)\times10^{22}$ kg) – attributed to dwarf planets. The period of rotation around the Sun is 557 years, around its own axis – a little more than 8^h. The orbit is highly elongated (eccentricity e = 0.442) and inclined to the ecliptic by 44.0231°, therefore, when passing through the orbit, the surface temperature varies within 30-55 K. At the time of discovery, its brightness was 18.7^m. The geometric albedo (~0.86 ± 0.07), characteristic of snow cover, turned out to be extremely high. This allowed us to assume that at the minimum distance (37.77 AU) Eris may have an atmosphere, which at the maximum distance (97.56 AU) will freeze again. Observations in the IR range indicated that its surface may now be covered with methane ice.

A combination of data on the magnitude and intensity of thermal radiation, carried out on the 30-meter radio telescope IRAM in Spain, allowed us to estimate its brightness temperature of ~25 K, which practically excludes the presence of gaseous methane. A satellite (object S/2005) was also discovered around it, which was initially called Gabriel, later Dysnomia. Its diameter is 300-499 km, and its rotation period is about 14 days [39].

TNO Haumea (2003 EL61, 136108) was discovered in 2005. It is a dwarf planet with dimensions of 1960×1518×996 km (~1400 km). It is named after the Hawaiian goddess of fertility and childbirth Haumea; it has 2 moons: 136108 Haumea 1 and 136108 Haumea 2 [40, 42], which are named after Haumea's daughters: Hi'iaka, the goddess of dance and patroness of the Big Island of Hawaii (where the Mauna Kea Observatory is located), and Namaka, the goddess of water and the sea, who cooled the lava of her sister Pele, which flowed into the sea, and turned it into a new island.

The satellites are believed to be part of the Haumea family, formed billions of years ago from ice fragments knocked off the surface by collisions, since the IR spectrum of the larger satellite Hi‘i‘aka (diameter ~ 310 km) at λ ~1.5 and 2 μm shows strong absorption, consistent with almost pure water ice on the surface [20, 40], its orbit is almost circular with a period of rotation of 49.462 ± 0.083 days. The ten-time

lighter satellite Namaka has an elliptical orbit with a significant eccentricity (e = 0.23) and a period of rotation around Haumea of 18.2783 ± 0.0076 days.

Such an elongated orbit indicates that Namaka's orbit is perturbed by an 8:3 orbital resonance with the more massive satellite Hi‘i‘aka. At least three other slightly smaller TNOs with similar spectra orbit Haumea. The mass of the Haumea system has been determined from the nature of its rotation and orbital parameters to be ~28% of the mass of the Pluto system, and the density is slightly less than 3 g/cm^3. The albedo of the planet has been measured by the Spitzer Space Telescope. In 1999, the orbit of Haumea's satellite Hi'iaka could be observed from Earth almost exactly in the position when it passed over the disk of the central body. Observations of such a passage would provide precise information about the size and shape of both Haumea and its larger satellite, as happened, for example, in the late 1980s with Pluto and Charon. However, the next time such a geometry will be in 2129. [150] For the satellite Namaka, due to the ellipticity of its orbit, the possibility of a transit of the central body remains for several more years.

The dwarf planet Makemake with a possible diameter of 1300-1900 km was discovered on March 31, 2005 by M. Brown's group and is a classic Kuiper belt object. It was initially designated (2005 FY9), later assigned the number 136472 and finally named after the deity of Rapanui mythology - Makemake.

Recall that classic Kuiper belt objects do not have an orbital resonance (2:3) with Neptune, and elements of their orbits are not perturbed by the latter, and therefore on June 11, 2008, the IAU in the class of dwarf planets allocated a subclass of plutoids, to which Pluto, Eris, Haumea and Makemake were attributed. A characteristic feature of plutoids is that they orbit the Sun in orbits with a radius larger than that of Neptune, and are of sufficient mass to allow gravitational forces to give them an almost spherical shape, which clears the space around their orbit, that is, other small objects cannot be near them. This TNO is estimated to have a diameter of 50 to 75% that of Pluto and is the third (or fourth) largest Kuiper belt object. Unlike other large trans-Neptunian objects, it has not yet been discovered to have any satellites, and therefore its mass and density remain uncertain.

3.4. Optical properties of trans-Neptunian objects.

Observations of Kuiper belt objects in visual rays have shown that their geometric albedo is within 0.41-0.73 [44]. According to R-photometry data, within the phase angles α = 0.1-1.5°, among the 10 large Kuiper belt bodies, 4 of them had a linear change in brightness with a phase coefficient of 0.09-0.26^{m}/degree; other optical characteristics [40, 42, 64, 100, 104, 123, 129, 189] are summarized in Fig. 22-25. As we can see, the spectrum of most TNOs contains methane absorption bands, some of them may also contain absorption bands of CO_2, CO, nitrogen, and water, while small bodies lack methane absorption bands. All this indicates the presence of an internal source of methane replenishment on the surface of some TNOs and its absence on others. The following is proposed as a mechanism for the reddening (Fig. 25) of objects with a sufficiently thick surface layer of methane: methane ices in outer space are bombarded by charged particles and the action of hard ultraviolet light, which lead to the formation of more complex hydrocarbons, including the reddish material tholin [104, 129].

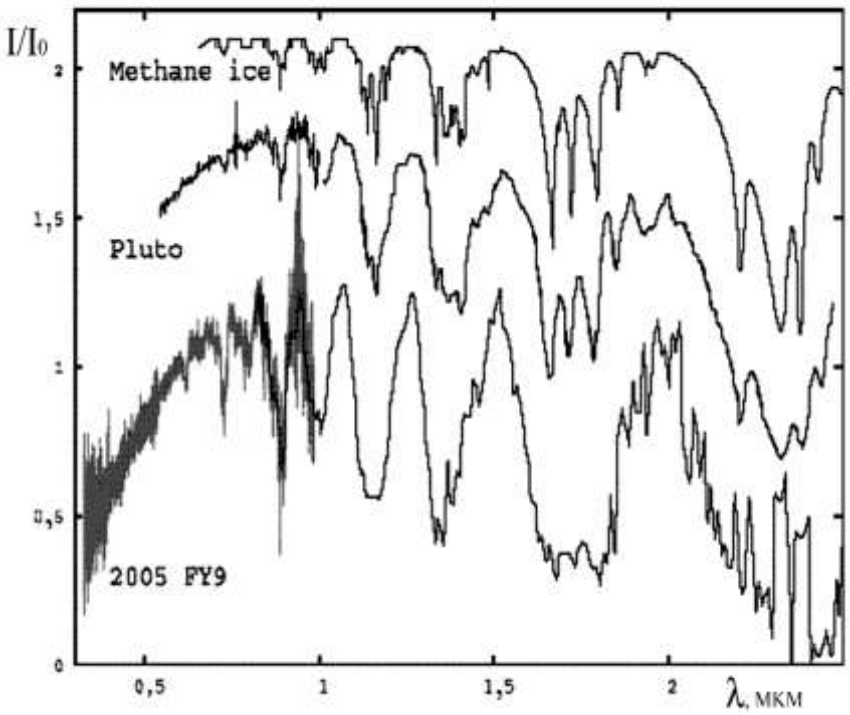

Fig. 22. Relative reflectivity of object 2005 FY9, Pluto and methane [114].

The degree of reddening can be determined by the surface area covered by tholins, and this allows, for example, to explain the fact that the albedo variations on 2003 UB313 are much smaller than on Pluto and that its albedo should be much higher than Pluto's at present [149]. These processes affect the thermal regime of TNOs, since the lower temperature of 2003 UB313 compared to Pluto also explains the difference in the mechanism of methane formation on their surfaces. It is expected that at a distance of 97 AU at the subsolar point of such a body with a surface albedo of 70% the surface temperature will be about 30 K. At this temperature, the vapor pressure of nitrogen N_2 over pure water ice is 420 nanobar, while the vapor pressure over pure methane ice will be lower than a picobar [167].

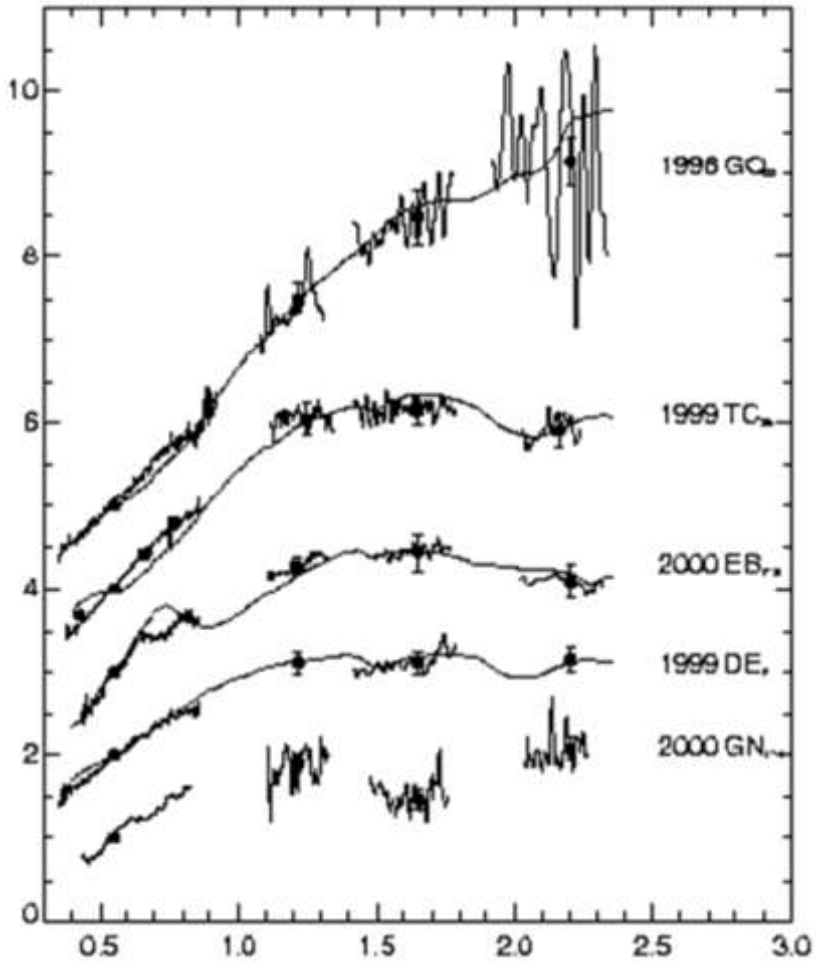

Fig. 23. Relative distribution of observed and calculated (smooth line) reflectivity of 5 Kuiper belt bodies [39].

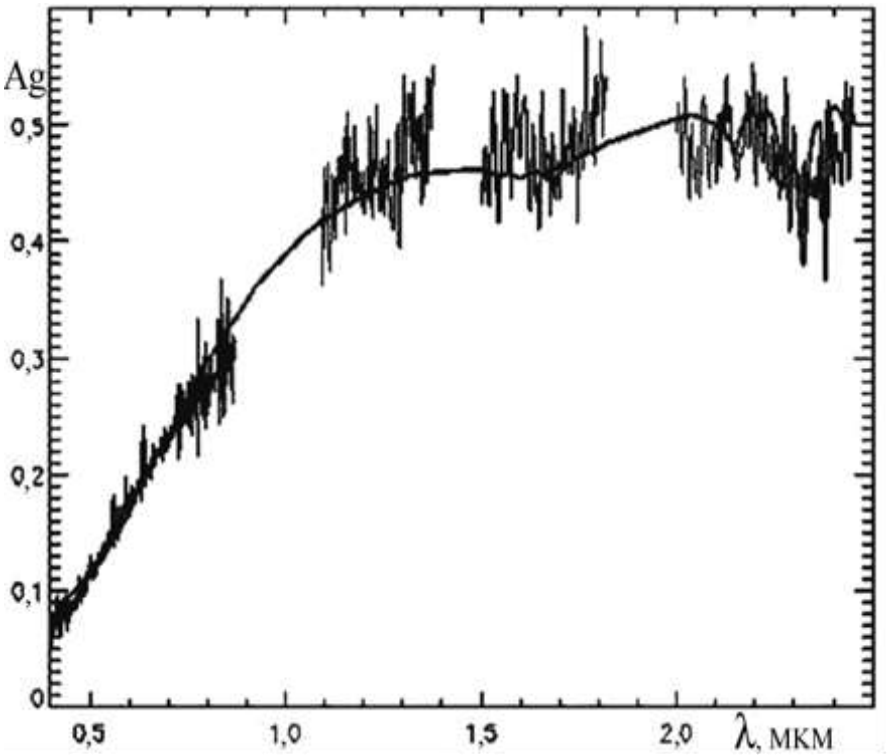

Fig. 24. Comparison of the observed spectrum of Sedna (separate fragments) and the one calculated for the model consisting of 24% tholin, 7% carbon, 10% N2, 26% CH_3OH and 3% CH_4 (smoothed line) [22].

Therefore, unlike Pluto, on the object 2003 UB313 methane in the gaseous state is currently practically absent. However, when approaching perihelion, an atmosphere of methane gas will appear on the object and the object will become similar to Pluto. It is proposed that the surface layer of TNO may also consist of the following mixture: ~70% carbon, 3% olivine, 12% frozen tholin, etc.

But with this composition, the surface corresponds to an albedo of ~ 0.09. As can be seen from Fig. 22, 25 The IR spectra of TNO are very similar, but, for example, the methane absorption bands in the spectrum of 2005 FY9 are deeper than in the spectrum of Pluto, which can be interpreted as the presence of a thicker ice cover on its surface, or a different size of ice particles. Fig. 25 suggests the presence of nitrogen and CO bands in the spectrum of Quaoar, but like Charon, strong water ice absorption bands and weak absorption by hydrated ammonia at $\lambda = 2.2$ μm are also noticeable there [100].

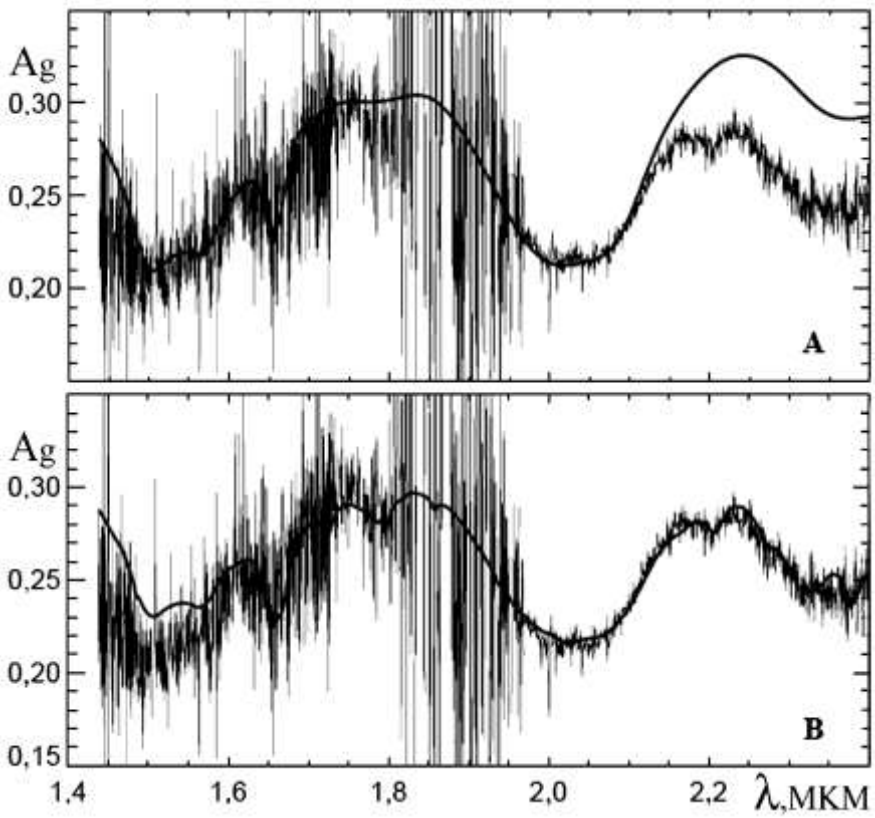

Fig. 25. Observed and calculated spectra of the dwarf planet Quaoar. The smoothed line shows the spectrum of a mixture of water ice and tholin (A) and with the addition of ethane (B) [155].

This means that once upon a time on the surface of this TNO the temperature exceeded the critical value of T ~105÷125 K at which ice crystallized. Since the radiative equilibrium temperature for a surface with an albedo of ~ 0.1 at a distance of 43 AU is only 50 K, the difference in these temperatures can be explained by its significant increase at one time due to heating in the process, for example, of radioactive decay in the deep layers of Quaoar, while heating by micrometeorite bombardment could be significant only for the outer part of the icy surface of these bodies. But observations show that water ice is present only on some large TNOs, while the vast majority of them have methane absorption bands. The so-called “methaneoids” include Pluto, Eris (136199) and 2005 FY9 (136472). Since the concentration of methane is determined by the thermal escape velocities of molecules, its presence will be more stable on large (over 1000 km in size), distant and colder TNOs than on warmer and smaller ones [39]. The dwarf planet Haumea exhibits brightness

fluctuations that may be due not only to its ellipsoidal shape but also to possible optical inhomogeneities in the disk. The spectrum of Haumea shows that its surface, like, for example, the surface of Charon, is covered mainly with water ice (H_2O and CH_4 bands are clearly visible). Episodic polarimetric observations of dwarf planets and TNOs [19, 23, 32] were obtained in the phase angle range $\alpha < 2°$, i.e. for the negative polarization branch (Fig. 26), and for TNOs show an extremely high degree of negative polarization. For objects with D < 1000 km at $\alpha \rightarrow 0°$, the value of the degree of polarization P ≈ 0% and increases rapidly with increasing α, reaching 1% at $\alpha = 1°$. For larger TNOs, the value P < |0.7|% and almost does not change throughout the observed phase angle range α. Since the groups of these objects differ not only in size, but also in surface albedo, which is noticeably higher for larger objects, two different surface chemical compositions and different surface structures are proposed to explain this fact. Darker surfaces usually give much higher negative polarization than brighter ones, which resembles the dependence of Pmin on albedo for asteroids [120]. Finally, these data practically do not show the opposition peak caused by coherent scattering. When individual fragments of the gas-dust cloud were compressed over billions of years, it evolved to its present state.

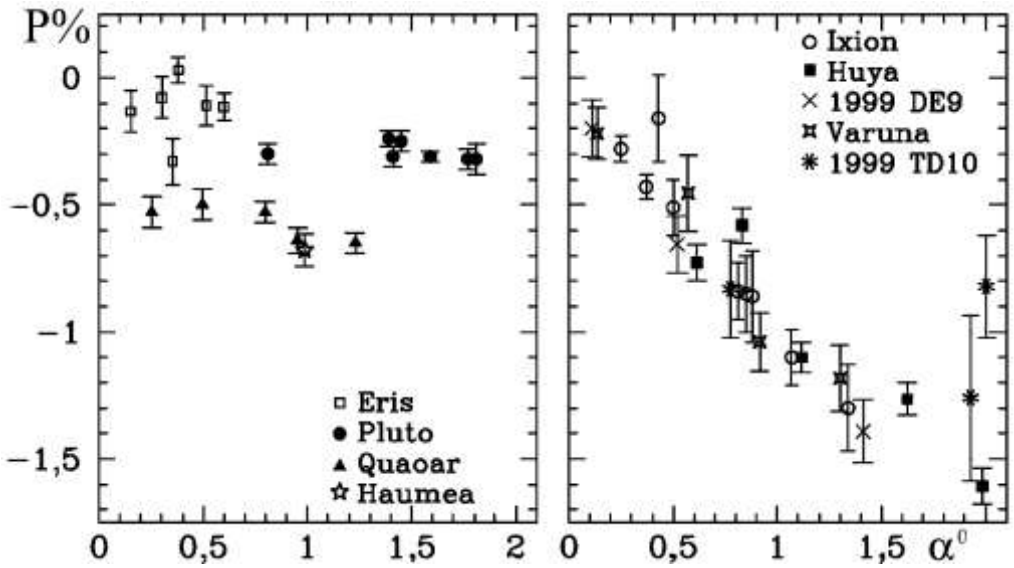

Fig. 26. Phase dependence of linear polarization of four dwarf planets and five TNOs [19].

Thus, the surfaces of atmosphereless planetary bodies changed over time due to volcanic and tectonic processes, bombardment by other cosmic bodies, under the influence of hard radiation from the central star, etc. This caused the formation of a rather complex relief with the appearance of craters of various sizes and microrelief on its individual details. Surface layers with microrelief are called rough, or porous.

The optical properties of the surface layers also changed under the influence of hard radiation from the Sun. This is confirmed by many laboratory studies. After all, bombardment of solid SiO_2 with γ – rays leads to a decrease in its reflectivity [68]. And when bombarding solid surfaces with a proton beam with an energy of 60 keV, their polarization properties also changed. Moreover, not only the maximum value of their degree of polarization Pmax changed, but also its spectral characteristics changed, and the reflectivity of the irradiated surfaces decreased several times.

Conclusions to Section 3.

A brief summary of the results of the study of atmosphereless celestial bodies allows us to draw the following generalizing conclusions.

1. Large bodies of the Solar System are divided into classical planets (Mercury, Venus, Earth, Mars, Jupiter, Saturn, Uranus and Neptune), dwarf planets (Ceres, Pluto, some other Kuiper belt bodies), small planets (asteroids) and comets, their satellites and rings.

2. As of mid-2012, more than 560,000 asteroids had been discovered; half of them had precise orbits and official numbers assigned to them; 15,615 of them had received proper names by September 6, 2011. Despite such a large number, their total mass was estimated to be only $\sim 10^{-3}$ Earth masses.

3. Satellites have also been discovered around some of the dwarf planets and asteroids; some of them are multiple bodies consisting of 2 to 5 bodies. Among these bodies, only a dozen have a diameter exceeding 1,000 km; several hundred asteroid bodies have a diameter of more than 100 km; the bulk of asteroid bodies range in size from a few tens of kilometers to 30 m or less.

4. Large bodies (with diameters of more than 100 km) usually have a close to spherical shape, small ones are fragments of arbitrary shape.

5. According to the spectral features of the surface of the bodies of the Solar System, they are divided into predominantly ice, mineral, or mixed surface types. Their albedo varies from a few units to 80-99%.

6. The surface layers of atmosphereless bodies are usually heavily cratered, and the craters themselves are caused by meteorite bombardment and active volcanism. The so-called ice bodies are an exception, the saturation of the surface layers with craters of which is insignificant. The surface layers are characterized by a complex relief in the form of mountain ranges, cracks, cliffs, etc. The surface layers of many bodies of the Solar System are characterized by optically inhomogeneous details, the photometric contrasts of which change with wavelength.

7. The above-mentioned diversity of the surface shape of the bodies of the Solar System is manifested in the rotation-induced light curves, and the optical heterogeneity of their surface is also manifested in the change in the degree of polarization. The results of such remote studies are used to determine the rotation period, the orientation of the rotation axis in space, to reconstruct the structure of the surface layer and search for satellites around them.

8. Almost all atmosphereless celestial bodies have a clearly pronounced opposition effect, i.e. a nonlinear increase in brightness when approaching the value of the solar phase angle $\alpha=0°$. Some bodies also have polarization opposition effects, which are manifested in a very narrow polarization peak at $\alpha\approx0.5°$. This is attributed to the optically coherent mechanism.

There is strong evidence that in this peak the orientation of the polarization plane corresponds to the value $\psi \sim 45°$. It has been established that for some asteroids the position of the polarization plane is within the range $0° < \psi < 90°$, or $90° < \psi < 180°$; the change in the value of ψ by 90° does not occur by a jump at the inversion point, but by a smooth rotation within certain limits $\Delta\psi$.

4. Details about the discovery and new information about the now dwarf planet Pluto

Thanks to the prediction made on the basis of the deviation of the apparent motion of Uranus from the calculated position in the orbit, in 1846 it was possible to discover the eighth planet in the Solar System – Neptune [105, 193]. This prompted astronomers to search for new planetary bodies [200, 204] in this way, because even after accurately accounting for the perturbations caused by the motion of Neptune in its orbit, the deviations in the motion of Uranus, although significantly reduced, still remained noticeable. In 1848, B. Peirce drew attention to this.

Several astronomers, including P. Lowell and W. Pickering, began calculations to predict new planetary bodies, based on the deviations in the motion of cometary bodies known at that time. P. Lovell (Fig. 27) did a tremendous job calculating the orbit of a new planet, which he called "Planet X", based on observations of deviations in the motion of the planet Uranus.

Fig. 27. Percival Lovell [213].

He began his search in 1905 at his own observatory. But in 1916, P. Lovell became disappointed in his research and stopped searching. He died soon after. But P. Lovell bequeathed all his savings to the development of his observatory. However, continuing the search was prevented by a long lawsuit with the scientist's widow, who tried to

recover the money he had bequeathed to the now well-known observatory. It was possible to resume full-fledged work only in 1929. An astrograph with an aperture of 32.5 cm was ordered specifically to continue the search for a new planetary body. Photographic images taken with this device covered an area of the sky (12×14)°; with an exposure of one hour, the maximum stellar magnitude reached 17m. In January 1929, amateur astronomer Clyde Tombaugh was invited to the observatory specifically to work with this equipment (Fig. 28).

Fig. 28. Clyde Tombaugh with a homemade telescope [213].

After the final adjustment of the telescope in April, he began photographing the starry sky. And although Pluto was already on the tenth photographic image, it remained unnoticed for some time. And only in September of the same year was it possible to establish a method for searching for objects moving across the sky. It consisted in three times photographing sections of the sky at a point opposite the Sun with an interval of several days. Then these photographic plates were compared on a blink comparator, and objects were searched for that during the time between the obtained images shifted relative to the fixed stars.

Viewing the obtained images required a lot of time due to the huge number of stars. Therefore, only on February 18, 1930, K. Tombaugh on the plates obtained on January 23 and 29 discovered an object that was moving at a very low speed. This fact

proved that this celestial body was located beyond the orbit of the most distant planet at that time – Neptune. This object was then in the constellation Gemini and had a magnitude of 15m. This was 2m weaker than previously expected according to calculations.

13.03.1930, on the 75th anniversary of the birth of P. Lovell and on the 149th anniversary of the discovery of the planet Uranus, the director of the Lovell Observatory V. Slipher announced the discovery of the ninth planet in the Solar System [195, 197, 212]. It was literally stated as follows: "Systematic long-term searches, supplementing Lovell's research on the trans-Neptunian planet, led to the discovery of an object that for seven weeks had a speed of movement and a trajectory consistent with the data of a trans-Neptunian body" [55].

For almost half a century after this point, estimates of Pluto's mass were revised downwards [71]. It was only in 1978 that the discovery of the moon Charon [239, 241] made it possible to measure [57] its mass with a fairly high accuracy for the first time. It became clear then that such a small value, about 0.002 of the mass of our Earth, was too small to cause a noticeable perturbation in the orbit of the planet Uranus. Therefore, the search for another "Planet X" was launched, which was still unsuccessful [203, 206].

Thanks to the flyby of the spacecraft (SC) "Voyager-2" in 1989, it was possible to clarify the mass of this planet. It turned out to be almost half a percent less than that which was previously considered correct. Therefore, calculations carried out in 1993 by the American astronomer Erland Miles Standish using these updated data practically nullified the possible gravitational influence of Neptune on the motion of Uranus. In this regard, the urgent need for the existence of a "Planet X" disappeared [187].

According to tradition, the right to name the new celestial body belonged to the Lovell Observatory. P. Lovell's widow – Constance, suggested such names as "Zeus", "Percival" and "Constantia". However, all these options were ignored. Three such proposals were received from the observatory workers: "Minerva", "Cronus" and "Pluto". As a result of the voting, almost all the votes were given to the last option [193]. The proposal for this name was first published by V. Slipher on 1.05.1930 [165].

And on 25.05.1930, the proposal was publicly announced and submitted for consideration to the American and London Royal Astronomical Societies. Both of these organizations unanimously approved it. According to Slipher's later reports, the name "Pluto" was first suggested to him on 14.03.1930 by an eleven-year-old schoolgirl from Oxford – Venice Burney. She was interested in astronomy and classical mythology. The astronomical symbol for Pluto is a nomogram of the Latin letters P and L. They are the first letters in its name and the initials of the founder of the observatory, Percival Lovell.

Since the discovery of Pluto in 1930, there have been many facts indicating that it is significantly different from the rest of the planets [67, 132, 133] in the Solar System. Indeed, unlike the practically circular orbits of all other planets, it revolves around the Sun in a very elongated orbit with an eccentricity of 0.25. And the inclination of its orbit to the ecliptic plane of 17° is quite significant, compared to no more than 7° for the orbits of all other planets. But until a certain time, such differences were not considered critical.

Indeed, in 1978, the satellite Charon was discovered around Pluto, observations of Pluto's coverage of stars allowed us to detect a thin atmosphere around it [212], the main component of which was molecular nitrogen. And the surface layer of Pluto mainly consisted [207, 210] of frozen molecular nitrogen and methane, and mountain ranges of frozen water [211, 242]. Since Pluto is quite small and it is very far from the Sun, it was practically impossible to learn more about it from Earth. Even with the Hubble Space Telescope, images of its surface were obtained only with very low resolution. Although it was possible to notice several dark and bright spots on the surface.

Why did Pluto cease to be a planet and become a dwarf planet?

In the middle of the 20th century, it was suggested that there was “construction debris” beyond Neptune’s orbit from the formation of the Solar System. But only in 1992 was the first trans-Neptunian asteroid actually discovered. After that, similar discoveries followed one after another. And in the trans-Neptunian space, which is now called the Kuiper Belt, an increasing number of rather large bodies began to be found.

That is, Pluto ceased to be a unique object in its environment. And this significantly distinguished it from other planets in the Solar System.

In addition, in 2005, another trans-Neptunian object comparable in size to Pluto was discovered – Eris [200]. Therefore, the question arose, what exactly should be called a planet? The International Astronomical Union, at its General Assembly in 2006, which was held in Prague, approved a list of features according to which a planet should be distinguished from a non-planet. And one of these features was the requirement that a real planet “clear” the area in its orbit of other bodies. Pluto could not cope with this task [166] and on August 24, 2006 it became a dwarf planet.

On January 19, 2006, a new, cosmic stage in the study of Pluto began. It was then that the New Horizons space probe was launched to it. After launching from Earth, in early 2007, the spacecraft performed a so-called gravitational maneuver near Jupiter [193, 194, 203, 204, 212]; this gave it additional acceleration. Planning such a maneuver allowed the probe to significantly save on fuel and increase the mass of the installed scientific equipment. During the gravitational maneuver, the operation of all seven scientific instruments of the probe was checked. Some of them were intended to obtain images in different wavelength ranges, others studied the properties of the surrounding plasma. On board the space probe were cameras, spectrometers, a device for illuminating Pluto's rarefied atmosphere using radio waves. The data obtained by them made it possible to study the global geology and morphology of the surfaces of Pluto [203] and Charon, to make their maps and to study Pluto's atmosphere. The maximum approach to Pluto occurred on July 14, 2015, when the New Horizons probe flew only 12,472 km from the surface (Fig. 29). Scientific observations of Pluto began 5 months before this moment and continued for at least a month after the approach. Within a few hours, the scientific instruments of the apparatus conducted a significant number of the most diverse observations and accumulated a huge amount of information. All the information was transmitted to Earth only at the end of 2016. The shape of Pluto turned out to be almost perfectly spherical, quite unexpectedly.

Fig. 29. Image of Pluto taken by New Horizons on July 14, 2015 from a distance of 35,445 kilometers (https://en.wikipedia.org/wiki/Pluto#/media/File:Pluto_in_True_Color_-_High-Res.jpg).

Fig. 30. The Sputnik Plain is covered with geologically young nitrogen ice “cells” formed by “dry” convection (https://en.wikipedia.org/wiki/Pluto#/media/File:Pluto%E2%80%99s_Heart_-_Like_a_Cosmic_Lava_Lamp.jpg).

Quite unexpected was the finding of the most diverse landforms on Pluto. Especially unexpected was the finding of extensive flat areas on which not a single impact crater was found. And the vast plain turned out to be divided into peculiar cells, which indicated the existence of possible convective movements in the ice layer (Fig. 30). All this indicated the relative youth of these areas of the surface. This plastic ice could consist of frozen molecular nitrogen and carbon monoxide. However, for such processes to occur, a sufficiently powerful source of internal energy is required. Despite the enormous thinness of Pluto's atmosphere [195], it was found to be capable of supporting a haze extending to a height of almost 150 km from the surface (Fig. 31). All these facts have raised a huge number of questions for researchers that will need to be answered in the future.

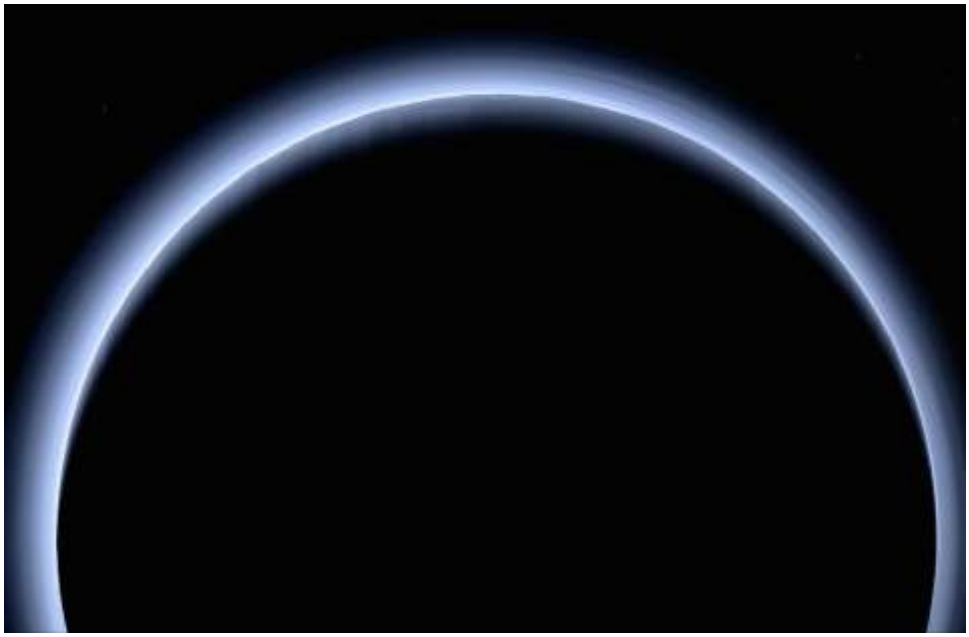

Fig. 31. A near-true-color image taken by the New Horizons spacecraft after its flyby. Numerous layers of blue haze are visible in Pluto's atmosphere. (https://en.wikipedia.org/wiki/Pluto#/media/File:PIA21590_%E2%80%93_Blue_Rays,_New_Horizons'_High-Res_Farewell_to_Pluto.jpg).

5. Features of Pluto's rotation around its axis and around the Sun.

It is known that the orbits of the large planets [193, 194, 197, 235, 237, 239, 240, 242] of the Solar System (except Mercury) are almost circular and close to the plane of the ecliptic. And as follows from the data in Table 4, the orbit of the dwarf planet [166, 199 211] Pluto (Fig. 32) differs significantly from them.

Table 4. Main characteristics of Pluto and its orbit.

Orbital characteristics	
Semi-major axis	5906.38 million km 39.482 AU
Perihelion	4436.82 million km 29.658 AU
Aphelion	7375.93 million km 49.305 AU
Eccentricity	0.249
Orbital period	247.94 Earth years
Orbital period	14179 Pluto solar days
Mean orbital velocity	4.67 km/s
Mean anomaly	14.86°
Orbital inclination to the ecliptic	17.14°
Orbital inclination to the Sun's equator	11.88°
Longitude of ascending node	110.303°
Longitude of pericenter	224.067°
Time of last pericenter	5 September 1989
Pericenter argument	113.763°
Physical characteristics	
Mean radius	1187±4 km 0.186 of Earth
Oblateness	<1%
Surface area	17.7 million km^2
Mass	(1.303 ± 0.003)×1022 kg
Mean density	0.0022 mass of the Earth
Surface acceleration due to gravity	1.860 ± 0.013 g/cm^3
Second cosmic velocity	0.617 m/s^2 (0.063 g)
Rotation period	1,210 km/s
Equatorial rotational velocity	-6.387 p
Axis inclination to orbit	122.53°
Right elevation of the north pole	132.99°
North pole inclination	−6.16°
Bond albedo	0.4-0.6
Geometric albedo	0.5-0.7
Surface temperature	33-55 K
Apparent magnitude	>13.65 (average 15.1)

Apparent angular size	0.06-0.11"
Axis inclination to orbit	122.53°
Atmosphere	
Surface pressure	1 Pa (as of 2015)
Altitude scale	about 60 km
Composition	nitrogen with admixtures of methane and carbon monoxide

It turned out to be more than 17° inclined to the ecliptic and significantly elongated. The average distance between Pluto and the Sun is 39.53 AU (5.913 billion km). But due to the large value of the eccentricity of the orbit (0.249), the distance to the Sun varies from 29.66 AU at perihelion to almost 49.31 AU at aphelion (4.437 – 7.376 billion km). The intensity of illumination differs by a factor of 2.8. This leads to a change in the temperature on its surface from 33K to almost 60K [208, 212]. The period of Pluto's rotation around the Sun is about 248 years. It last passed the place of perihelion on September 5, 1989, and is currently beginning to move away from the Sun [122]. Pluto's motion along its orbit is quite chaotic and is described by highly nonlinear equations. Therefore, it can only be predicted a few million years ahead or a few million years ahead. And this can only be noticed after fairly long observations of it. The typical time for the development of such changes for Pluto is about 10–20 million years [122]. If observations are made over shorter periods of time, its movements will appear to be almost regularly periodic along an elliptical orbit. Although in reality, Pluto's orbit shifts slightly with each revolution, and over time it changes significantly from the initial movements. Therefore, predicting Pluto's movements for more distant moments in time is quite difficult [179, 249]. Pluto is in a 3:2 orbital resonance with the giant planet [132, 194, 206] Neptune. That is, Pluto periodically approaches Neptune [243]. In each such cycle, when Pluto passes through perihelion, Neptune is 50° behind Pluto; and when Pluto passes perihelion a second time, Neptune will have already made one and a half revolutions around the Sun and will be at about the same distance, but in front of Pluto. And when Neptune and Pluto are on the same line with the Sun and on the same side of it, Pluto will be at aphelion.

Thus, for part of its orbit, Pluto is even closer to the Sun [204, 208, 211, 212] than Neptune (Fig. 32). The last time this happened was from 02/07/1979 to 02/11/1999.

Calculations have shown that before that Pluto occupied the same position for 14 years from 11.07.1735 to 15.09.1749. Due to the rather large value of the inclination of Pluto's orbit to the plane of the ecliptic, it does not intersect with the orbit of Neptune. After all, passing the perihelion point, Pluto is at a distance of 10 AU above the plane of the ecliptic. For this reason, Pluto cannot approach the planet Neptune closer than 17 AU. But Pluto can approach Uranus by almost 11 AU. [179, 249]. Such an orbital resonance between Neptune and Pluto is very stable and persists for millions of years [243, 248]. It is believed that Pluto acquired a resonance with Neptune over billions of years of numerous approaches, and this changed its orbit.

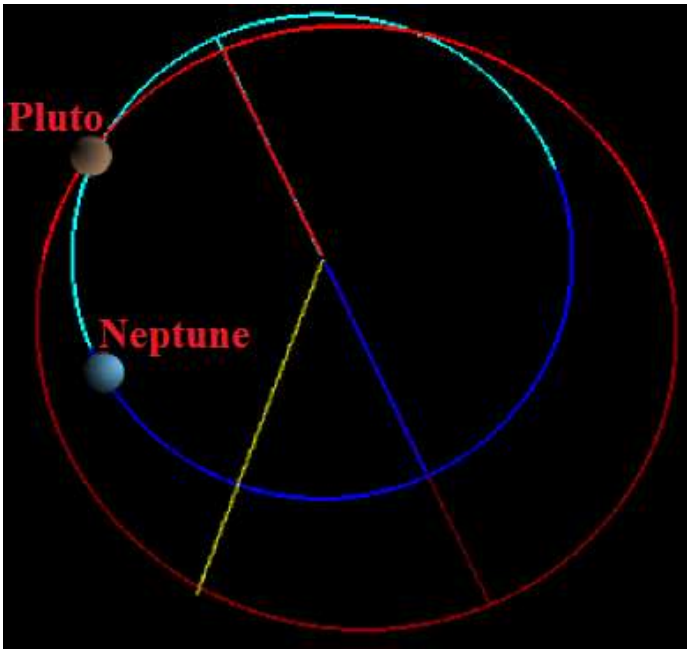

Fig. 32. Scheme of the intersection of the orbits of Pluto and Neptune (https://upload.wikimedia.org/wikipedia/commons/a/a0/TheKuiperBelt_Orbits_Pluto_Polar.svg).

However, it turned out that in addition to the 3:2 orbital resonance, several other resonances and influences [186, 202, 204, 207] are of great importance, which are also reflected in certain features of their relative motion and additionally stabilize the features of Pluto's orbit.

The argument of the perihelion of Pluto is close to 90° [248]. It is this value that provides a significant distance both to the plane of the ecliptic and to the nearby giant planets during the passage of perihelion. All this together allows avoiding the rapprochement of Pluto with Neptune. This is a direct consequence of the so-called Kozai effect [243], which compares the values of the eccentricity and inclination of Pluto's orbit with respect to a more massive body, which, in this case, is Neptune.

The moments when the angular difference between the inclination of Pluto's perihelion and Neptune's orbit is the smallest occur approximately every 10,000 years [7]. And the longitudes of the ascending nodes for the orbits of these two planetary bodies (i.e., the points at which they cross the plane of the ecliptic) are in resonance with the mentioned oscillations. And if these two longitudes coincide, then the point of perihelion of Pluto's orbit will make an angle of 90° with the ecliptic (Fig. 33).

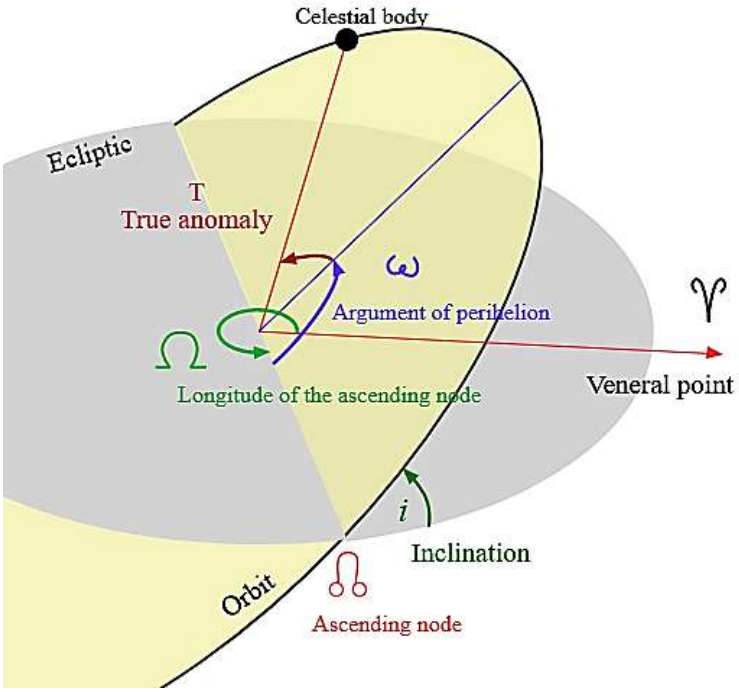

Fig. 33. Kepler orbital elements relative to the main plane (https://upload.wikimedia.org/wikipedia/commons/0/01/Orbit.svg).

At such times, Pluto will be in a 1:1 superresonance above the plane of Neptune's orbit at its highest and furthest away from it [30]. A full cycle is completed in about 20 thousand years [7, 122]. The period of Pluto's rotation around its own axis is 6.387

Earth days. The same value is equal to the period of rotation of Charon around Pluto and around its axis. For this reason, Pluto and Charon always face the same way to each other. They are the largest bodies in the Solar System with mutual synchronous rotation [57]. This phenomenon has been used as a natural starting point for longitudes. That is, the zero meridian on Pluto passes through the center of the hemisphere facing Charon [14, 16].

The Pluto-Charon system [57] is distinguished by the fact that, due to the large mass of the satellite Charon, their center of mass is located outside the limits for both bodies (Fig. 34). Therefore, they are sometimes called a double planet [157].

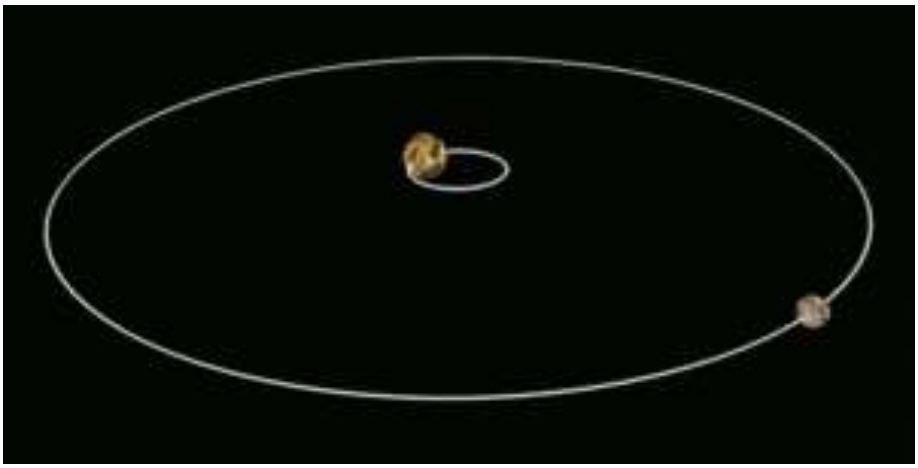

Fig. 34. Rotation of Pluto and Charon around a common center of mass (https://my.science.ua/wp-content/uploads/2016/05/898-3.gif).

The axis of rotation for Pluto is oriented relative to the orbital plane in almost the same way as for Uranus. Its inclination exceeds 122°. Therefore, Pluto also practically “lies on its side” and rotates around its axis in the opposite direction from most planets. The last equinox for Pluto took place on December 16, 1987 [5]. And the solstice will occur in the late 2020s [60]. Thus, the equinox on Pluto now almost coincides with the moment of passing the perihelion of the orbit.

6. Physical parameters of Pluto based on remote sensing results and the earliest data from the flight path

Pluto is the most famous minor planet in the Solar System and the largest trans-Neptunian object to date [199, 200, 203]. It was the first Kuiper Belt object discovered [165, 173, 213]. It is currently the ninth largest and tenth most massive celestial body orbiting the Sun (excluding several planetary satellites [237, 239-242,254]). Pluto's surface is highly heterogeneous. Studies have shown that it is the second most contrasted body in the Solar System after Iapetus [30]. The albedo of individual areas on its surface varies from 10% to almost 70% [173]. This heterogeneity leads to periodic changes in Pluto's brightness as it rotates, sometimes reaching 0.35^{m}. Also, its spectrum changes significantly as Pluto rotates. This allowed us to obtain certain data on the distribution of various substances on its surface from ground-based observations [62, 86, 88, 89].

The considerable distances to Pluto and the capabilities of ground-based telescopes did not allow us to obtain high-quality images of its surface. And only the largest albedo details are visible in the images obtained by the Hubble Space Telescope [86]. The very first images of Pluto's surface were albedo maps made during observations of its eclipses by the satellite Charon, which took place in 1984-1990 (Fig. 35). The principle of their construction is based on the fact that the eclipse of a brighter area of the surface causes greater changes in brightness than when the eclipse of a darker area. Computer processing of such observational data on changes in brightness at the moments of eclipses makes it possible to create an albedo map of the hemisphere of Pluto facing the satellite Charon.

Only the largest albedo details are also visible on such maps. In particular, a wide, rather dark band was visible south of Pluto's equator [173]. Pluto's average magnitude is about 15.1^{m}. And only at perihelion can it reach 13.65^{m}. Spectral and polarimetric observations [132, 134, 143], performed by the employees of the Main Astronomical Observatory of the National Academy of Sciences of Ukraine at the Sanglok

Observatory in May 1988 [2] (i.e. 1 year and 4 months before Pluto's passage through the perihelion point) gave an average visual magnitude of 13.99^m.

In the sky, Pluto is a light brown point with an angular diameter of up to 0.11″. The color index B−V varies within $0.70 \div 0.98^m$. Moreover, in 2000, the color of Pluto's surface became less saturated with a color index of $0.70 \div 0.87^m$ [2, 3, 28]. One of the reasons for such changes could be the decrease in the strength of its small atmosphere [111, 112, 211]. Pluto is currently in a stable orbital resonance with Neptune, and therefore their collision is impossible.

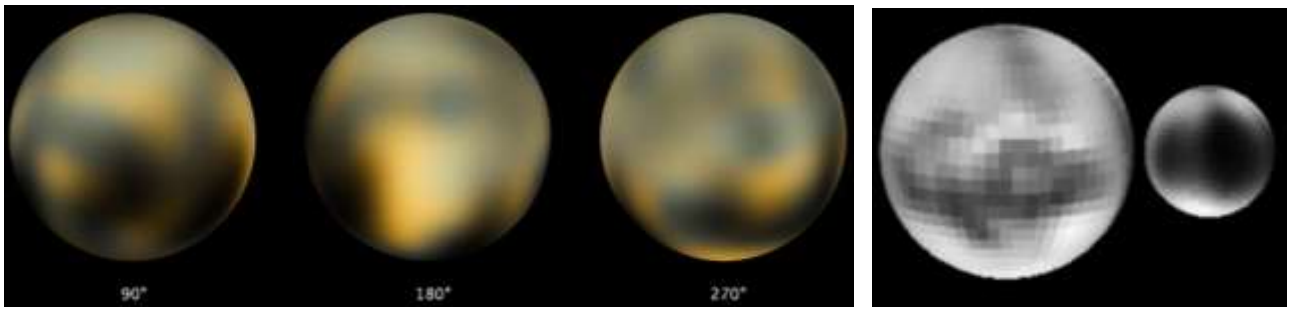

Fig. 35. On the left – images of Pluto, built in 2010 from images of the Hubble Space Telescope (2002-2003) (https://upload.wikimedia.org/wikipedia/commons/0/0b/Pluto-map-hs-2010-06-a-faces.jpg). On the right – albedo maps of Pluto and Charon, compiled in 1992 from observations of mutual eclipses in 1984-1990 (https://upload.wikimedia.org/wikipedia/commons/8/85/Pluto_%26_Charon_%28Sub-earth_10_degrees_latitude%2C_10_degrees_longitude%29.png).

From the day of its discovery in 1930 and until 2006 – Pluto was considered the ninth planet. However, in the late 20th and early 21st centuries, other rather massive objects were discovered in the outer part of the Solar System [200]. In this regard, in 2006, the International Astronomical Union had to adopt a formal definition for the term “planet” for the first time. After that, Pluto ceased to meet the accepted definition and, together with Eris and Ceres, it was assigned to a new category of bodies in the Solar System: dwarf planets. Also, at that time, under the number 134340, Pluto was also included in the list of so-called minor planets. Although some researchers continue

to believe that Pluto should be restored to the status of a planet. The average density of Pluto is 1.860±0.013 g/cm^3 [143]. Therefore, most likely, its interior consists of 50÷70% of rock and 30÷50% – mainly of water ice in the so-called modifications I, II, III, V and VI [96, 112]. Since the heat obtained during the decay of various radioactive elements would be enough to separate ice from rock, Pluto's interior should be differentiated. In this case, the denser rocky core should be surrounded by a mantle of ice, the thickness of which can be up to 300 km [112]. It is possible that the heat received could have been sufficient to form a vast ocean of liquid water beneath the surface [181]. When the liquid water froze there, the traces of ice stretching and compressing that are now observed on Pluto's surface could have appeared: ridges and ledges [111]. Spectral observational data have shown that water ice is also present on Pluto's surface. Although most of the surface is covered with other, more volatile ices [60], and most of it – over 95% – is nitrogen ice. In addition, spectral observations have also indicated the presence of frozen methane (according to various estimates, from 1.5 [88] to 3% [96]), carbon monoxide (from 0.01 [62] to 0.5% [86]), and also – in small quantities – some other compounds, which may well be formed from methane and nitrogen under the influence of hard radiation. These, in particular, may be more complex hydrocarbons and nitrites [62, 91], as well as the so-called tholins [14], which give the surfaces of Pluto and some other bodies located far from the Sun a brown color (Fig. 36).

Fig. 36. 80-kilometer-wide image taken during New Horizons' closest approach to Pluto, with a resolution of about 80 meters per pixel, near Sputnik Planum (https://photojournal.jpl.nasa.gov/catalog/PIA20213).

Among the above substances, nitrogen, carbon monoxide and, to a lesser extent, methane – are distinguished by significant volatility for Pluto's conditions. And therefore they are capable of moving on its surface [198, 206, 208, 212]. Images of Pluto's surface with excellent resolution were only obtained in 2015 using equipment on the New Horizons spacecraft.

The images obtained at that time revealed a large, very bright region on Pluto's surface (Fig. 37). It had a fairly smooth surface, most likely made of water ice.

Fig. 37. The image shows a part of the Sputnik Planitia plain approximately 400 kilometers across, taken by the multispectral camera in the visible range of the spectrum from the New Horizons spacecraft, 07/14/2015. (https://en.wikipedia.org/wiki/File:Pluto%E2%80%99s_Heart_-_Like_a_Cosmic_Lava_Lamp.jpg).

Also, many other features have been recorded on the surface of Pluto [89]. The most noticeable geological feature on the visible part of Pluto's surface [143] is the Sputnik Planitia plain. This depression, with dimensions of more than 1000 km, occupies about 5% of its entire surface. Most likely, it is a heavily destroyed impact crater. It is now filled with frozen gases (mainly nitrogen). This plain is crossed by many furrows, which divide it into separate cells with sizes of tens of kilometers. They

are explained by the result of convection in the “streams” of nitrogen ice. And water ice at temperatures on the surface of Pluto is very strong. And studies show that, most likely, it is from it that the surrounding mountains of darker color with heights of up to 5 km are composed. It is lighter than nitrogen ice and can form icebergs floating in it. It is likely that such icebergs are the small dark elevations between the cells in Fig. 36, 37. It is believed that such blocks of water ice can float under the influence of convection across the entire surface of Pluto. And the somewhat larger, dark mountain ranges located at the edges of the light region can only slightly shift and rotate [203]. Computer simulations of these effects have shown that the rate of ice movement across the surface of the plains on Pluto is measured at only a few centimeters per Earth year [143].

7. The history of the discovery and study of Pluto's atmosphere

As early as 1846, the eighth planet of the Solar System, Neptune, was discovered based on the deviations of the observed orbit of the giant planet [193, 194] Uranus from the calculated values. However, even after taking into account the observed perturbations caused by the presence of this giant planet [205, 206, 237, 242], the deviations in the orbit of Uranus, although significantly reduced, still remained noticeable. Therefore, some astronomers began to search for new planetary bodies based on the analysis of deviations in the motion of known orbits of comets [97]. The most notable in this direction were the works of Lowell P. [211]. In 1905, he began searching for the next planet at his own observatory. However, he was unable to find the planet, and in 1916, Lowell P. stopped the next stage of the search and soon passed away. Later, when Pluto was already discovered, it was still found on a pair of photographic plates taken by Lowell in 1915 [59].

It was only in 1929 that the search for the planet at this observatory was resumed. An astrograph with an aperture of 32.5 cm was made especially for these observations. With its help, pictures of sky areas with a size of 12×14° with a maximum magnitude of 17m were obtained with exposures of one hour. An amateur astronomer, Tombaugh K., was invited to work with this device, who, after setting up the telescope in April 1929, began photographing the starry sky [186]. Comparison on a blink comparator of two photographic plates taken with an interval of several nights, made it possible to find celestial objects that had shifted slightly during the specified time. And already on 18.02.1930, on the images of the constellation Gemini taken on 23 and 29 January, Tombaugh managed to detect a moving object [200, 213]. Its speed indicated the location of this celestial body 15m beyond the orbit of Neptune. Moreover, it was 2m weaker than Lowell had expected at the time [186]. On 13.03.1930, on the day of Lowell's 75th birthday and on the 149th anniversary of the discovery of Uranus, the director of the Lowell Observatory, W. Slipher, announced the discovery of the 9th planet in the Solar System. It was named Pluto. And then the same name was approved by the American and London Royal Astronomical Societies.

Over the next almost 4 decades, estimates of the mass of Pluto were revised towards its decrease [74]. And only in 1978, the discovery of the satellite Charon allowed it to be measured for the first time [4]. And then it became clear that a mass of 0.002 Earth masses is too small to noticeably perturb the orbit of the planet Uranus. Signs of the presence of an atmosphere on Pluto [57] were searched for in its spectrum by J. Kuiper in the 1940s, but without success [252]. In the 1970s, some astronomers suggested the presence of a dense atmosphere and even oceans of neon there. After all, this gas was then considered the only widespread gas in the entire Solar System that would not freeze and disperse into space under Pluto's conditions. However, this hypothesis was based on a significantly overestimated estimate of Pluto's mass. After all, in those years, there was no observational data on the characteristics of its atmosphere and chemical composition [252]. Only in 1976 did the first significant, albeit rather indirect, signs of the existence of an atmosphere on Pluto appear. According to the results of infrared photometry, which was obtained using a 4-meter telescope, methane ice was detected on its surface [62]. At the temperature existing on the surface of Pluto, it was this ice [203, 208] that should have noticeably evaporated.

However, it was possible to clearly verify the presence of a noticeable atmosphere only through observations of the phenomenon of Pluto covering stars. If a star is covered by an object without an atmosphere, then the light from it will disappear quite sharply. But when Pluto covers the star, the light disappears gradually. This effect of weakening the light from the star is explained by the fact that it is caused not so much by absorption in the atmosphere itself or scattering in it, but by refraction [73]. Pluto's atmosphere was first detected in 1985 during observations of its occultation of a star [37].

The existence of an atmosphere around Pluto was finally confirmed by occultation observations in 1988. In addition to photometric observations of Pluto's occultation of stars [10], in the 1980s Pluto's atmosphere was also studied using spectral methods [114]. Thus, the very first observational evidence of the existence of an atmosphere was obtained on August 19, 1985 by Noah Brosch and Haim Mendelson at Wise Observatory in Israel [38]. However, the quality of these data was low due to

unfavorable observation conditions. Moreover, their detailed description was published only 10 years later. More successful observations of Pluto's occultation of stars from as many as 8 different points were made on June 9, 1988. It was they who finally confirmed the existence of an atmosphere around Pluto. The best results were obtained at the Kuiper Airborne Observatory.

Thanks to these studies, it was possible to determine the so-called height scale in Pluto's atmosphere. And from its value, the ratio of the temperature near the surface to the average molecular mass of the atmospheric components was calculated. However, it was not possible to calculate the values of the temperature and pressure near the surface at that time due to the lack of observational data on the chemical composition of the atmosphere itself. There was also a huge uncertainty in the values of Pluto's size and mass of this planetary body [74]. The question of chemical composition was resolved in 1992 thanks to the study of the infrared spectrum of Pluto on the 3.8-meter United Kingdom Infrared Telescope.

It turned out that its surface is covered mostly with nitrogen ice. Since it is much more volatile than methane ice, this meant that nitrogen also predominates in Pluto's atmosphere. But gaseous nitrogen could not be registered in the planet's spectrum at that time. In addition, an admixture of frozen carbon monoxide was also discovered based on these same observations [143]. In the same year, the 3-meter infrared telescope IRTF was the first to reliably detect methane lines [198, 236] in the gaseous state [255]. The surface temperature was best estimated from observations of thermal radiation from Pluto. The earliest values were calculated in 1987 from observations from the orbital observatory IRAS. They turned out to be close to 55-60 K. While the results obtained during subsequent observations gave only 30-40 K [252].

In 2005, the Submillimeter Array, which consisted of eight six-meter diameter radio telescopes, was able to measure thermal radiation separately from Pluto and Charon. The average temperature on Pluto's surface was found to be 42±4 K. Other data obtained showed that the temperature on different parts of its surface varied quite significantly, and could vary from 40 K to almost 60 K. After 1988, Pluto's occultation of stars was observed by teams from the Paris Observatory [162] and the Michigan

Institute of Technology [73] on July 20 and August 21, 2002. According to their observations, the atmospheric pressure was almost twice as high as it was in 1988. The next occultation of stars was observed on June 12, 2006 [8]; and then they began to occur more and more often [34].

Processing of many of these observational data showed that the pressure in Pluto's atmosphere continued to increase. Of particular interest was the occultation of a fairly bright star, which was almost 10 times brighter than Pluto itself [151]. After all, it took place on June 30, 2015, just 2 weeks before the New Horizons spacecraft flew by the then dwarf [199] planet Pluto. On July 14, 2015, the New Horizons spacecraft first examined Pluto’s atmosphere up close. When observing at a phase angle of 147° (Fig. 38), the spacecraft’s instruments were able to detect up to 20 separate layers in Pluto’s atmosphere.

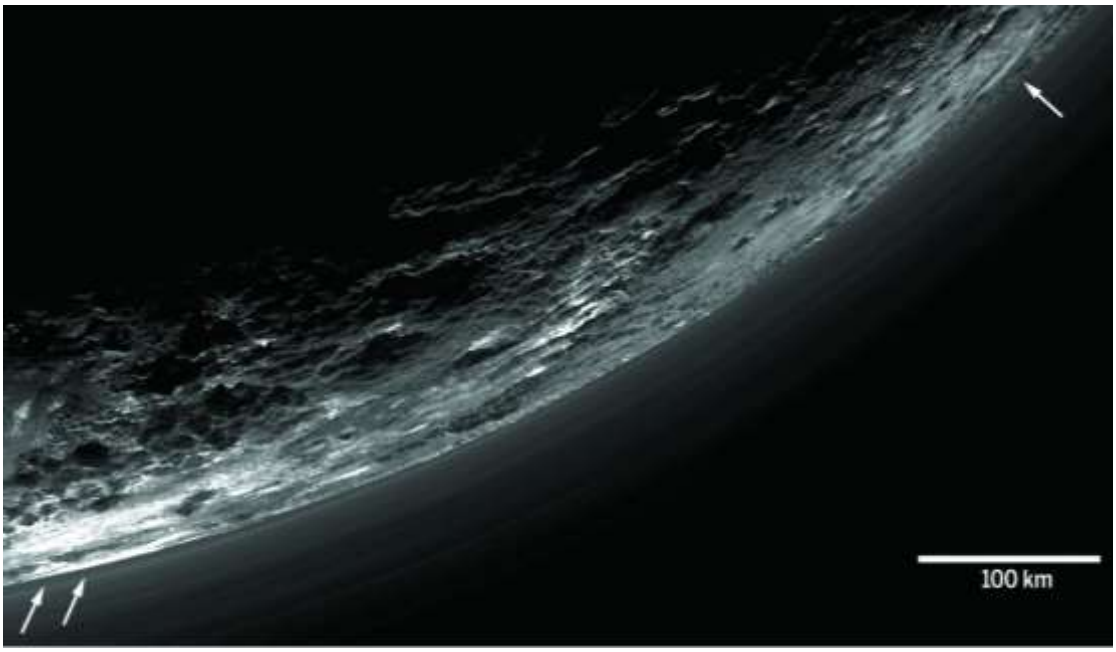

Fig. 38. Image of haze layers above Pluto’s limb (https://www.science.org/cms/10.1126/science.aad8866/asset/a3bb0081-3d24-4701-ad65-f2fceae4196e/assets/graphic/351_aad8866_fa.jpeg).

The image shows that some of the layers extend horizontally for hundreds of kilometers. And others lie not quite horizontally. Some of them may be formed with the participation of aerosols [134, 212]. For example, the white arrows on the left

indicate a layer that was at an altitude of about 5 km above the surface; and then on the right it practically descended to the surface.

The space probe also passed through Pluto’s shadow, recording the absorption of solar radiation by the atmosphere. It also conducted an experiment on the transillumination of the atmosphere with radio waves. In this experiment, waves were emitted from the Earth's surface, and the probe recorded them with its equipment. This was the first direct study of the lower layers of Pluto's atmosphere. In particular, it was the first time that the pressure near the surface of the dwarf planet was reliably measured. Its value turned out to be 1.0–1.1 Pa [85].

8. Updating data on the physical characteristics of the dwarf planet Pluto thanks to the study of the New Horizons probe

Immediately after its discovery, Pluto was considered the same planet X, and attempts were made to calculate its mass based on its influence on the orbits of Uranus and Neptune [55, 187]. Lovell expected the mass of this planet to be 6.6 Earth masses. By the early 1970s, mass estimates had decreased to the mass of Mars. And only the discovery of Charon [188] allowed, using Kepler's third law, to measure the mass of Pluto. It turned out to be only 0.0022 of the mass of the Earth [71]. And the size of Pluto, after several redeterminations, decreased to 2368±8 km. According to the results obtained in 2015 by the New Horizons space probe, the diameter of Pluto was estimated at 2374±8 km. The shape of the planet turned out to be very close to spherical with an oblateness of less than 1%.

Thus, among the objects of the Solar System, it is inferior in size and mass to all the giant planets [67, 193, 194, 197, 198] to all the terrestrial planets and even to some of their satellites [132, 134, 237, 239]. It turned out to be smaller than seven satellites: Ganymede, Titan, Callisto, Io, the Moon, Europa and Triton. But it is 14 times more massive and 2.5 times larger than the largest object of the Main asteroid belt – another dwarf planet Ceres. Thus, among the trans-Neptunian bodies known today, Pluto is the largest body. However, in terms of mass, it is slightly inferior to another dwarf planet [242] Eris from the scattered disk [199]. Like most bodies in the Kuiper belt, Pluto consists mainly of rock and ice. Pluto's orbit has a large eccentricity (0.25) [211, 214]. Therefore, it is quite elongated, and also has a significant inclination to the ecliptic plane (17.1°). Due to this elongated orbit, Pluto approaches the Sun at perihelion by almost 29.6 AU (about 4.4 billion km), and therefore is even closer to the orbit of Neptune; and at aphelion, it is more than 49.3 AU (7.4 billion km). Pluto's magnitude averages 15.1m, and at perihelion it reaches 13.65m. This means that telescopes with an aperture of more than 0.3 m are required for its observations. But even with very large telescopes, Pluto looks like a star-like object, since its angular diameter at such

distances is only 0.06-0.11". Its color is light brown with a B−V color index in the range of 0.70-0.98m.

Pluto's surface is very heterogeneous in contrast. After all, the albedo of different areas on its surface varies from 0.10 to 0.70. Such heterogeneity during rotation around its axis leads to changes in its brightness by almost 40%. Since its spectrum also changes, this allowed ground-based observations [215] to obtain certain conclusions about the distribution of some of the substances [81, 88, 96] on Pluto's surface. However, the distance to Pluto and the capabilities of ground-based telescopes did not allow obtaining satisfactory images of its surface. Even images from the Hubble Space Telescope allowed to distinguish only the largest and most contrasting details [213]. Only in 2015, using the equipment of the New Horizons space probe, it was possible to obtain images with good spatial resolution. It was thanks to the New Horizons probe that it was possible to detect traces of unexpectedly intense and diverse geological activity on Pluto, including relatively recent ones. Based on the concentration of impact craters, the age of some of the areas on its surface is close to 4 billion years; while the age of others often does not exceed several million years. The origin of many of the observed details on the surface of Pluto is explained, for example, by tectonic processes, asteroid impacts, cryovolcanism, surface erosion, movements of fairly large glacial masses, convective processes in the ice layer, condensation and sublimation of gas components, as well as the action of winds. The main bright albedo detail and especially different from other regions on the surface Pluto has a very bright area measuring 1500×1800 km. It is located on the side of the dwarf planet opposite Charon and is well known as Tombaugh Regio. The western part of this bright plain area has a very flat relief and has been called “Sputnik Planitia”. It has a rounded shape with a narrowed protrusion in the southern direction. In terms of its size, it occupies almost 5% of the entire surface area of Pluto (Fig. 39). This depression is filled with frozen gases and has a very young surface. After all, it has practically no impact craters of noticeable sizes. Its surface is also covered with curvilinear grooves that divide it into peculiar “cells.”

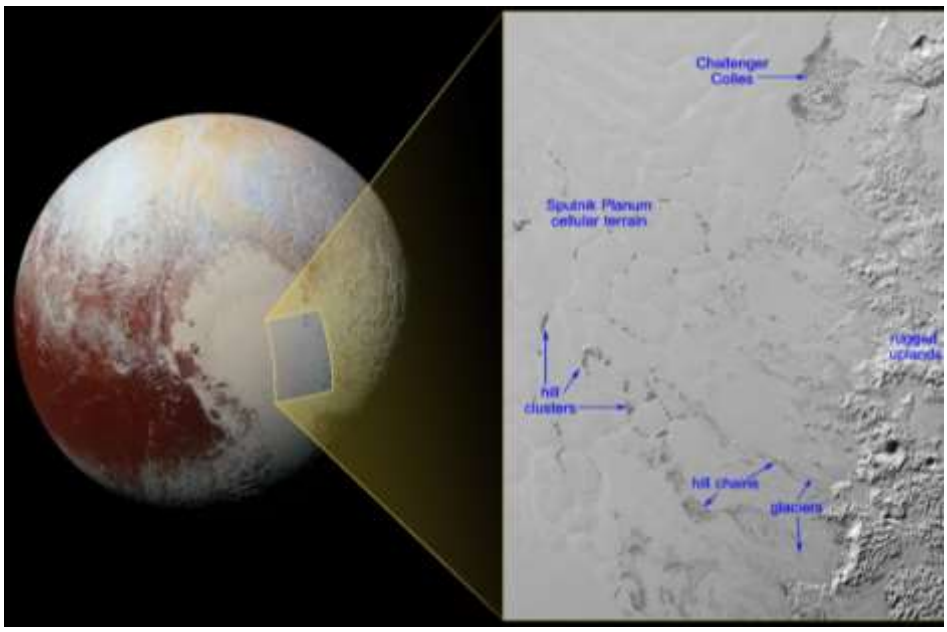

Fig. 39. Nitrogen ice from glaciers on Pluto creates isolated "cells," the edges of which may be dark fragments of water ice. They are an example of Pluto's geological activity (https://www.americaspace.com/wp-content/uploads/2016/02/nh-plutosfloatinghills-context-lables_v3-sml-02-04-16.jpg).

It is believed that the pattern of cells appears due to the slow thermal convection of nitrogen ice dominant on the surface of Pluto. After all, they fill the surface of "Sputnik Planitia." Considerable reservoirs of solid frozen nitrogen are located in some places under the surface at a kilometer depth. There they are heated from the depths of Pluto by insignificant internal heat flows. Later, they become buoyant and rise in fairly large clumps. After cooling for a certain time, they sink down again, renewing cyclic transformations. However, most of the entire surface of Pluto is quite uneven. Although meteorite craters among the many hills and depressions are for some reason not common. The largest of the hills reaches about 260 km in length, and canyons have a tectonic origin with a length of up to 600 km.

Many of the craters found were heavily damaged, sometimes cut by canyons, or filled with ice. Some of the areas on the surface are cut by branched, branching valleys. It is believed that such formations may have been formed by nitrogen glaciers. Also on the surface, quite peculiar relief formations have been found. These include extensive hills covered with small ridges elongated in one direction. The height of such ridges

reaches several hundred meters; the intervals between them are from 5 to 10 km. A possible cause of such formations is considered to be the sublimation of ice under the influence of sunlight and the subsequent freezing of liquefied gases on these hills.

Also found are regions covered with many smaller parallel ridges with distances between them up to 1 km. They are also found in craters and on hills. It was even possible to detect two oval hills with peculiar depressions in the center. It is believed that they may be cryovolcanoes [241]. Their diameters are about 225 and 150 km at heights of 6 and up to 4 km, respectively. Elongated dark stripes extend from some of the low hills, which could have been formed, for example, under the influence of the wind. At almost right angles to them are other elongated features, which, most likely, can be dunes of methane "sand". The reason for the very bright color of the entire eastern part of Tombaugh Regio may be various ices, which, under the influence of winds, migrate across the entire plain.

From the hills located in the gorges with the plains, glacial structures slowly move, cutting out branched valleys on their way. On the western edge of the light plain are mountain ranges with heights of up to 5 km. Due to the considerable distance of Pluto's orbit from the Sun, at certain distances the temperature on its surface can drop to as low as 33 K. Under such conditions, water freezes, as well as all other liquids and gases that may exist on Pluto's surface: nitrogen, methane [60, 62] and carbon monoxide. Although they have much lower freezing points than water. Due to the elliptical shape of Pluto's orbit, at some points it approaches and at others it moves away from the Sun. For this reason, at the closest point at a temperature of up to 60 K, that part of the surface that consists of nitrogen must heat up so much that nitrogen can sublimate from a solid state, turn into a gaseous state, and even form a huge diffuse cloud around Pluto. When the temperature changes, precipitation can fall from the cloud, which quickly freezes and takes the form of "snow". Pluto therefore has a very thin atmosphere, consisting mainly of nitrogen, but also of carbon monoxide and methane. The latter two chemical elements can also be in equilibrium with their ice form on the planet's surface. For this reason, the pressure near the surface varies from 0.65 to 2.4 Pa. Due to such seasonal [201, 208] changes in surface illumination, volatile

ices migrate around the planet: they can evaporate in some places and condense in others. According to some estimates, seasonal changes in the thickness of their layer reach values of the order of a meter [141]. Such processes, together with changes in the viewing angle, lead to noticeable changes in the brightness and color of Pluto over time [113]. A high-resolution image (Fig. 40), taken about an hour and a half before the New Horizons spacecraft made its closest approach to Pluto, at a distance of 77,000 kilometers from the planet's surface, shows a region near Pluto's equator. It shows a series of young mountains about 3.5 kilometers above the average level of the icy surface. It is believed that these mountains could have formed no more than 100 million years ago.

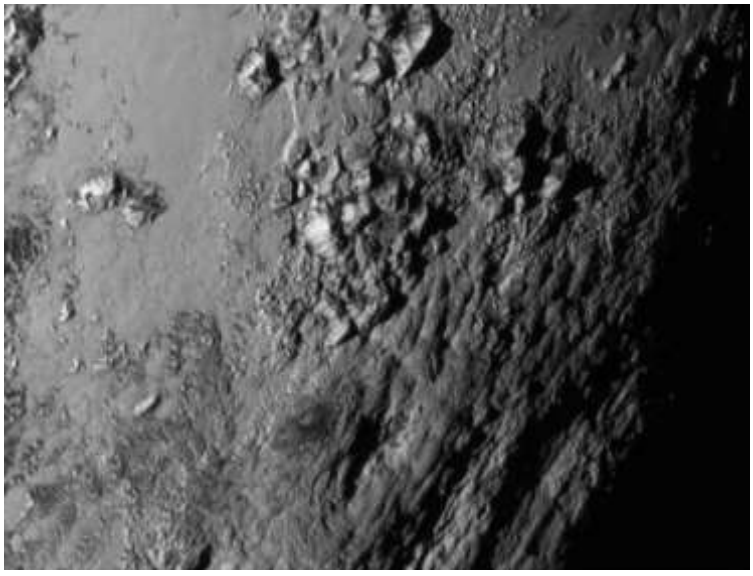

Fig. 40. New close-up images of a region near Pluto's equator show a series of young mountains (https://www.nasa.gov/wp-content/uploads/2023/03/nh-plutosurface.png).

Therefore, they are quite young compared to the age of the Solar System, which is more than 4.56 billion years. It is quite possible that they are still in the process of updating their relief. Although this region covers up to 1% of Pluto's surface area, it may still be geologically active [200, 208]. This relatively young age is based on the almost complete absence of impact craters on this part of the surface.

9. Physical parameters of the atmosphere of the dwarf planet Pluto

Due to the distance of Pluto's orbit from the Sun (from 29.657 AU at perihelion to 48.87 AU at aphelion), the temperature near its surface at this distance can vary from 33 K to almost 60 K. Under such conditions, not only water H_2O freezes, but also other liquids and gases found on the surface of this dwarf planet.

For example, nitrogen N_2, carbon monoxide CO [85] and methane CH_4 have been found there. All of the above compounds freeze at much lower temperatures than water. Due to the elongated orbit of Pluto, the temperature conditions on its surface vary significantly. For this reason, at the point closest to the Sun, its surface heats up so much that some of its components can change their phase state. According to numerous observational data, the main component of Pluto's surface is nitrogen ice. Due to its physicochemical properties, nitrogen, due to heating near the perihelion point, has the ability to transition from a solid to a gaseous state. As a result of sublimation of nitrogen around Pluto, its amount increases and this leads to an increase in pressure in the predominantly nitrogen atmosphere. Again, due to the physicochemical properties of this chemical element, aerosol clouds can also form at certain altitudes in Pluto's atmosphere. However, due to the small values of gravity, it is not enough for a long time to hold the gas-aerosol shell around this dwarf planet for a long time. Therefore, over time, the newly formed molecules fly away into outer space. And when the dwarf planet is far from the Sun, it can cool down so much that its atmosphere will freeze out so much that it will almost completely settle back to the surface. After a long search, Pluto's atmosphere was discovered only in 1985 [216] during observations of its coverage of the star. If the object under study has no gas atmosphere, the light flux from the star will disappear very abruptly. But in the case of Pluto, the light disappeared gradually (Fig. 41). The final confirmation of the existence of an atmosphere around this celestial body was made during large-scale observations of the star's cover in 1988 [28].

Pluto's atmosphere was also studied by spectral methods. A careful analysis of the obtained observational data showed that Pluto's atmosphere is very rarefied and

consists of those gases that evaporate from the ice on its surface. It turned out that mainly – the main component of the surface – nitrogen; impurities of methane (0.25÷0.4%) and carbon monoxide (about 0.05÷0.10%) were also found.

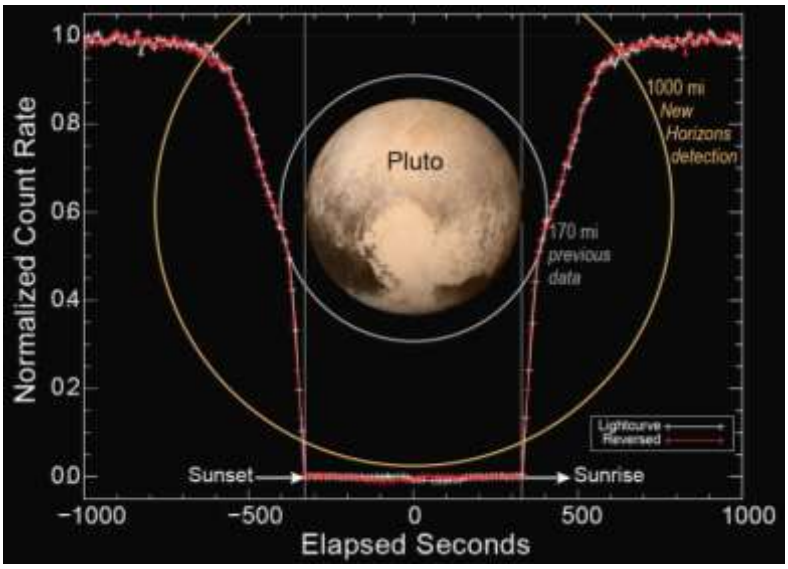

Fig. 41. The absorption curve of solar ultraviolet radiation by the atmosphere of Pluto, measured during the flight of the New Horizons spacecraft through the shadow of Pluto (https://upload.wikimedia.org/wikipedia/commons/a/a3/PIA19716_Alice_Solar_Occultation_%28cropped%29.jpg).

Under the influence of the hard component of solar radiation, some other more complex compounds are formed from these compounds. These include, in particular, ethylene, ethane and acetylene. Over time and with changes in physical conditions on Pluto, these and other compounds fall to the surface of the dwarf planet. Presumably, it is particles of this composition that form separate gas-aerosol layers of fogs, which were observed at altitudes slightly higher than 200 km from the surface. And although Pluto's atmosphere is very thin, the haze turned out to be quite noticeable. Moreover, thanks to the sunlight scattered by it, it was even possible to obtain images of individual details located on the surface on the night side of Pluto. The atmospheric pressure near the surface of Pluto turned out to be very small, and its value varies significantly over time. Moreover, it also changes in a rather unexpected way. After all, due to the

elongation of its orbit, Pluto at aphelion receives almost three times less heat than at perihelion. Such values should lead to significant changes in its atmosphere. According to the proposed predictions, when Pluto is at aphelion, most of the atmosphere should cool, freeze and fall to the surface. At the same time, its pressure should decrease many times.

However, observations of Pluto's coverage of stars made between 1988 and 2015 showed that the value of atmospheric pressure gradually increased almost threefold. And this despite the fact that after 1989 Pluto began to move away from the Sun. The most likely explanation for this atmospheric behavior is that in 1987, Pluto's north polar region began to emerge from shadow into sunlight for the first time in almost 124 years; the resulting heating of the surface layers could well have contributed to the evaporation of nitrogen from the circumpolar region. Measurements made in 2015 by the New Horizons spacecraft showed (Fig. 42) that the atmospheric pressure near the surface was about 1 Pa.

Fig. 42. The image of the night side of Pluto shows the lower layers of the atmosphere backlit by the Sun (https://en.wikipedia.org/wiki/Atmosphere_of_Pluto#/media/File: Blue_hazes_over_backlit_Pluto.jpg).

This value is practically consistent with the results of observations of stellar coverages over the previous few years. However, Pluto's atmosphere was also notable for strong and not fully understood seasonal variations that arise due to the peculiarities of Pluto's orbital and axial rotation. Observational data of Pluto's stellar coverages obtained with the help of the New Horizons spacecraft show how the temperature in its atmosphere changed over time at sunrise and sunset. The biggest changes occurred when the Sun first emerged from behind Pluto, and then as it began to pass through the atmosphere. Molecular nitrogen N_2 begins to absorb sunlight within the upper part of Pluto's atmosphere; as the spacecraft begins to approach the planet's shadow, the light flux from the Sun decreases significantly. While the effect of the eclipse increases, atmospheric methane and hydrocarbons can also absorb sunlight and further reduce the light flux. It becomes the smallest when the space probe completely passes into Pluto's shadow. And at that time the photon counting rate drops to almost zero. Since the space probe was leaving Pluto's shadow at sunrise, then the reverse process began to occur. By analyzing the observed rates of photon counting in the reverse direction, it was possible to notice that the structure of the atmosphere on opposite sides of Pluto is almost identical. Also, the equipment of the New Horizons space probe revealed a layered haze (Fig. 43) of blue color in the atmosphere of Pluto, which covered the entire dwarf planet. In the obtained images, the height of the haze reaches a height of more than 200 km, and in the images obtained using an ultraviolet spectrometer, the haze was registered even at altitudes of about 300 km [56].

The best quality images show about 20 individual layers. They extended for at least 1000 km horizontally. The height of the same individual layer of haze could be somewhat different at different locations above the surface [85]. It was also found that the haze was 2–3 times denser over the northern polar region than over the surface in the equatorial region [1]. The thickness of the individual layers varied in height from 1 to more than 10 km [56]. And the vertical distance between these layers was also not much different from 10 km [85].

Fig. 43. Images of individual layers of haze in Pluto's atmosphere, taken over part of the Sputnik Planitia plain with surrounding mountains, obtained 15 minutes after the spacecraft's closest approach to Pluto (https://upload.wikimedia.org/wikipedia/commons/0/0e/MVIC_sunset_scan_of_Pluto.jpg).

Estimates of the optical thickness of the haze thickness give values from 0.004 [67] to 0.013 [74]. Such values lead to a decrease in the intensity of light rays vertically from 0.4% to 1.3%. The so-called height scale of such a haze in the atmosphere of Pluto (i.e., the height at which its density decreases by a factor of ≈e) is 45÷55 km [67, 74]. Such values approximately coincide with the height scale for pressure changes in the middle layers of the planetary atmosphere [75]. At altitudes of 100÷200 km, its value decreases to about 30 km [74]. The size of particles in the haze is still little studied. After all, its blue color indicates a radius of these particles of about 10 nm. While calculations on the phase dependence of the brightness of the atmosphere at different phase angles indicate a radius of more than 100 nm. This behavior of brightness changes can be explained, for example, by the combination of small particles (tens of nm) into larger conglomerates with sizes of hundreds of nm [85]. It is believed that this haze, under the physical conditions in the atmosphere of Pluto, most likely can be formed from particles of those non-volatile compounds that were able to synthesize from well-known atmospheric gases under the influence of hard solar

radiation. Subsequently, these particles slowly fall to the surface of Pluto over time [173]. Their settling time ranges from several Earth days to several weeks [56]. The stratification of the haze may well be associated with gravitational waves in the atmosphere. Their presence is indicated by some results obtained during observations of stellar coatings [173]. Gravitational waves themselves can arise during atmospheric movements under the influence of wind blowing over relief irregularities [85]. Most likely, it is the haze that causes the break in the observed curve of the decrease in the intensity of solar radiation as it passes through the atmosphere, obtained by the New Horizons space probe during its passage through the shadow of Pluto (Fig. 44).

It is clearly seen there that below altitudes of about 150 km the atmosphere attenuates sunlight much more strongly than it did above this level [173]. The same “break” was observed during observations of the stellar envelopes in 1988. Initially, this absorption behavior was interpreted as the attenuation of the light flux by the haze [4]. However, after the data obtained by the New Horizons space probe, it was possible to establish that the observed pattern of changes in atmospheric absorption may arise due to the rapid increase in temperature with height in the lower layers of Pluto’s atmosphere [57]. In subsequent observations of the star's coverage, when Pluto's atmosphere had become more than twice as dense, such a break in the change in light absorption was practically no longer observed [162]. A somewhat different sign of the presence of haze in Pluto's atmosphere was observed during the 2002 star coverage. At a time when Pluto had already completely covered the star, some of the light from the star was still able to reach the Earth due to the refraction effect in its atmosphere. Then it turned out that the intensity of such light increases with increasing wavelength [73].

This fact is usually interpreted as a reliable [94, 113] sign of light scattering by aerosol particles. However, in subsequent observations of the coverage (including the observations of June 29, 2015 [94]) such a behavior of the change in the light flux was no longer observed [113].

10. Chemical composition of Pluto's atmosphere

Pluto's atmosphere has been studied extensively since the mid-1980s using photometric observations of its stellar coverage [75, 141] and spectral methods [114, 255]. In 2015, Pluto's gaseous atmosphere was closely studied using the New Horizons spacecraft [85, 173]. Extensive studies to date show that Pluto's atmosphere is a thin gas envelope surrounding the entire dwarf planet [199, 200, 203, 208, 211, 212]. It consists of various substances that are frozen on its surface and, under certain conditions, sublimate from its surface [39]. These components are almost 98% nitrogen N_2 with minor admixtures of methane CH_4 and carbon monoxide CO [218].

According to the New Horizons spacecraft, the methane concentration was about 0.25% [173]. Ground-based observations showed a value of 0.4–0.6% in 2008 [114] and about 0.4% in 2012. Ground-based observations estimated the carbon monoxide content at 0.025–0.15% in 2010 [113] and 0.05–0.075% in 2015 [90]. As New Horizons was moving away from Pluto, the Alice spectrometer observed Pluto's eclipse of the Sun, providing data on the extent and chemical composition of its atmosphere. Signs of the atmosphere were detected at a distance of 1,500 km from the dwarf planet's surface, much further than could be observed from Earth. Above other molecules in Pluto's atmosphere are nitrogen molecules; below them methane is added; finally, near the planet's surface, signs of several heavier hydrocarbons appear in the atmospheric absorption spectrum.

It is known that methane is the first representative of the homologous series of the so-called alkanes. Methane is followed by ethane, propane-butane and a number of other substances. The formulas of the limiting hydrocarbons are expressed as C_nH_{2n+2}. Methane and ethane belong to substances that are identical in chemical properties, but different in composition, and, therefore, in their physical properties.

The composition of the so-called homologues differs by the CH_2 group. Therefore, methane is used as a starting material for obtaining ethane; ethane is a raw material for the synthesis of ethylene, etc. To obtain ethane from methane at

temperatures characteristic of Pluto, methane must first be oxidized to acetylene, and then acetylene must be hydrated to ethane.

The oxidation of methane to acetylene should proceed as follows:

$4CH_4 + 4O_2 \rightarrow CH{\equiv}CH + CO_2 + CO + 5H_2O + 2H_2$.

Then, acetylene needs to undergo double hydration and the final product of this reaction will be ethane:

$CH_3{\equiv}CH_3 \rightarrow CH_2 = CH_2 \rightarrow C_2H_6$.

Usually, this method should be used when the starting substance can only be methane. Under the influence of hard radiation, various more complex compounds are formed from these atmospheric compounds that are not volatile at the “winter” temperatures on the surface of Pluto [81, 96] and therefore they gradually settle on it. This, in particular, applies to such chemical elements as ethane, ethylene and acetylene [91], as well as to somewhat heavier hydrocarbons and nitriles [60, 61], to hydrogen cyanide and to such high-molecular compounds as tholins. The latter give Pluto's surface a brown color [173]. At altitudes above 200 km [91], it is particles of somewhat more complex compounds, which under the influence of strong solar radiation [91] were synthesized from the above-mentioned basic atmospheric gases, that form clearly visible haze layers [132, 134] in Pluto's atmosphere.

According to data from the New Horizons space probe in 2015, the pressure of Pluto's atmosphere near the surface was 1 Pa [85, 173]. The temperature near its surface can vary from 34 to almost 60 K. However, with altitude, due to the methane-induced greenhouse effect [193, 194, 197, 198], the temperature increases quite rapidly. And already at an altitude of about 30 km it reaches as much as 110 K. After this altitude, the temperature begins to slowly decrease [66, 85]. According to the data of the New Horizons space probe, the following estimates of their content were made for ethylene and acetylene: 0.0001% and 0.0003%, respectively [173].

The most volatile component of Pluto's atmosphere is nitrogen; carbon monoxide is in second place and methane is in third place. The main indicator of the volatility of this chemical element is the saturated vapor pressure. For example, at a temperature

close to the minimum for Pluto's surface of 40 K, this value is about 10 Pa for nitrogen, almost 1 Pa for carbon monoxide and only 0.001 Pa for methane.

With increasing temperature, the saturated vapor pressure value increases sharply. And already at a temperature of 60 K (which is close to the maximum temperature on Pluto's surface at the perihelion of its orbit), the corresponding values of saturated vapor pressures increase up to 10,000, 3,000 and 10 Pa, respectively.

The saturated vapor pressures of hydrocarbons heavier than methane, as well as carbon dioxide, at such a relatively high temperature still remain quite small (less than 10–5 Pa). This indicates the practical absence of these chemical elements in Pluto's conditions, at least at the levels of the cold lower layers of its atmosphere. Chemical components such as water, ammonia, and hydrogen cyanide remain nonvolatile components even at the temperature of 100 K typical of Pluto's upper atmosphere [81, 96]. For the minor components of Pluto's atmosphere, one would still expect larger deviations from the equilibrium state with surface ices than for nitrogen, and slightly stronger changes in concentrations with time and space (over the surface and with height in the atmosphere) [113].

However, for such a component as methane, at least in the lower part of the atmosphere, it was not possible to reliably detect its changes with altitude, longitude, or time [188, 261]. However, it is clear that with the distance of Pluto from the Sun in its orbit, the absolute and relative values of the methane content should decrease. This fact is indicated by the dependence of the saturated vapor pressure on temperature for methane and nitrogen [188, 261]. Moreover, the methane concentration turned out to be 2 orders of magnitude higher than the calculated value based on the values of its concentration in the surface ice layer, as well as on the ratio between the saturated vapor pressures for methane and nitrogen [188, 261].

One of the hypotheses explaining this fact may be the presence on the surface of Pluto of separate areas with relatively pure methane ice; Another possibility is the increased methane content, at least in a thin layer near the surface, in a mixture of existing ices [113, 188]. Methane and carbon monoxide, despite their low content, significantly affect the temperature of Pluto's atmosphere. After all, the first of these

chemical elements significantly heats it [114], while the second can slightly cool the atmosphere [66, 112]. A similar break was observed during the occultation of a star by Pluto in 1988. It was also initially interpreted as the attenuation of light by haze in the atmosphere [74].

However, after the appearance of data from the New Horizons space probe, it was established that such a break should arise mainly due to the rapid increase in temperature with height in the lower layers of the atmosphere [56]. In later observations of the occultations of stars (when the atmosphere around Pluto had already become more than twice as dense), this was practically no longer observed [66, 75, 162]. Another sign of the presence of haze in the atmosphere was observed during the observation of the cover in 2002. After Pluto had completely covered the star, but due to refraction in its atmosphere, some of its light was still able to reach the Earth. At that time, it was found that the intensity of this light increases with increasing wavelength [73]. This was then interpreted as a very reliable sign of light scattering by the aerosol component in the atmosphere [75, 94].

However, during subsequent observations of the covers [94], such a phenomenon was not detected. And on July 14, 2015, observations from the New Horizons space probe revealed that the color of the haze over Pluto is blue. Due to its small mass, Pluto is quite actively losing its gas envelope. At altitude, it is picked up and ionized by the solar wind. Therefore, after the flyby of Pluto, the New Horizons space probe continued to fly for a long time through the ion tail that trailed behind the dwarf planet. Estimates have shown that the rate of loss of its gas envelope is about 500 tons per hour. This indicates that during its existence, Pluto as a whole could have lost an amount of nitrogen equivalent to an ice shell on the surface with a thickness of several hundred meters to more than two kilometers.

Since the presence of many mountain ranges on its surface indicates a relatively small current thickness of the frozen nitrogen layer, it should not be ruled out that the nitrogen in the modern atmosphere is not only a product of the sublimation of N2 ice from the surface, but is also partially emitted from some underground storage. According to estimates based on data from the New Horizons probe, Pluto's

atmosphere dissipates into space at a rate of 1×10^{23} nitrogen molecules and 5×10^{25} methane molecules per second. This corresponds to the loss of a layer of nitrogen ice a few centimeters thick and a layer of methane ice a few tens of meters thick over the lifetime of the Solar System [85].

Before measurements by the New Horizons spacecraft, the temperature of Pluto's upper atmosphere was thought to be higher. This fact implied a very high rate of atmospheric dissipation [188]. The rate of atmospheric loss was previously estimated at 10^{27}–10^{28} molecules (50–500 kg) of nitrogen per second. At this rate, a surface layer hundreds or even thousands of meters thick would have evaporated during the existence of the Solar System [164]. In this case, the relative rate of atmospheric loss for Pluto would be greater than for all the large planets [188]. And then there would be nothing to replenish the existing nitrogen reserves. After all, calculations show that the mere fall of small bodies onto Pluto's surface would not be sufficient for this [188, 242]. Molecules that have enough speed to overcome Pluto's gravity escape into space and are ionized by the ultraviolet part of the solar wind. When the solar wind encounters a barrier of atmospheric ions, it slows down, deflects to the side, picks up ions, and carries them with it, creating a long tail behind Pluto.

Behind Pluto, a peculiar cavity at least 100 thousand km long remains in the solar wind stream, filled with relatively cold ionized nitrogen. This was detected by the SWAP solar wind particle parameter meter on the New Horizons space probe, which flew through this cavity. The region of interaction of Pluto's atmosphere with the solar wind on the side of the Sun is located at a distance of about 6 Pluto radii (7 thousand km), and on the opposite side - more than 400 Pluto radii (500 thousand km). These estimates refer to the zone where the solar wind slows down by 20% [17]. In 2014–2015, the Chandra space telescope detected low-energy (0.31–0.60 keV) X-rays coming from Pluto. It is believed that these may be the result of the interaction between gases from Pluto's atmosphere and the solar wind [117].

11. Gaseous and aerosol components in Pluto's atmosphere

Observations of stellar envelopes in 1988 confirmed that Pluto has a gaseous atmosphere [242]. This very thin atmosphere of Pluto consists of gases that evaporate directly from various substances that are on its surface in a frozen state. It is almost 98% nitrogen with minor admixtures of methane (0.25-0.60% [173]) and carbon monoxide (about 0.05-0.15% [90]). Under the influence of hard radiation, various more complex compounds are formed from these components. In particular, these include ethane, ethylene and acetylene [91]. Over time, all of them gradually fall to the surface of Pluto. Presumably, it is particles of this composition that form a layered [Fig. 44] aerosol component in the atmosphere [132, 134], which reaches heights of more than 200 km [91]. Despite the considerable thinness of the atmosphere, this aerosol haze [67] is quite visible. And thanks to the light scattered by it, the New Horizons space probe even managed to photograph some details on the night side of Pluto.

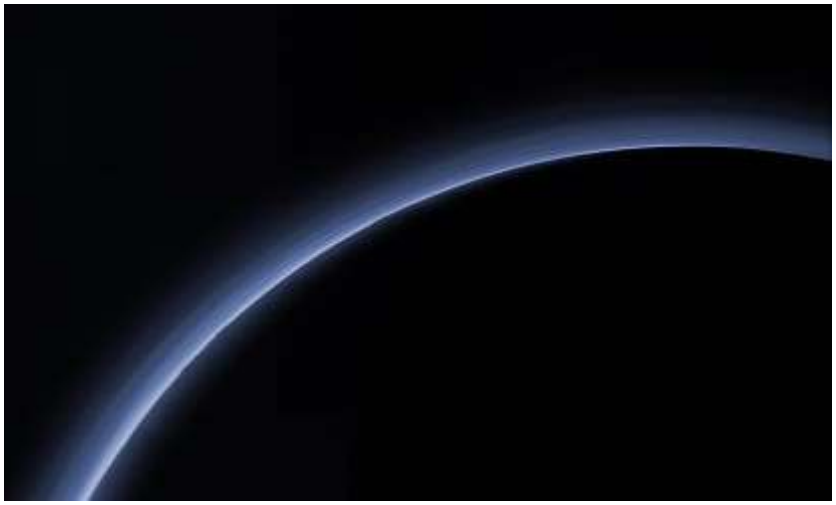

Fig. 44. Layered aerosol component in Pluto's atmosphere (https://gagadget.com/media/cache/0d/5c/0d5cda4d7d3a7b4914b23eb504a0f2ab.jpg).

The pressure of such a gas-aerosol atmosphere of Pluto is very small and changes significantly over time. Due to the elongated orbit at aphelion, Pluto receives almost three times less heat than at perihelion. And this should cause significant changes in its atmosphere. According to some predictions, when Pluto is near the aphelion point,

most of the gaseous part of the atmosphere freezes and falls to the surface in the form of frost and snow. And then the atmospheric pressure near the surface of the dwarf planet decreases many times [141]. However, observations of Pluto's eclipses have shown that between 1988 and 2015, the atmospheric pressure there continued to gradually increase, and during this time it increased almost threefold. And this happened despite the fact that after 1989 Pluto began to move further and further away from the Sun [141, 255]. It is likely that this fact is related to the fact that in 1987 the northern circumpolar region of Pluto came out of the solar shadow for the first time in 124 years; and this contributed to the processes of nitrogen evaporation from the frozen surface of the circumpolar cap. In 2015, measurements by the New Horizons space probe showed that the atmospheric pressure near the surface of Pluto was about 1 Pa [85]. This value is approximately consistent with observations of eclipses over the previous few years [85].

Measurements made in 2002 revealed that even then Pluto's atmosphere was much thicker (Fig. 45) than previously thought.

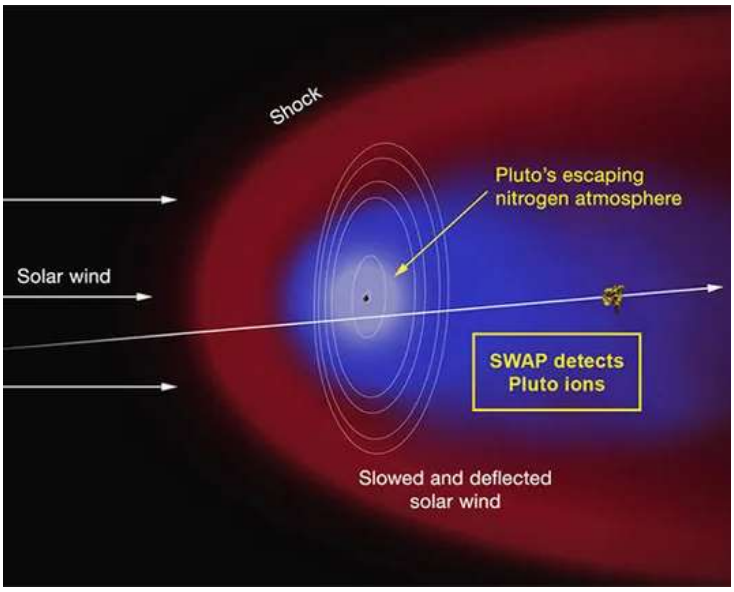

Fig. 45. Pluto's atmosphere creates a vast region of cold, dense ionized gas hundreds of thousands of kilometers beyond Pluto's orbit. The emissions are mostly nitrogen ions (https://cdn.mos.cms.futurecdn.net/z4P7tET7LjkUuGU4UZiFi7-650-80.jpg.webp).

It has been suggested that this may be a seasonal phenomenon [193, 197, 198, 212]. Nitrogen on the surface of the previously shaded polar regions of the dwarf planet [199] began to be exposed to direct sunlight. This caused its evaporation to increase, which led to a gradual expansion of the atmosphere. Formed under the influence of the hard component of solar radiation from the above-mentioned gases, various more complex compounds, at the temperatures existing on Pluto, already cease to be volatile [81, 96]. Therefore, they freeze and gradually settle on the surface of the dwarf planet in the form of aerosol particles.

Such components include, in particular, acetylene, ethane, ethylene, heavier hydrocarbons, nitriles [260, 61, 91], as well as hydrogen cyanide and high-molecular compounds called tholins. The latter, in places where they fall to the surface, give these areas of Pluto's surface a brownish color [173]. According to observations with the equipment of the New Horizons space probe, estimates of the content of ethylene and acetylene were made. They showed values of 0.0001 and 0.0003%, respectively [73]. For the minor components of Pluto's atmosphere, one can expect larger deviations from the equilibrium state with surface ices than for nitrogen. And therefore, for them, stronger temporal and spatial changes in their concentration occur [6]. However, for methane, it was not possible to reliably detect its changes with altitude (at least in the lower atmosphere), with longitude, or with time [36]. But it is clear that as Pluto moves away from the Sun, both the absolute and relative methane content should decrease. This is indicated by the calculated dependences of the saturated vapor pressure of methane and nitrogen on temperature [261].

It is interesting that the value of the methane concentration turned out to be 2 orders of magnitude higher than the calculated values. This was obtained based on the measured values of its concentration in the upper layer of ice near the surface and the ratio between the values of the saturated vapor pressures of methane and nitrogen [112, 261]. One of the proposed hypotheses explains this fact by the possible presence of separate areas with relatively pure methane ice on the surface of Pluto. Another hypothesis suggests an increase in the content of frozen methane in a thin surface layer of a normal mixture of ices [112, 188].

Indeed, despite the rather small absolute content of methane and carbon monoxide, these components significantly affect temperature changes in Pluto's atmosphere. After all, methane heats it quite strongly [114, 194]; while carbon monoxide, on the contrary, leads to some cooling of it [60, 112].

Also, a layered haze has been registered in Pluto's atmosphere [200]. It is believed that it is formed by more complex newly formed compounds that are synthesized from the above-mentioned gases under the influence of hard radiation [91]. Indeed, if the temperature on the surface of Pluto is in the range of 34-60 K, then with height the temperature in the atmosphere increases rapidly due to the greenhouse effect caused by methane. At an altitude of about 30 km it reaches a value of 110 K. After this height the temperature decreases slowly again [66, 85].

Calculations have shown that the atmosphere, despite a very small pressure, is able to effectively smooth out daily temperature fluctuations [255]. Areas of the surface from which nitrogen ice evaporates are cooled by up to 20 degrees. This causes a wind near the surface with speeds reaching values of the order of 1-10 m/s [182]. It is difficult to say anything about the size of the particles of this haze. Its blue color may indicate a particle radius of up to 10 nm. While the brightness ratio at different values of phase angles gives a radius value an order of magnitude larger, over 100 nm. One explanation for this fact may be the aggregation of smaller particles into larger formations with sizes exceeding a hundred nm [85].

The most likely is that this haze could have formed from particles of non-volatile compounds that were synthesized under the influence of hard solar radiation from known atmospheric gases. And then they change their aggregate state, and therefore in the form of aerosol particles can slowly fall to the surface of Pluto [91, 173]. The time of their settling can be measured in Earth days, or even weeks [56]. When in 2002 Pluto completely covered the star, but still some of its light, due to refraction in its atmosphere, still reached the Earth. Then it turned out that the intensity of this light increases with wavelength [73]. This was then interpreted [94, 113] as a sign of light scattering by aerosol particles of small sizes.

Within the thin and discontinuous atmospheric boundary layer, the measured temperature near the surface was relatively constant [85]. This layer was then detected by radio transmissions of the atmosphere from the New Horizons spacecraft as the spacecraft passed Pluto. The thickness of this gas layer was about 4 km; and this layer had a temperature of about 37 ± 3 K. At this temperature, the saturated nitrogen vapor pressure is equal to the observed atmospheric pressure.

It is possible that this boundary layer consists of gas that has just evaporated from the planet's surface [203, 208, 211] and has not yet had time to mix with the rest of the atmosphere. This explanation is also supported by the fact that this layer was observed in the young flat region of Sputnik Planitia, which is a huge reservoir of volatile ices and on which there are now practically no noticeable impact craters [253]. The observed evaporation could have occurred either at the time of the observations or very shortly before them. Calculations have shown that without constant renewal this layer could last no more than two Earth years [85].

12. The vertical structure of Pluto's atmosphere

Pluto's atmosphere is a relatively thin gaseous envelope [200]. It consists mainly of nitrogen, but also methane and carbon monoxide. The presence of such an atmosphere is maintained by constant evaporation from the surface ice layer. From 2000 to 2010, the atmosphere expanded significantly due to sublimation [203, 208, 211, 212] of surface ice from the northern polar region. It was this polar region that began to emerge from the polar night in the 1990s after a break of more than 124 years. At the turn of the 20th and 21st centuries, the atmosphere was visible up to an altitude of 100–135 km above the surface. And according to the results of measurements in 2010, it was clearly observed even at altitudes of more than 3000 km. This was already about one sixth of the distance to the nearest satellite Charon. Thermodynamic calculations indicate that Pluto's atmosphere should consist of about 98% nitrogen, up to 0.5% methane, and slightly less than 0.2% carbon monoxide. As Pluto moves away from the Sun, its atmosphere will gradually freeze and settle onto the dwarf planet's surface [199]. As it approaches the Sun again, the solar heat will again heat Pluto's surface more and more. As the ice sublimates, more and more of it will gradually turn into a gas.

This will create a kind of anti-greenhouse effect [132, 133]. As matter evaporates from Pluto's surface, it will cool this surface as a result of sublimation processes. Calculations have shown that even at such moments, the temperature on Pluto's surface can rise above 43 K. While the upper part of Pluto's atmosphere becomes much warmer than the surface, having a temperature of over 100 K.

Thus, the atmospheric pressure near the surface undergoes significant changes when Pluto approaches or moves away from the Sun. This means that when Pluto is at perihelion, the temperature near the surface increases, and the icy components begin to change their state to a gaseous state; and when Pluto approaches aphelion, the atmosphere freezes, turning into a solid state. Observations made during the flyby of the New Horizons space probe allowed us to obtain a detailed report on the current state of Pluto's atmosphere [85]. The lower layers of the atmosphere at altitudes below

200 km correspond to data obtained from ground-based observations of stellar eclipses. While the upper atmosphere was much colder and more compact than model calculations based on the flyby data indicated.

However, molecular nitrogen N_2 dominated the atmosphere at altitudes below 1,800 km. While methane CH_4, acetylene C_2H_2, ethylene C_2H_4 and ethane C_2H_6 are common minor gases in the atmosphere and are likely to be responsible for the large haze formations that cover the entire planet. Such colder upper atmospheres somewhat hinder the previously expected escape of Pluto's atmospheric components into outer space. According to data obtained in 2015, the temperature of Pluto's lower atmosphere increased with altitude at a rate of several degrees per kilometer.

At an altitude of 20-40 km, it reached a maximum value of about 110 K, and then began to slowly decrease. At altitudes of several hundred kilometers, the temperature values reached a level of about 70 K and then practically did not change. According to the results obtained in 2005-2008, the average temperature of the atmosphere was about 50° higher than on the surface. This temperature behavior is explained by the results of the greenhouse effect caused by the presence of methane in the atmosphere. Interaction with the atmosphere also significantly affects the temperature values on the surface of Pluto. The calculations showed that the atmosphere, despite a rather small pressure value, effectively smoothes out daily temperature fluctuations. But those areas of the surface from which nitrogen ice evaporates are cooled by almost 20 degrees. Due to daily temperature changes, wind speeds near the planet's surface can reach up to 10 m/s.

Pluto's atmosphere turned out to be divided into separate layers by height. On this dwarf planet, the troposphere is distinguished, separated from it by a fairly wide stratopause, the stratosphere and the mesosphere. The physical characteristics of each of these layers are distinguished by their own characteristics [67, 193, 197].

According to the indicators of the calculation of light fluxes through the atmosphere of Pluto in the ultraviolet (UV) region of the spectrum during observations of a solar eclipse with the equipment of the New Horizons space probe, the following structure of changes was noted. Absorption by nitrogen N_2 began at an altitude of 1670

km from the surface of Pluto; absorption by methane CH_4 began to appear at altitudes below 960 km, and absorption by various hydrocarbons C_2H_x began at altitudes below 420 km; starting from altitudes below 150 km, a layered structure of haze began to appear.

Observations at the beginning and end of the eclipse showed nearly symmetrical vertical absorption profiles in the direct line of sight. These results indicate a global homogeneity of the structure of Pluto's upper atmosphere. The data obtained during the solar eclipse observation best fit a methane CH_4 fraction in this part of the atmosphere of 0.25%. This turned out to be somewhat lower than the previous estimate of 0.44%. Such changes indicate that the atmosphere has become somewhat cooler. Observations in the far UV also allowed the discovery of two new atmospheric constituents. These were ethylene C_2H_4 and acetylene C_2H_2 with atmospheric ratios of about 0.000001 and 0.000003, respectively. Their opacity is consistent with a relatively constant atmosphere at altitudes of 50 to 300 km. Analysis of star obscuration and CH_4 spectral line data prior to the spacecraft flyby showed that the global mean surface pressure ranged from 6 to 24 μbar and varied over time [114, 253]. In particular, from 1988 to 2003, the pressure due to sublimation increased almost 2-fold, and remained virtually constant after 2003 [173]. Results from the New Horizons spacecraft showed that Pluto's troposphere is represented by a relatively thin and discontinuous layer near the surface with a surface pressure of ~10 μbar [173, 260].

Within the troposphere, the temperature was relatively constant [85]. These features were detected by radio scanning of the atmosphere using instruments on the New Horizons spacecraft. The thickness of this layer was only about 4 km, and it had a temperature of about 37±3 K. To explain such features, it is believed that this boundary layer may consist of gas that has only recently evaporated from the surface and has not yet had time to mix with the rest of the atmosphere.

In favor of such a development of events, observational data indicate that this layer was observed in the area of the Sputnik Planitia plain. And this plain is a huge reservoir of various volatile ices. Evaporation should have occurred either at the time of observations or shortly before them. Calculations have shown that without constant

renewal due to sublimation, this layer could exist for no more than two Earth years [85]. Above this boundary layer begins the stratosphere. It is a region where the temperature is characterized by an increase in temperature with height. The rate of increase varies significantly in different places. For example, for the lower 10 km of the stratosphere, when the spacecraft entered Pluto, the value was measured to be 6.4±0.9; when the spacecraft left its shadow, this value was almost half as low – 3.4±0.9 K/km [85]. According to ground-based observations, the same value was estimated at 2.2 [75], 3–15[114] or 5.5[113] K/km. This increase in temperature is the result of the greenhouse effect caused by methane. The average surface temperature according to 2005 data was 42±4 K [89], with an average temperature over the atmosphere of 90(+25−18) K in 2008 [113, 114].

In the stratopause at an altitude of 20–40 km, the temperature reached a maximum value of 100–110 K; and then the temperature slowly decreased at a rate of about 0.2 K/km [66, 75, 113]. The reason for this drop could be the cooling effect of acetylene, hydrogen cyanide [66, 85] and/or carbon monoxide [112]. At altitudes slightly above 500 km, the temperature reached 70 K, and then it practically did not change [73, 75, 85]. According to the same data, no significant dependence of temperature on latitude and time of day was found. That is, the temperature remained approximately the same over the entire surface. This indicates a fairly rapid mixing of the atmosphere [113]. However, in 2015, using equipment on the New Horizons space probe, a noticeable difference was observed between the curves of temperature dependence on height on different sides of Pluto [85].

Small vertical temperature inhomogeneities were also detected in Pluto's atmosphere. They manifest themselves in sharp and short bursts of brightness during stellar eclipses. The magnitude of these inhomogeneities is estimated at 0.5÷0.8 K at altitude intervals of several kilometers. They may be the result of the influence of turbulence in the atmosphere caused by convection or winds [162]. The interaction of the surface layers with the atmosphere also affects the temperature of the surface of Pluto. Calculations show that the atmosphere, despite the very small pressure near the surface, is able to significantly smooth out daily temperature fluctuations [253].

However, there are still temperature variations of about 20 degrees. This may be because the areas of the surface from which nitrogen ice evaporates are significantly cooled.

Observations of Pluto's occultations of stars have shown that the pressure value gradually increased by almost threefold between 1988 and 2015. This is despite the fact that Pluto has been moving away from the Sun since 1989 [161]. A possible reason for this pressure behavior may be that in 1987, after a very long break, a polar day began to set in at Pluto's north pole. This began to promote the evaporation of nitrogen from this polar region [162]. The opposite hemisphere, however, was still quite warm, which still made its condensation impossible [151, 161]. This trend between 1988 and 2013 was confirmed by independent works [34, 73, 146, 253], and continued in data from 2015 [161]. The data obtained exclude a decrease in atmospheric temperature associated with Pluto's distance from the Sun. However, they are consistent with the high thermal inertia in the atmosphere and with the existing N_2 ice cap in Pluto's north polar region.

13. The earliest data on the general characteristics of Pluto's relief

As was already visible in the images taken by the Hubble telescope [213], the surface of the dwarf planet [199, 200] Pluto [212] is very heterogeneous. The albedo of different parts of the surface varied from 0.10 to more than 0.70 [28]. Such changes in albedo values made it the second most contrasting object in the Solar System after the satellite of the giant planet [194] Saturn [67, 132, 197] Iapetus [173]. Such heterogeneity during the rotation of Pluto around its axis leads to periodic changes in both its brightness and spectrum. And such changes reach more than 30% [143]. It was the changes in the spectrum from ground-based [238] observations that made it possible to learn that molecular nitrogen and carbon monoxide are much more abundant [60] on the side of Pluto facing away from the moon Charon. This is where the region now commonly called the “heart of Pluto” is located. While methane was found to be most abundant approximately 120° from this region [88].

The New Horizons spacecraft began its journey to Pluto on January 20, 2006, with a speed of more than 16 km/s, given to it by rocket engines at launch. A gravitational maneuver near Jupiter [131, 194, 197, 206] was able to add about 4 km/s more. The probe also has its own engines and a very small fuel supply. But they will be used only for small changes in the probe’s orientation in space and for minor corrections of its orbital trajectory.

Changes in orientation in space were used, for example, to turn the probe with the necessary instrument for observations to the object of study. A total of seven instruments were installed on the New Horizons spacecraft. One of them is the black-and-white visible range camera LORRI. It is a 0.2-m telescope with a CCD matrix. Its field of view is 0.29°, and it has an angular resolution of about one arc second per pixel. To obtain color images, the 7.5-cm Ralph telescope was used with the MVIC camera with a field of view of 5.7° and an angular resolution of about four arc seconds per pixel. The camera covered the visible range and a very small section of the infrared range.

The same Ralph instrument also included the LEISA panoramic infrared spectrometer. With its help, the absorption bands of ices from molecular nitrogen, carbon monoxide, methane, water, etc. were studied. The Alice panoramic ultraviolet spectrometer was used to study the chemical composition of Pluto's atmosphere [218]. Two of the installed instruments – SWAP and PEPSSI – were used to study the plasma around the space probe. The probe also carried the SDC dust detector and the REX instrument, designed to observe Pluto's atmosphere [221] and, possibly, the existing atmosphere of Charon in the radio range. The main Pluto study program began in January 2015 and ended in January 2016. The closest approach observation program itself with Pluto was carried out from July 13 to 15, 2015. At that time, the probe operated in a fully automatic mode. Its operating program was downloaded in advance. After that, the device began transmitting the results of the observations obtained during the flyby to Earth. In February 2017, the International Astronomical Union approved a list of topics for naming features on Pluto (Fig. 46).

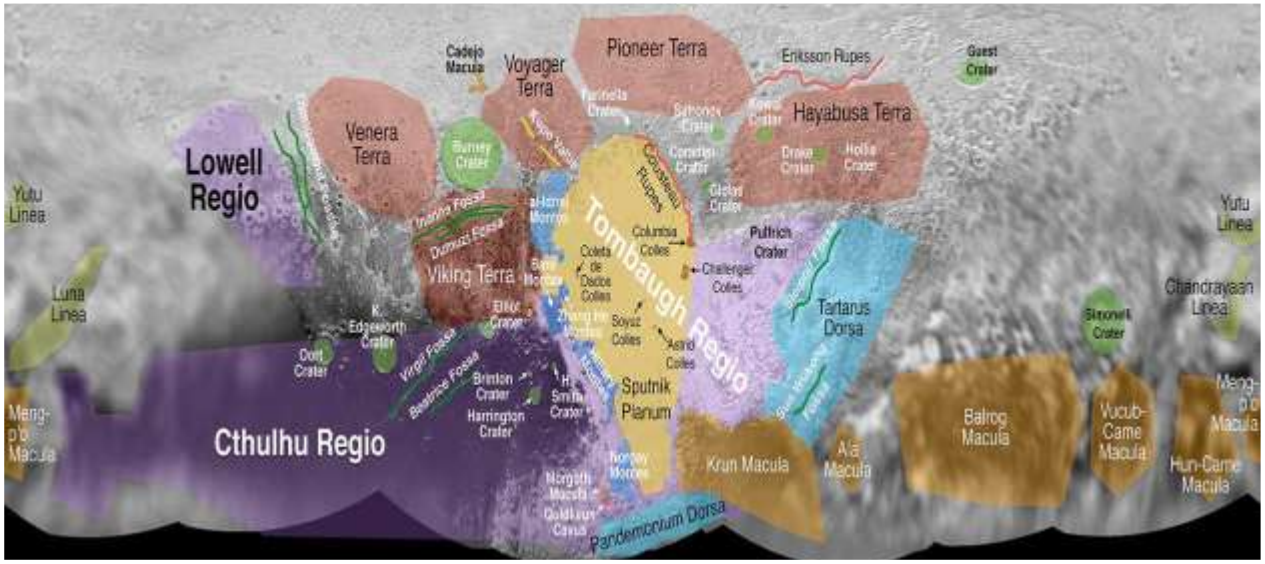

Fig. 46. Maps with names of objects on Pluto. Geomorphological regions are colored as follows: red – terrae; green – craters; light yellow – chasmata; orange – spots; blue – mountains; purple – plateaus; yellow – plains; cyan – hills; pink – cavi; light green – linear formations; golden yellow – hills; red lines – cliffs; green lines – ditches; yellow lines – valleys [173].

The names should correspond to the following topics. These should be the names of gods, goddesses, other beings, heroes, explorers of the underworld, the names of the underworld itself and individual places in that world that occur in mythology, folklore and literary sources and that were in some way associated with the underworld; as well as the names of scientists and engineers associated with the study of Pluto and the Kuiper Belt, with space missions, spacecraft, historical pioneers who reached certain new horizons in the study of the Earth, sea and sky. Thanks to observations with the New Horizons spacecraft, traces of unexpectedly intense and diverse geological activity were discovered on Pluto [203, 212, in particular, quite recent ones.

Judging by the concentration of impact craters, the age of some parts of the surface turned out to be close to more than 4 billion years, while the age of others often could not exceed 10 million years [113, 173]. The origin of many of the observed features on the surface is explained by the impacts of asteroid bodies, active tectonic processes, possible cryovolcanism, glacier movement, erosion, even convection in ice [208], as well as sublimation and condensation of gases in aerosols [134], and also the action of the wind near the surface [91, 130, 143]. The main albedo features on the surface of the dwarf planet are some global features in the images of Pluto transmitted from the New Horizons spacecraft.

Among such features, equatorial regions with low albedo of reddish color stand out. They extend somewhat south of the equator for almost its entire length (Fig. 47, top); these include, for example, Cthulhu Regio and Krun Macula (Fig. 46); also visible is the northern, hitherto summer polar region, Lowell Regio, and part of the southern, formerly winter hemisphere. And among the regions with high albedo, the most noticeable detail is a bright area with dimensions of 1800×1500 km, located on the hemisphere opposite Charon. Its name is well known as the “heart of Pluto” or Tombaugh Regio. Its western half is distinguished by a very light and flat relief; it was called Sputnik Planitia. It has a rounded shape with a small protrusion in the southern direction (Fig. 46, 47).

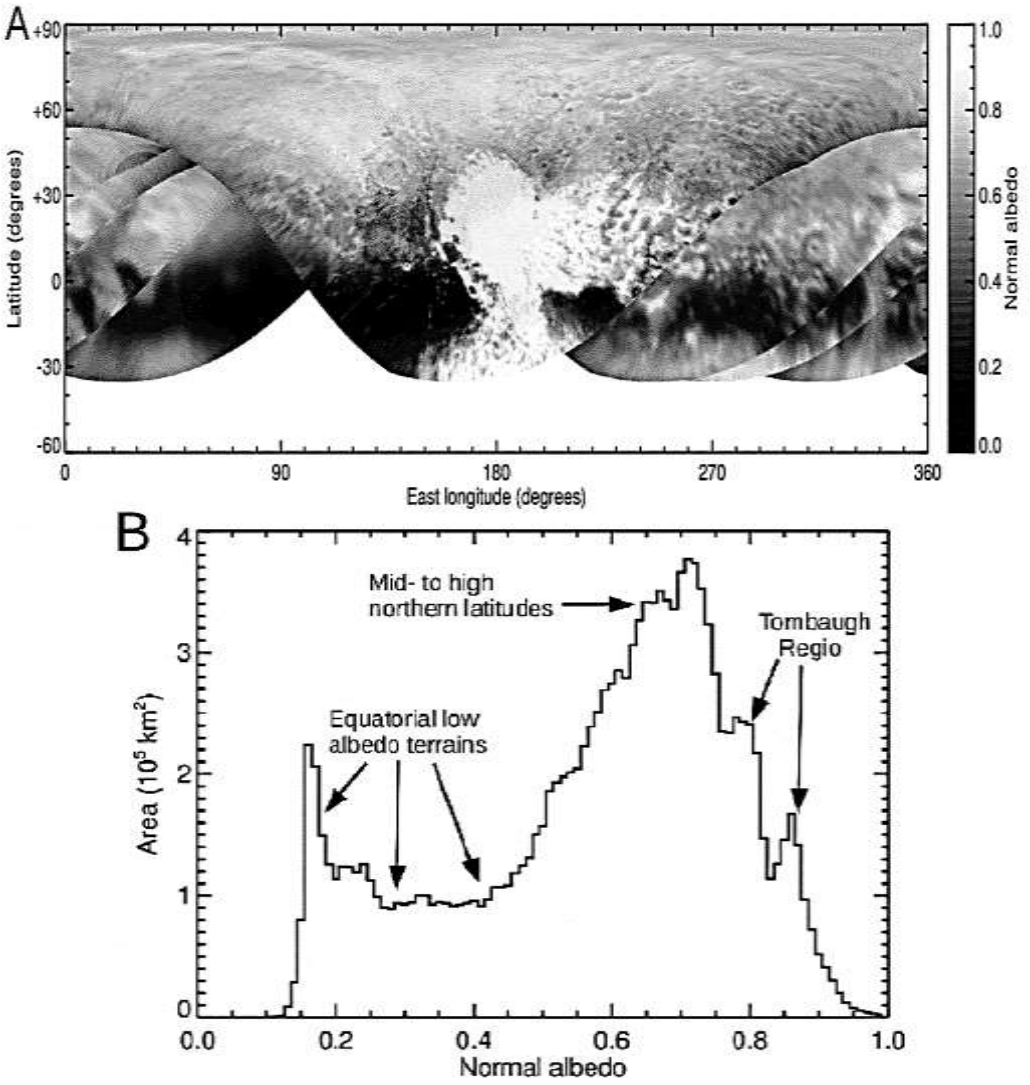

Fig. 47. Above – normal reflectance of Pluto's surface according to images obtained at wavelengths of 350-850 nm. Below – histogram of normal albedo values over Pluto's surface [3].

Its area is almost 5% of the area of the entire surface of Pluto [130]. This depression is believed to be of impact origin [130, 184], and later it was probably filled with frozen gases. It now has a very young surface. This is indicated by the almost complete absence of impact craters of noticeable size on it [130, 174].

Many inexplicable and often mysterious objects have also been found on this plain. For example, it is crossed by curvilinear, often double grooves with a depth of about a hundred meters. They divide its entire surface into separate "cells" with dimensions of tens of kilometers. The centers of some of the cells are raised by almost 50 m relative to their edges. Although some of them have smaller heights.

Such their geologically recent recovery on the surface of Pluto and its topographic relaxation are in good agreement with the weak rheology of this ice. Among such ices, ice from molecular nitrogen N2 should dominate. The large cells can be interpreted as potentially active, almost solid-state convection in a thick layer of such ice. Most likely, these cells are of convective origin [130].

The southern region and the eastern edge of Sputnik Planitia do not exhibit cellular morphology. Instead, they show plains without any features and numerous pits that reach several kilometers in diameter. Some of these areas were found to be dotted with numerous small, lined-up depressions. It is believed that their appearance may be associated with very recent sublimation of ice. Long dark stripes extend from some of the hills on Pluto's surface, which may have been formed under the influence of near-surface winds [174]. Numerous elongated features are often observed perpendicular to them.

They are most likely methane sand dunes [182, 256]. It is ice migrating from the plain under the influence of winds that may be responsible for the very bright color of the entire eastern part of Tombaugh Regio [113].

14. Update of data on the characteristics of Pluto's terrain

t was known from remote observations that Pluto's surface is very heterogeneous. The albedo of individual areas of Pluto's surface varies from values less than 0.10 to more than 0.70 [213, 222]. Later, these data were confirmed by numerous images obtained using the equipment installed on the New Horizons spacecraft. The observation program at the closest approach to Pluto was carried out by all instruments of the space probe in a fully automatic mode from July 13 to 15, 2015. After this date, the device began transmitting the results of observations obtained during this flyby to Earth. Based on these data, a detailed study of impact craters on the surface of this dwarf planet was carried out, which made it possible to establish that its surface went through at least three separate phases in the process of its formation [60, 132, 199]. With an age of more than 4 billion years for Pluto's ancient surface, Pluto has had a long history of geological activity [215].

The dwarf planet's surface has been found to contain both very old rocks and relatively young rocks that could have formed only in the last few million years (Fig. 48). These include, for example, the heart-shaped relief feature called Tombaugh Regio. New data also show the presence of a so-called "intermediate" area of intermediate age. This suggests that Pluto has been geologically active throughout its long history. The main reason for the very bright color of the entire eastern part of Tombaugh Regio may be ices carried by winds across this plain [113]. Images taken by the spacecraft show that this large, bright area, called Sputnik Planitia, appears to be covered in "soft" nitrogen ice that hides old impact craters. The entire Sputnik Planitia valley lies several kilometers below its surroundings. Its surface features indicate that it is composed of exceptionally elastic ice, unique in the entire Solar System. Glaciers flow from the adjacent highlands, carving out extensive valleys along their path [115]. On the western edge of Tombaugh Regio, numerous mountains up to 5 km high stretch for hundreds of kilometers along the entire western edge of Sputnik Planitia [96].

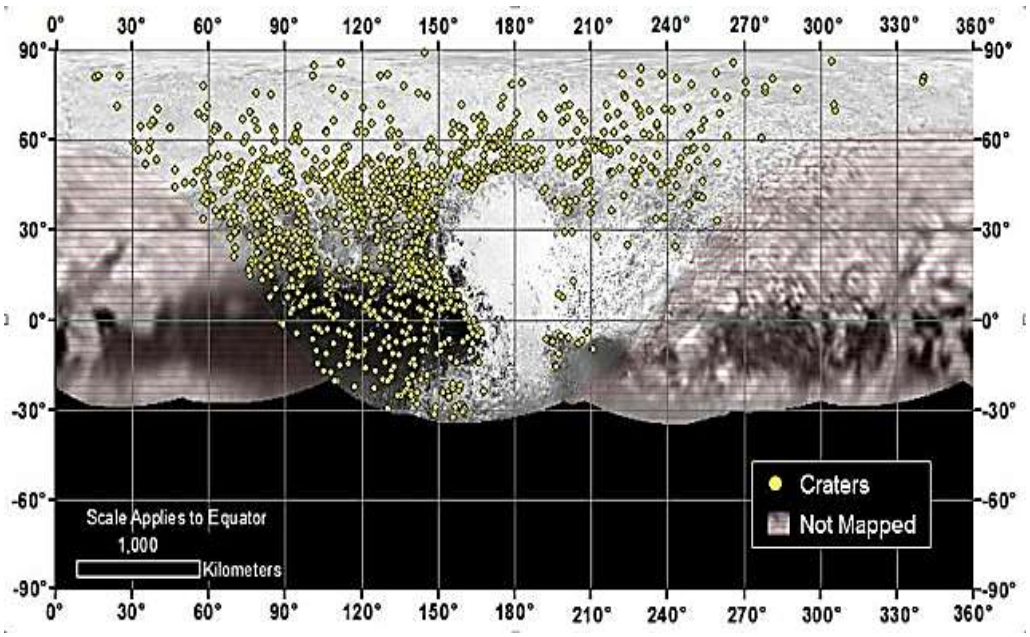

Fig. 48. More than a thousand craters have been discovered on Pluto. They vary considerably in size and appearance (http://photojournal.jpl.nasa.gov/jpeg/PIA20154.jpg).

The chains of these high mountains consist of individual blocks with sharp-edged rocks on slopes with a rather random orientation and dimensions up to 40 km across (Fig. 49, Left).This giant ridge must consist of water ice. After all, frozen nitrogen, methane [67, 131, 193, 194] and other frozen materials available on the surface of Pluto are not able to support such a huge mass of rock material. In [173] it was first proposed that the steep slopes and high mountain blocks should consist of water ice; and observations from the New Horizons probe confirmed this spectroscopically [86]. Thus, the very bright region of Sputnik Planitia borders the dark, heavily cratered Cthulhu Regio. It bears the traces of massive asteroid bombardments that all the young planetary bodies in the Solar System were subjected to four billion years ago. The dark color of the surface in this place may be due to methane, which has undergone chemical processing in the atmosphere [172, 197, 198]. It also settles at the poles, where it is carried by wind currents. The surface of Sputnik Planitia appears somewhat darker on the western side. This suggests a change in the chemical composition, or rather the structure of the surface itself. Randomly located raised dark blocks at the edges of individual convective cells [220, 222] are likely to be icebergs of frozen water floating

in the somewhat denser frozen nitrogen (Fig. 49, right). Since water ice is less dense than nitrogen-dominated ice, it is believed that these water ice hills are likely fragments of rocky hills that broke off from glaciers around Sputnik Planitia and now seem to be floating in a sea of frozen nitrogen for a long time, like icebergs. As the hills enter the cellular relief of the central part of Sputnik Planitia, they become subject to convective movements of nitrogen ice and are pushed out to the edges of the cells, where clusters of hills in groups reach up to 20 km.

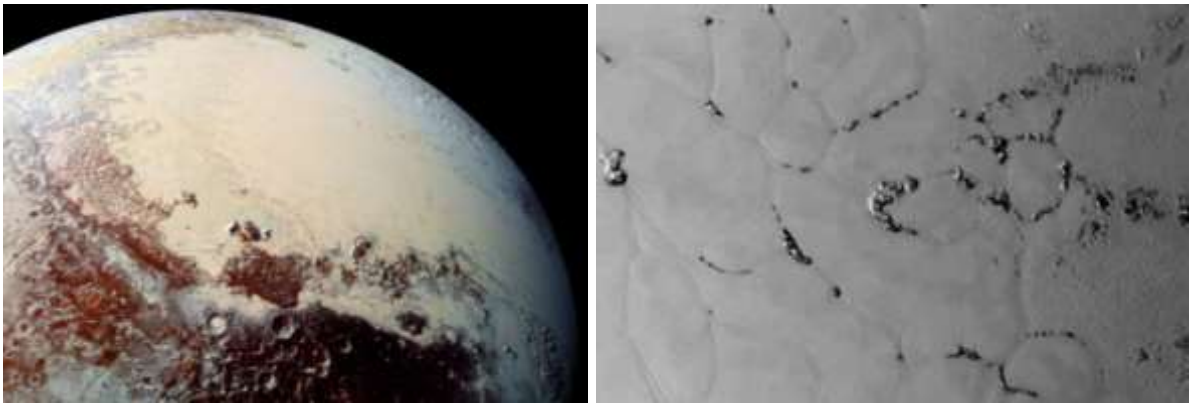

Fig. 49. On the left, mountains of hard water ice border the “soft” surface of the large frozen nitrogen sea Sputnik Planitia [96]. On the right, Sputnik Planitia contains cells that have small dark hills of water ice along the edges of the cells (https://planetary.s3.amazonaws.com/web/assets/pictures/20151221_lor_0299174905_0x632_sci_8_crop.jpg).

As shown by careful studies, most of Pluto’s surface is quite uneven. Among the various hills and depressions, meteorite craters [242] have been found. The largest of the discovered craters is up to 260 km in diameter. Canyons of tectonic [209, 211, 212, 241] origin have also been found there; their length reaches 600 km. Many of the craters are quite destroyed; some of them are even crossed by canyons; other craters may be filled with ice [173]. Some areas were cut by branched valleys. It is very likely that they could have been formed during the movement of nitrogen glaciers [130]. Quite peculiar relief forms are also found on the surface, such as extensive hills covered with small ridges elongated in one direction.

The height of such ridges is several hundred meters with a width of the gaps between them from 5 to 10 km. One explanation for the formation of such structures is the result of sublimation of ice under the influence of sunlight, or the gradual freezing of gases under the influence of constant winds on the hills or some other processes [91, 130, 206, 220]. Some of the regions are crossed by numerous parallel, smaller ridges of unknown origin, spaced about 1 km apart. They cover various surface features, including hills and craters [130].

The Al-Idrisi Montes system (Fig. 50, left) is located in the west of the Sputnik Planitia plain and is almost 380 km across. These mountains are quite densely packed. Many of the mountain blocks have either flat or gently sloping upper surfaces with textures that are similar to some of the surrounding highlands [200]. This indicates the gradual breakdown of the ancient surface that once existed here.

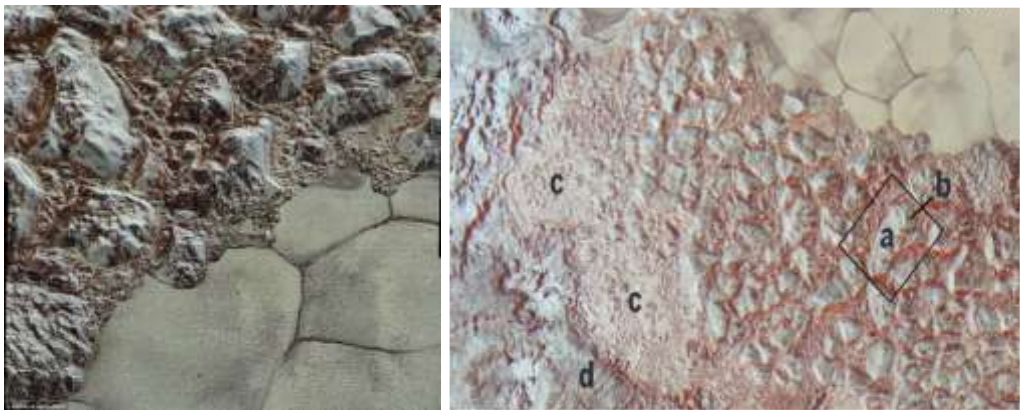

Fig. 50. Left: Images of the Al-Idrisi Montes mountains bordering Sputnik Planitia, with a resolution of 630 meters per pixel, were taken from a distance of 17,000 km 15 minutes before New Horizons approached Pluto. Many small patches of water ice have been found on the surface of Pluto (https://astro-swiss.ch/wp-content/uploads/2018/06/pluto-5.gif). Right: The chaotic Al-Idrisi Montes mountains on the northwestern edge of Sputnik Planitia. a) Textured surface, possibly preceding block formation; (b) steep fault surface with possible open bedding; (c) chaotic area consisting of small blocks; (d) inward-facing terraces [130].

The material between the individual blocks has a characteristic reddish color (Fig. 50, right). The Al-Idrisi Montes region contains two depressions "c", covered by somewhat finer interblock material and smaller blocks. Terrace "d" surrounds this depression. Among the numerous craters on Pluto's mountain ranges, two volcanically similar hills [203], Piccard Mons and Wright Mons, stand out. Their height is about 4–5 km, and their diameters are almost 160 km (Fig. 51). They have calderas at the top, typical of volcanoes. However, these volcanoes, instead of hot lava, spew a mixture of frozen water and methane, nitrogen, and ammonia.

This suggests that geological activity may still be occurring in the interior of this celestial body [208]. And these two peaks may be so-called cryovolcanoes. The peculiar hilly texture on their slopes may indicate cryovolcanic flows. If these formations are indeed volcanic, then the depressions on the peaks most likely formed as a result of collapse after the eruption. The strange hilly texture on the mountain slopes may indicate certain volcanic flows that descended from the summit to the plains located at the foot of these mountains. Images from the New Horizons spacecraft also revealed several large cracks on Pluto, up to four kilometers deep.

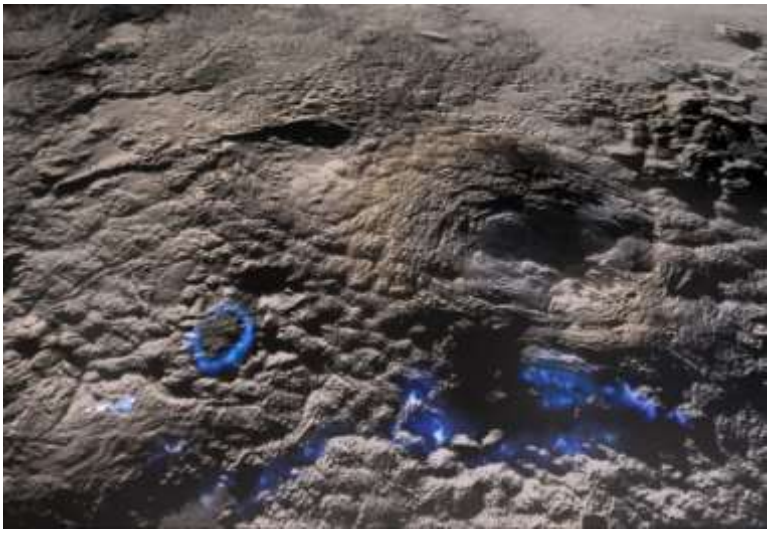

Fig. 51. Image of Pluto's surface obtained by the New Horizons space probe in 2015, with evidence of potential cryovolcanism (marked in blue) (https://thealphacentauri.net/wp-content/uploads/2022/03/29sci-pluto1-superJumbo.jpg).

The longest of them stretches for 322 km. Their presence can be explained by the decay of natural radioactive elements in the core or other global changes that once occurred on Pluto's surface. That is, Pluto's geological activity is due to the remnants of radioactive elements that have survived since the formation of the dwarf planet, and the same volatile compounds that circulate between the surface and the atmosphere. Pluto orbits the Sun in an elliptical orbit every 248 Earth years, and these substances either fall out as frost and remain frozen for decades (a kind of winter), or seasonally [172, 177, 196, 197, 201, 206, 212, 253] heat up and release methane, nitrogen, and carbon monoxide (summer). We believe that the processes of surface formation must be occurring even now. The young surface of the planet means that Pluto has some renewal mechanisms that require an internal heat source. It is assumed that Pluto may have once had a liquid ocean, which gradually gave off its heat and froze. Perhaps Pluto has radioactive materials that, decaying, release heat, forming ice volcanoes. Regardless of the source, it is safe to say that Pluto is the first icy planet that does not orbit a giant planet and therefore does not have tidal forces to influence geological processes. This tells us that geological activity can occur on icy worlds without tidal energy. This is a very important discovery in planetary science.

15. Features of the internal structure of Pluto

Pluto is inferior in size and mass not only to the large planets of the Solar System, but also to some of their satellites (Fig. 52). It is also smaller than seven planetary satellites: Ganymede, Titan, Callisto, Io, the Moon, Europa and Triton.

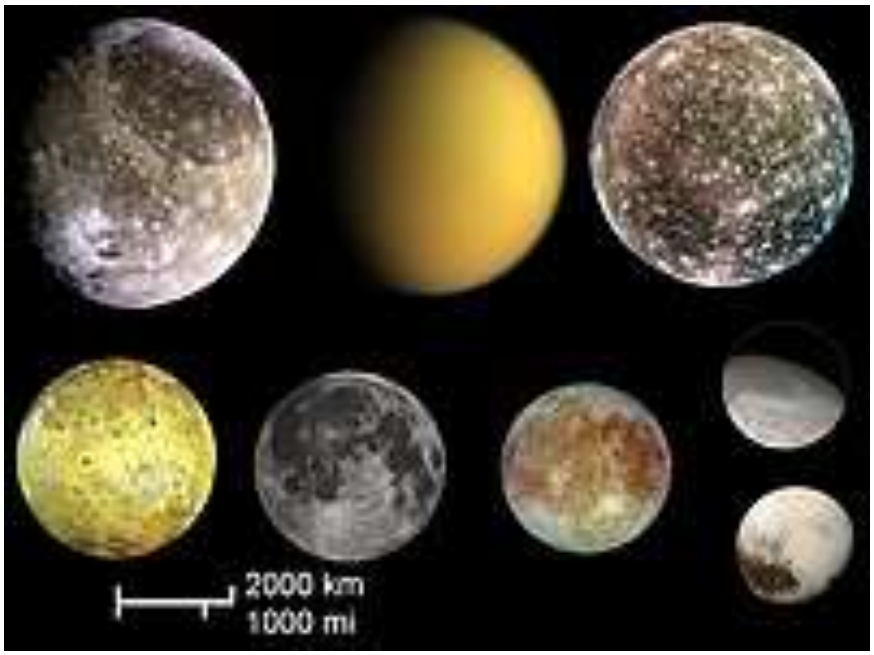

Fig. 52. Pluto (bottom right) compared to the largest satellites of the Solar System (from left to right and top to bottom): Ganymede, Titan, Callisto, Io, Moon, Europa and Triton (https://upload.wikimedia.org/wikipedia/commons/2/23/Pluto_compared2.jpg).

For example, Pluto's mass is almost six times less than that of the Moon, and its diameter is only 2/3 of the diameter of the Earth's natural satellite. However, it is 2.5 times larger and 14 times more massive than the dwarf planet Ceres, the largest cosmic body in the Main Asteroid Belt.

However, among the known trans-Neptunian objects, Pluto has the largest diameter. Although it is almost a quarter smaller in mass than another dwarf planet Eris, which is located in the scattered disk [140]. The diameter of Pluto, 2376±32 km, was only obtained in 2015 based on data from the New Horizons spacecraft [139, 173]. The oblateness of its surface was found to be less than 1%.

Very little is still known about the structure of Pluto's interior. Rough conclusions about its composition can be drawn from its average density, which is 1.860±0.013 g/cm^3 [173]. Pluto is likely to be composed of rock and ice; and judging by the high prevalence of water in the Solar System, the ice there should be mostly water. The proportion of rock may be about 65%. It is believed that, like many satellites of the giant planets and larger asteroids, Pluto's internal structure should also be differentiated (Fig. 53).

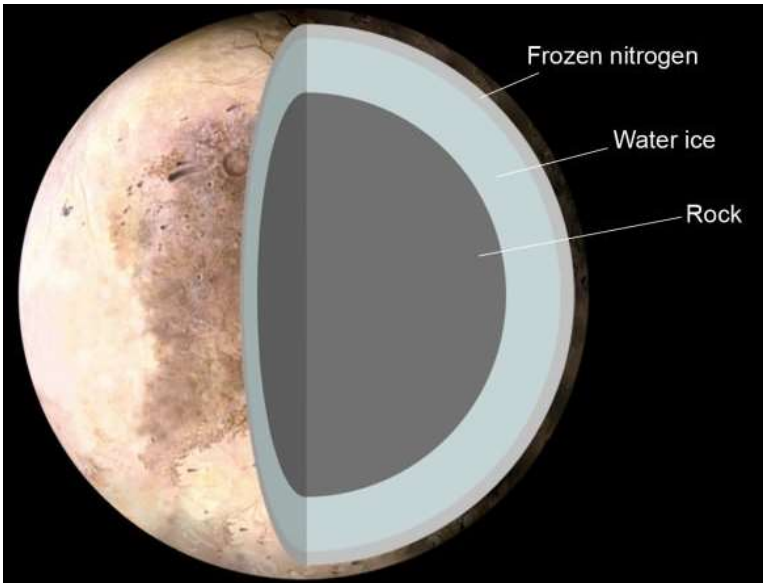

Fig. 53. Possible internal structure of Pluto (https://www.universetoday.com/wp-content/uploads/2008/05/Internal_Structure_of_Pluto.jpg).

That is, it should have a fairly dense core, most likely made of rocky material. This core may be surrounded by an icy mantle. It is likely that the diameter of the core should be about two-thirds of the diameter of the entire Pluto; that is, its size may be about 1,700 kilometers. And the thickness of the ice layer located on the boundary of the core and mantle may range from 100 to more than 200 kilometers.

Under certain conditions, at the very beginning of its formation, during the decay of radioactive elements near the core, the ice could even melt so much that the rocky rocks in its central part should separate from it. Under such conditions, it is quite possible that a huge ocean of liquid water could even have formed between the mantle and the rocky core of Pluto at that time.

And if such a model for thermal changes in the internal state of Pluto were true, then this could somehow be reflected in the nature of changes in the visible layer of this celestial body. After all, the presence of a liquid ocean under the upper mantle should have caused certain changes in the temperature gradient in the mantle and led to noticeable changes in the stress in the near-surface layer. In turn, these effects should have caused visible ruptures and compression in certain parts of the surface. That is, the surface of Pluto at that time should have been covered with surface faults, which should have covered the entire globe of the planet. And after that, frozen nitrogen, water ice and silicates could also appear on the surface of Pluto. Thus, Pluto could once have had certain sources of heat. These could be the accretion of matter during its formation, the decay of radioactive elements (which may still be ongoing to some extent), and some periodic tidal deformations by its moon Charon at a time when it was not yet turned to it on one side. It is also assumed that Pluto could have collided with another body of comparable size, and then this could have led to the formation of the current system of satellites around it. Then this could also have made a noticeable contribution to the heating of its interior.

Most likely, all this heat could have been enough to melt the ice and separate it from the rocky core [21]. It is for this reason that Pluto's interior could have become differentiated when the rocky core could have become surrounded by an icy mantle several hundred kilometers thick.

According to some model calculations, this heat could even be enough to form the above-mentioned subsurface ocean of water, as is the case for some satellites of the giant planets [132, 193]. Existing spectral data show that water ice now sometimes reaches the surface of Pluto. Although, for the most part, it is masked by a thin layer of other volatile ices [4], mainly nitrogen (up to 98%). In addition, frozen methane (according to various estimates, from 0.4% [113] to 3% [181]) and carbon monoxide (0.01-0.2% [181]) have been found there, as well as impurities of more complex compounds formed from methane and nitrogen under the influence of hard radiation. These include ethane, possibly heavier hydrocarbons or nitriles, and high-molecular-weight tholin compounds, which give Pluto (as well as some other bodies far from the

Sun) a brownish color [60, 86, 88, 96]. The frozen gases common there are colorless, and areas rich in them are quite light (Fig. 49, 50). Among the substances mentioned, nitrogen, carbon monoxide, and, to a lesser extent, methane are distinguished by significant volatility under Pluto's conditions and are therefore capable of seasonal movements on the surface, which also affects its color. Water ice is distinguished by its great strength. And therefore, only it can form relief details with a height of several kilometers. And since water ice is also light, the peculiar ice icebergs that can float in the noticeably heavier and more fluid nitrogen ice are also composed of water [91]. True, methane ice is even lighter [130]. But unlike frozen carbon monoxide, it does not dissolve well in frozen nitrogen [60] and in some places, presumably, exists in its pure form [113].

Since Pluto is located about 40 times further from the Sun than Earth, the flux of solar energy on it is 1600 times weaker. The surface temperature of Pluto varies quite significantly in different areas: from less than 40 K to almost 60 K. Higher values are observed in dark areas, lower ones in bright areas. This may be a consequence of both differences in the absorption of solar radiation and the fact that the bright surface is rich in frozen gases; and their evaporation further cools this surface. [164] suggests that Wright Mons and Piccard Mons are actually the merger of many smaller modern cryovolcanoes. This may indicate a modern source of heat on Pluto at levels previously thought impossible.

16. Features of the system of satellites around Pluto

Five moons are known to orbit the dwarf planet Pluto [217, 241] (Fig. 54). In order of distance from it, they are Charon, Styx, Nyx, Cerberus, and Hydra.

The largest of these moons is Charon [18]. Charon is also the closest moon to Pluto. It is massive enough to share a common barycenter with Pluto. It is around this that the two celestial bodies rotate in synchronous motion. This moon is named after a demon from Greek mythology who transported human souls to the afterlife.

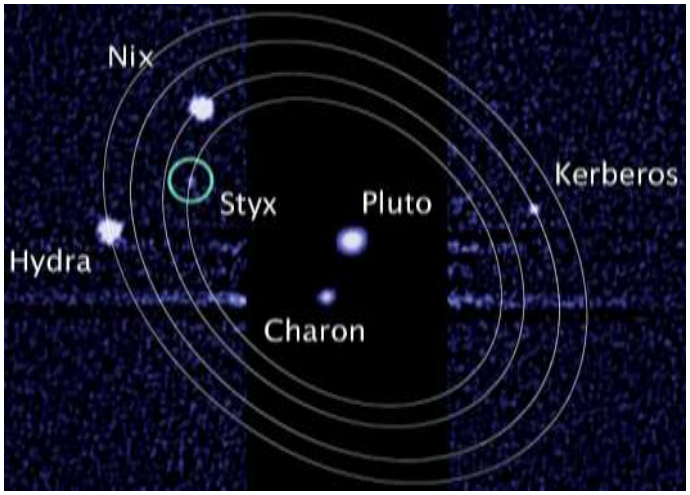

Fig. 54. Satellites orbiting Pluto (https://en.wikipedia.org/wiki/File:Pluto_moon_P5_discovery_with_moons%27_orbits.jpg).

It was discovered on 22.06.1978 by the American astronomer J. Christie. This discovery allowed to significantly reduce the estimate of the size of Pluto [86]. After all, until that moment it was believed that only Pluto reflects sunlight. According to the then estimates, in the year of its discovery in 1978, the satellite Charon had a diameter of ≈1200 km, which was half the diameter of Pluto. Pluto has a red tint, and Charon appears grayish (Fig. 55). It is assumed that the difference in color is due to the fact [60] that most of Charon's surface is covered with water ice [86]. The sizes of Pluto and Charon were determined quite accurately due to the observation of Charon passing in front of Pluto's disk. This allowed making appropriate calculations based on the

change in the brightness of the Pluto-Charon system. Charon synchronously revolves around Pluto in 6.4 Earth days at a distance of 19,640 km. As a result of the discovery of Charon's satellite, it was possible to clarify the mass of Pluto itself. It turned out to be much smaller than previously expected. Calculations showed that the center of mass of the Pluto-Charon system is located slightly above the surface of Pluto. For this reason, Pluto and Charon are sometimes considered to be a double planet.

Fig. 55. Pseudo-color photographs of Pluto and Charon taken by the New Horizons spacecraft in July 2015 (https://gdb.rferl.org/30cc6875-aaf9-489e-82be-2b68649d9a50_w1597_n_s.jpg).

Pluto’s moon Charon appears relatively smooth and not particularly cratered in the photographs. At Charon’s north pole, there is a fairly well-defined dark region (called Mordor) with an extended and diffuse reddish halo [139]. The thickness of the dark matter layer covering Mordor was found to be small.

This conclusion was reached after the discovery of several bright spots in this region. They are considered impact craters [238]. Around them, the dark layer on the surface turned out to be covered from above with a light substance, which is thrown out from a rather shallow depth. To the south of Mordor, the satellite is surrounded by a system of faults and ridges that extend up to a thousand kilometers. Another canyon several kilometers deep was found on the limb of Charon. The absence of numerous impact craters on Charon is much more difficult to explain than the smooth areas that are on the surface of Pluto [199, 200, 203]. However, it should be taken into account that the images of Charon obtained from the space probe have a much worse resolution than the images of parts of the surface of Pluto. Although it should be said that the

landforms on Pluto [218] and on its largest satellite Charon turned out to be significantly more diverse than could be expected. Moreover, the surfaces of both these bodies turned out to be very active [208, 210, 217]. The combination of chemical components and thermodynamic processes on their surfaces leads to a fairly wide range of diverse processes [211, 212]. In preparation for the launch of the New Horizons space probe, a group of astronomers from the special Pluto Companion Search Team managed to detect two other outer satellites (Fig. 56) around Pluto in images taken in May 2005 by the Hubble telescope.

Fig. 56. Pluto and its three larger satellites: Charon, Hydra and Nix (https://en.wikipedia.org/wiki/File:Pluto_and_its_satellites_(2005).jpg).

These satellites were then assigned the temporary designations S/2005 P 1 and S/2005 P 2. Their discovery was announced in October 2005. A little more than a year later, on 21.07.2006, the International Astronomical Union officially assigned them the proper names Nix, or Pluto II (formerly P 2) and Hydra, or Pluto III (formerly P 1). Since the albedo of the satellites at the time of their discovery was unknown, it was difficult to determine their sizes. If we assume that the albedo of the satellites is equal to the corresponding indicator for Charon, then their diameters were then estimated at 125 km and 140 km (with a possible error of two times). The radius of the orbit of the

smaller satellite is 49 thousand km; that is, it is 2.5 times further from Pluto than Charon. The other satellite moves in an orbit with a radius of almost 65 thousand km. Their periods of rotation around Pluto are about 11 and 14 Earth days, respectively. Charon and these two satellites are in an orbital resonance of 3:2:1. That is, in the time that Hydra makes one rotation, Nix makes two, and Charon – three. 06/28/2011 in images obtained with the Hubble telescope, it was possible to detect another satellite of Pluto S/2011 (134340) 1 (S/2011 P 1). It was given the temporary designation P4. According to preliminary estimates, its diameter was 13-34 km. The discovery of this fourth satellite, later named Kerberos, was officially announced on 07/20/2011.

A year later, on 07/07/2012, a fifth satellite was discovered, which was named Styx. It was discovered during a special search for possible potentially dangerous objects to lay a possible trajectory of the New Horizons space probe. During the rather intensive search, it was concluded that there are no other satellites, about 15 times dimmer than Styx, further from the orbit of Charon. It was also not possible to detect a possible ring system around Pluto.

The presence of four small satellites on Pluto raises many questions. After all, it remains unclear how exactly they could have condensed near another rather massive satellite, Charon. The circular nature of their orbits today indicates a very small probability of accidental capture of such bodies by Pluto's gravitational forces.

In this regard, a hypothesis was put forward that Charon and other satellites of Pluto could have arisen simultaneously as a result of some very powerful collision with Pluto of another large body. It is believed that even at the stage of its formation, Pluto could have been hit by another space object with some kind of sliding impact. As a result of such a collision, a powerful ejection of its matter should have occurred from Pluto. The incoming object itself should have completely collapsed. The main part of the fragments formed in this case formed the "new" Pluto, and from a smaller part of them Charon was formed and four more "fragments" of smaller sizes remained (Table 5). That is, the smaller satellites of Pluto were formed from the debris thrown out as a result of a massive collision between Pluto and another Kuiper belt object [178].

Table 5. Basic parameters of Pluto and its satellites.

Name	Mean diameter (km)	Mass ($\times 10^{21}$ kg	Semi-major axis (km)	Rotation period (days)	Year of discovery
Pluto	2376.6±3.2	13.05± 0.07	2390	6.387230	1930
Charon	1212±1	1.52 ± 0.06	19 571 ± 4	6.387230	1978
Nix	49.8×33.2×31.1	< 0.002	48675 ± 120	24.856 ± 0.001	2005
Hydra	50.9×36.1×30.9	< 0.002	64780 ± 90	38.206 ± 0.001	2005
Kerberos	19 × 10 × 9	0.002 ± 0.001	59 000	31	2011
Stix	16 × 9 × 8	< 0.002	42656±78	3.24 ± 0.07	2012

The information obtained by the New Horizons probe also revealed that Pluto's moon Charon is, and is currently, geologically quite active. Many dark and light areas have been found on Charon's surface. A significant part of the surface is covered with depressions and rocks up to 1000 km long. One of the rather massive canyons is up to ten kilometers deep, and another canyon is almost twice as deep. During the flyby of the New Horizons probe, in addition to Pluto and Charon, images were also obtained of all four of Pluto's moons: Styx, Nix, Cerberus, and Hydra [173]. More detailed images were obtained for Nix and Hydra. These images made it possible to specify the sizes of these moons. Recall that ground-based estimates of the size of Hydra ranged from several dozen to one and a half hundred kilometers. The surface of Hydra as a whole turned out to be very bright, although with significant variations in brightness. In terms of its albedo, it occupies an intermediate position between Pluto and Charon. This indicates that Hydra should also be covered with water ice. Nycta is somewhat smaller in size and has similar surface properties to Hydra. In general, all five of Pluto's moons have a grayer color than the dwarf planet itself. However, quite extensive red spots stand out on the surfaces of the moons of Charon and Nycta. They indicate the presence of a thin cover of tholins formed from methane [194, 2011] on these parts of the moon's surface.

17. The history of the discovery of Pluto's satellite Charon and its main characteristics

Pluto's moon Charon was discovered on June 22, 1978, by the American astronomer J. Christie [232]. This discovery led to a significant reduction in the estimated size of Pluto [231]. Up until then, it was believed that all the reflected sunlight belonged to Pluto alone. This moon of Pluto was named Charon, after the demon from Greek mythology who transported human souls to the afterlife. After the first blurry images of this moon (Fig. 57, left), images in which Pluto and Charon are separated as separate objects were first obtained by the Hubble Space Telescope in the 1990s (Fig. 57, center). And only in 1994, in the sharpest images obtained by the Hubble Telescope, it was possible to see two clearly separated disks of Pluto and Charon (Fig. 57, right).

Fig. 57. From left to right: at the time of discovery – 1978; before correction – 1990; after correction – 1994
(http://hubblesite.org/newscenter/archive/releases/1994/17/image/a/).

In July 2015, the New Horizons spacecraft was able to get as close as possible to the Pluto system. If Pluto was reddish in color [212], then Charon had a gray color (Fig. 55). It is assumed that such differences in color are due to the fact that Charon may be mostly covered with water ice [60, 86]. Based on observations of changes in brightness when Charon passes in front of Pluto’s disk, it was possible to perform appropriate calculations for the Pluto-Charon system. This allowed us to refine the parameters of both Pluto itself and its satellite (Table 6). It was also found that Pluto and Charon rotate synchronously, always facing each other with the same side.

Table 6. Main characteristics of Pluto and Charon**.**

Name	Pluto	Charon
Mean diameter, km	2372 ± 2	1208 ± 3
Mass ($\times 10^{21}$ kg)	13.05 ± 0.07	1.52 ± 0.06
Semi-major axis (km)	2390	19571 ± 4
Rotation period (days)	6.38723	6.38723

Charon is only 19,571 km from Pluto and it orbits Pluto in 6.38723 Earth days. Calculations have shown that the center of mass of the Pluto-Charon system is several kilometers above the surface of Pluto. Charon from the surface of Pluto has an angular size of about 4°; while the Sun has a size of only 39-65″. Such proximity of Charon to Pluto sometimes provides conditions when a large part of Pluto's surface can be eclipsed. And due to synchronous rotation – solar eclipses by Charon always experience the same hemisphere of the dwarf planet. This occurs when Pluto's satellite passes between Pluto and the Sun. This can only happen at two points in Pluto's orbit, which are not far from its aphelion and perihelion. The last such situation occurred on 02/25/1989. At that time, ground-based observations were possible. The next period of so-called syzygy with Charon will not begin until October 2103; it will have a maximum in 2110 and end in January 2117. At such times, solar eclipses on Pluto occur every day and last up to 90 minutes [200, 214, 215]. It was previously believed that the entire relief of Charon is covered with ancient impact craters [242]. However, images of the surface of the satellite Charon obtained by the New Horizons spacecraft have revealed that there are dark and light areas on the satellite, which are covered only by small depressions and rock formations; some of them are over 900 km long. Also on its surface, a huge canyon was found, more than 9 km deep, and the second canyon is twice as deep. That is, information from the New Horizons spacecraft revealed that Pluto's moon Charon, contrary to predictions, is a geologically very active [200, 208] cosmic body (Fig. 58). It is believed that Pluto was hit by another space object at the stage of its birth. As a result of such a collision with Pluto, matter was ejected from the dwarf planet. And the object itself, the culprit of the catastrophe, was destroyed. A

"new" Pluto was formed from the majority of its fragments and the ejected matter; and Charon was formed from a smaller part of them.

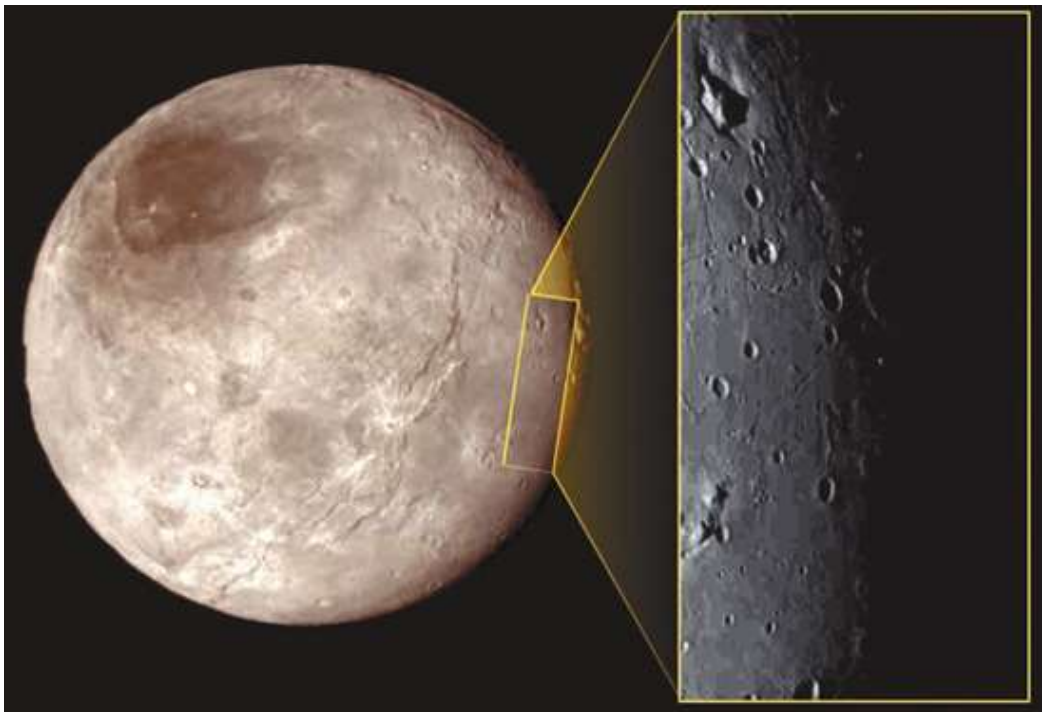

Fig. 58. Pluto's moon Charon close-up. The inset on the right with a vertical size of about 390 km shows a detail of the relief, which is a mountain in the depression (https://images.unian.net/photos/2015_07/1437121286-7680-pluton.jpg).

In the photographs obtained by the spacecraft, the surface of the moon Charon looks quite smooth and not particularly cratered. Around its north pole is a rather dark region called Mordor, with a long and diffuse reddish halo. It is believed that this reddish substance of small thickness may consist of so-called tholins [208]. Under the conditions on the surface of Charon, they are formed from methane. The methane itself may come from the atmosphere of nearby Pluto. Model calculations have shown that this satellite may receive up to 2.5% of the gases that Pluto's atmosphere is constantly losing [208].

Several spots have been found in the same region that may be impact craters. In them, the dark layer on top is covered with some light material that could have been thrown out from under the surface [231] from a relatively shallow depth. Around the Mordor region is a system of faults and ridges that extends for almost a thousand

kilometers. Another deep canyon is visible on the limb of Charon. However, it is quite difficult to explain the absence of numerous craters on the surface of Charon. However, there are extensive fairly smooth areas there.

Studies have shown that the landforms of Pluto and Charon turned out to be significantly more diverse than previously expected, and the surfaces of both these bodies are quite geologically active [139, 174]. Charon turned out to be massive enough to be in hydrostatic equilibrium [139]. The average density of Charon is slightly lower than that of Pluto and is equal to 1.702 ± 0.017 g/cm^3 [174]. This value suggests that it is about 55% rocky and up to 45% ice. After the flyby of the New Horizons spacecraft, features were discovered on the surface of Charon that clearly indicate that the internal structure of Charon has a differentiated structure. And many structural features have been found on its surface, indicating that Charon's ancient subsurface ocean may have triggered large-scale cryo-eruptions on the surface [18]. Its subsequent freezing would have caused the satellite to expand until Charon's core was warm enough again to begin the processes of the last period of compaction and contraction. It is this contraction that could have caused the appearance of the arc ridges observed in the Mordor region [121]. In contrast to Pluto's surface, which consists mainly of nitrogen and methane [132, 197] ices, Charon's surface is dominated by less volatile water ice. In 2007, the Gemini Observatory also detected patches of ammonia hydrates and water crystals on Charon's surface. This should indicate the presence of active cryogeysers and cryovolcanoes on Charon [209]. The fact that the ice was still in crystalline form suggests that it could have been deposited very recently. Solar radiation would have degraded it to an amorphous state in only about 30,000 years [58]. However, after new data were obtained during the New Horizons flyby, neither active cryovolcanoes nor geyser eruptions were detected. Later studies also questioned the cryovolcanic origin of the crystalline water ice and the characteristics of the ammonia. Instead, it was suggested that the ammonia could be passively replenished from some subsurface material [95]. Photometric mapping of Charon’s surface has shown a latitudinal range of albedo variations (Fig. 59).

Fig. 59. Map of Charon with names approved by the IAU (https://www.jpl.nasa.gov/images/pia00442-charons-first-official-feature-names).

There is a fairly bright equatorial region and much darker circumpolar regions. With the help of the New Horizons spacecraft, in addition to the Mordor region, evidence of significant geological changes in the past was found on the surface of Charon. They showed that most likely, Charon still has a differentiated structure inside. Moreover, its southern hemisphere has significantly fewer impact craters than the northern one, and it turned out to be much flatter. This may indicate that it was there that a significant surface renewal took place. It is possible that at some point in the past this was caused by the partial or complete freezing of the internal water ocean. And this led to the removal of many of the impact craters previously formed there. A system of large grabens and ledges has also been found on Charon. One of them extends almost 1000 km in the equatorial belt. Another, called Argo Chasma, may be up to 9 km deep. No noticeable atmosphere has been found on Charon [67, 173]. There are suggestions that it may be formed seasonally [197, 201, 212] on Charon for a short period during methane sublimation [183]. Under certain conditions, Charon's gravity can "drag" part of the upper atmosphere from Pluto. And any other gas that reaches Charon can be held there for some time near the surface. These may be nitrogen ions; evidence of the presence of CO_2 gas and H_2O vapor has been found there. However, their amount must be very small compared even to the amount of atmosphere on Pluto. Although the numerous spectral signatures of ice formations on Charon's surface suggest that the ice formations may provide some atmosphere, Charon's relatively low gravity causes any newly formed atmosphere to rapidly escape into space [76].

18. Hydra is a satellite of Pluto

The New Horizons team suspected that, like the giant planets [193-195, 198], Pluto [213] and Charon [225] might be accompanied by small moons [148, 224] and rings [239] associated with the Pluto system [222]. To test this hypothesis, they used remote sensing data [132, 172] from the Hubble Space Telescope. This led to the discovery of the moons Nix and Hydra [211]. Both of them were found to be quite close to Pluto and Charon. The images used for their discovery were obtained on 15 and 18 May 2005. The moons Hydra and Nix (Fig. 56) were discovered independently by M. Mutchler and E. Steffl. The discovery of these objects was announced on October 31, 2005, after previous archival images of Pluto taken with the Hubble Space Telescope in 2002 confirmed the discovery. The newly discovered moons were provisionally designated S/2005 P 1 for Hydra and S/2005 P 2 for Nix. The name Hydra was approved on June 21, 2006 by the International Astronomical Union (IAU) and was announced along with the name Nix.

Hydra was named after the Lernaean Hydra, a nine-headed serpent that fought Hercules in Greek mythology. In particular, Hydra's nine heads subtly allude to Pluto's former status as the ninth planet. In addition, the names of these two moons were chosen so that their first letters, "N" and "H," honor the New Horizons space mission to Pluto. The name Hydra was also chosen so that its initial “H” would honor the Hubble Space Telescope, which was used to discover this moon of Pluto.

The names of the features on the surface of bodies in the dwarf planet system [199, 200] Pluto [208, 212] are intended to be related to mythology, literature, and the history of exploration of this dwarf planet. In particular, the names of the features on the surface of Hydra are intended to be related to legendary serpents and dragons in literary sources, mythology, and history. All of Pluto's smaller moons, including Hydra, are believed to have formed from debris ejected from a massive collision [210, 242] between Pluto and another Kuiper belt object [178]. The debris from this collision eventually coalesced into Pluto and all of its moons. It has even been suggested that

Hydra originally formed closer to Pluto, and its orbit was altered by its tidal interactions [148].

In this case, Hydra, along with Pluto's smaller moons, would have migrated outward with Charon to their current orbits around the Pluto-Charon barycenter. Due to the "tidal damping" of mutual tidal interactions with Charon, Hydra's orbit around the Pluto-Charon barycenter gradually became more circular over time. Images obtained in July 2015 from the New Horizons spacecraft with detailed images of Hydra (Fig. 60) allowed for the first time to determine the size of this moon with sufficient accuracy: 50.9 km × 36.1 km × 30.9 km [192]. Hydra turned out to be the second largest moon of Pluto. Hydra is the fifth and most distant moon of Pluto, with a semi-major axis of 64,738 km [173]. Its mass is $(3.01\pm0.30)\times10^{16}$ kg and its average density is 1.220 ± 0.150 g/cm^3. Its synodic period is 10.31^h.

Fig. 60. A true-color image of Hydra taken by the New Horizons spacecraft on July 14, 2015 (https://commons.wikimedia.org/wiki/File:Hydra_reprocessed.png).

The average surface temperature of Hydra is about 23 K. Overall, Hydra's surface is very bright with a high degree of reflectivity, although with significant variations in brightness. On average, it reflects almost 83% of the sunlight falling on it. This means that Hydra's surface should be covered with water ice. Hydra's surface, like other small moons of Pluto, has a neutral spectrum. And the water ice on the surface of Hydra is quite clean and therefore does not show significant darkening, compared to Charon (Fig. 61).

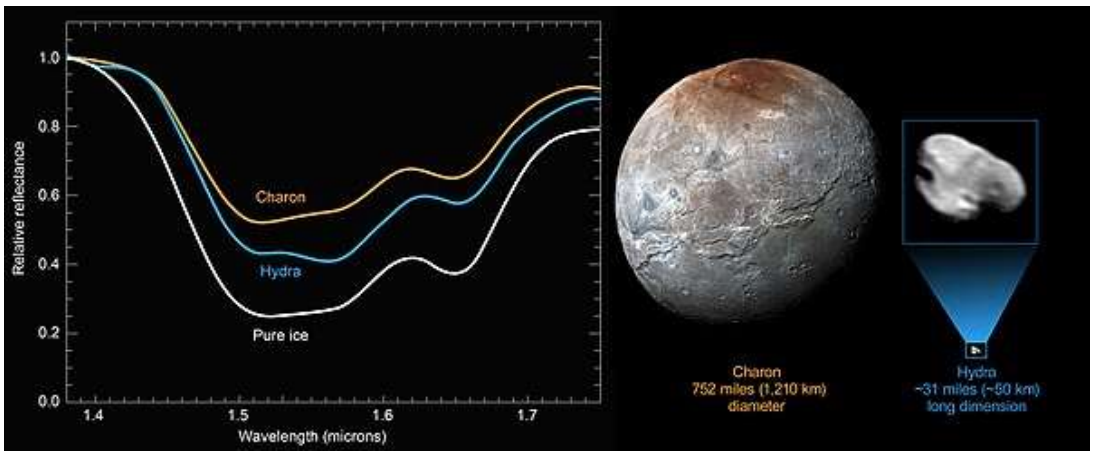

Fig. 61. Comparison of the spectra of the satellites Hydra and Charon. The spectrum of Hydra closely matches the spectrum of pure water ice, which is shown for comparison (https://photojournal.jpl.nasa.gov/jpegMod/PIA20581_modest.jpg).

One explanation for this is that Hydra's surface is frequently resurfaced by micrometeorite impacts, which eject lighter material from beneath the surface of the satellite. Hydra's surface composition, reflectivity, and other basic physical properties were measured during the close flyby of the New Horizons spacecraft through the Pluto system on July 15, 2015. A detailed image of Hydra, taken from a distance of 640,000 km, revealed variations in brightness on its surface and a rather dark circular formation with a diameter of about 10 km. The spectrum of Hydra appears slightly bluer because Hydra has a larger amount of water ice on its surface. This fact also explains the relatively high geometric albedo of this moon. According to crater counts from the New Horizons spacecraft, the age of Hydra's surface is estimated to be about four billion years [246]. Large craters and depressions on Hydra's surface indicate that it may have lost some of its original mass through impacts since its formation [246].

Studies of Hydra show that its surface is not tidally locked and rotates chaotically; its period of rotation and axial tilt vary rapidly on astronomical timescales, to the point that its axis of rotation regularly flips. The chaotic nature of Hydra's motion is largely due to the varying gravitational effects of Pluto and Charon, which orbit around their barycenter. The chaotic nature of the moon's motion is also enhanced by its rather irregular shape, which creates significant rotational moments [157]. During the New

Horizons flyby of Pluto and its moons, Hydra had a rotation period of about 10 hours; its axis of rotation was tilted by almost 110 degrees to the plane of its orbit [246].

Compared to the other moons of Pluto, Hydra rotates quite rapidly. The rotation periods of the other moons exceed one Earth day. This rapid rotation of Hydra is typical of the rotation periods of most objects in the Kuiper belt. Like all Pluto's moons, Hydra's orbit is nearly circular and coplanar with the orbit of Charon [173]. Because of such circular orbits, it is suggested that Pluto's moons should have undergone tidal evolution since their formation [148, 170].

Hydra has an orbital period of about 38.2 Earth days and is in resonance with the other moons of Pluto. Thus, the satellite Hydra is in a 2:3 orbital resonance with the satellite Nix and in a 6:11 resonance with the satellite Styx [157]. And with Charon, the orbit of Hydra is close to an orbital resonance of 1:6. It is believed that such resonances arose at the beginning of Charon's migration, immediately after the formation of all five known satellites of Pluto; and these resonances are supported by periodic local fluctuations in the Pluto-Charon gravitational field strength by about 5% [244].

19. Nix – Pluto's moon

Before the launch of the New Horizons spacecraft, a special group of astronomers was created - the Hubble Space Telescope Pluto Companion Search Team [213]. The members of this team suspected that, like other planets in the solar system [172, 193, 194, 196-198], Pluto [218] and its moon Charon may be accompanied by other moons and, perhaps, even rings [239]. Any of these objects could prevent a safe approach to these celestial bodies. Therefore, in 2005, a team of researchers used the Hubble Space Telescope to search for faint moons around Pluto [224]. Since the brightness of these moons should be much lower than even Charon, they obtained images of the sky with long exposures. For example, the luminous flux from the later discovered moon Nix was about 5000 times fainter than that from Pluto. The images used to discover the next two moons were obtained on 15 and 18 May 2005. Analysis of the images in mid-July 2005 revealed two previously unknown moons around Pluto (Fig. 62). These two outer moons were then designated S/2005 P 1 and S/2005 P 2. After careful verification of the data obtained, their discovery was officially announced in late October 2005 [46, 170]. Almost a year later, on 21 June 2006, the International Astronomical Union officially assigned them the proper names Nix, or Pluto II (P 2) and Hydra, or Pluto III (P 1). Nix was named after Nyx, Charon's ferryman of Hades in Greek mythology.

The initial proposal for the name Nix was to use the classical spelling Nyx. But to avoid confusion with the name of the asteroid 3908 Nyx, the spelling was changed to the Coptic spelling of the name Nix; the adjectival form of the name is Nictian. The names of individual elements on the bodies of the Pluto system should be associated with mythology, literature and the history of research on the central celestial body. In particular, the names of objects on Nix should be associated with the deities of the night mentioned in literature, mythology and history.

Since the exact albedo of the newly discovered satellites was then unknown, it was difficult to say anything about their sizes. Therefore, it was assumed that the albedo of the satellites is equal to the corresponding indicator for Charon [224, 225]. Under these conditions, the diameters of the satellites were estimated at 125 km and 140 km

with a possible error of almost twice. The orbital radius for the smaller satellite is about 48.71 thousand km. Thus, it is almost 2.5 times further from Pluto than Charon. Another, slightly larger moon, is in an orbit with a radius of 64.75 thousand km. Under these conditions, their periods of rotation around the dwarf planet [199, 200] Pluto and the period of the moon Charon are in orbital resonance 3:2:1 [148, 244, 246]. The moon Nix has similar dimensions and surface properties to Hydra [226]. For the moons Nix and Hydra, the New Horizons space probe obtained quite detailed images (Fig. 63) when it flew past the Pluto system in July 2015.

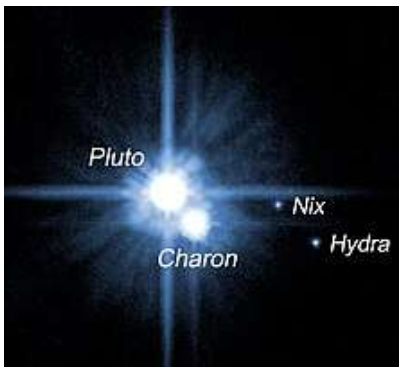

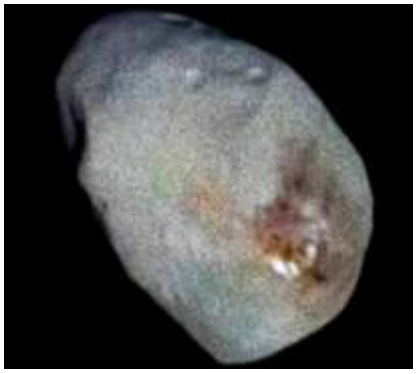

Fig. 62. Images of Pluto's moons obtained with the Hubble telescope (https://en.wikipedia.org/wiki/File:Pluto_and_its_satellites_(2005).jpg).

Fig. 63. Pocessed image of Nix (Enhanced color image of Nix, taken by “New Horizons”) (https://upload.wikimedia.org/wikipedia/commons/5/51/Nix_best_view.jpg).

At the same time, for Pluto's natural satellite [203, 208, 211, 212] Nix was able to measure its dimensions quite accurately: 49.8 km × 33.2 km × 31.1 km [192]. It turned out to be the third largest moon of Pluto, being only slightly smaller than Hydra. Nix is also the third satellite of Pluto and in distance [173].

Nix has no tidally-formed surface and moves erratically, like all of Pluto's smaller moons; its axial tilt and period of rotation vary greatly over short periods of time. Due to its erratic rotation, Nix can even flip its axis of rotation from time to time. The erratic motions of Pluto's small moons are caused by the gravitational effects of Pluto and Charon. The erratic motion of Nix is further enhanced by its elongated shape [157].

Nix orbits the Pluto-Charon barycenter between the orbits of Styx and Kerberos. All of Pluto's moons have circular orbits. And they all have very low orbital inclinations to Pluto's equator [119, 170]. This indicates that all of the moons have undergone tidal evolution since their formation [170]. Nix has an orbital period of 24.8546 Earth days, and its orbit is in resonance with other moons of Pluto. For example, Nix is in a 3:2 orbital resonance with Hydra and a 9:11 resonance with Styx [157]. As a result of this three-body resonance, it couples with Styx and Hydra in a 2:3 ratio. Nix's orbital period is close to the 1:4 orbital resonance with Charon, with a time difference of up to 3% [44, 148, 157].

Early remote observations of the moon showed that Nix's surface has a reddish color [44]. Other remote observations showed that Nix is spectrally neutral, similar to the other small moons of Pluto [172, 246]. Nix has also varied in brightness and albedo [175]. The brightness variations were thought to be caused by the appearance of regions of different albedo on the surface of Nix [175]. This was confirmed by close-up images taken by the New Horizons spacecraft. They showed a large reddish region on the surface of Nix, approximately 18 km across. The reddish region is thought to be a large impact crater where reddish material was ejected from beneath the water ice layer on Nix's surface and deposited on its surface.

In this case, Nix would likely have regolith originating from such an impact [178, 242, 246]. Another explanation suggests that the reddish material could have resulted from a collision of Nix with another object of slightly different composition. However, observations have shown that no significant color variations were detected in other impact craters on the surface of Nix [246]. The water ice present on the surface of Nix is likely responsible for its high reflectivity.

Traces of frozen methane may also be present on the surface of Nix [201]. They may be the reason for the reddish material on its surface; most likely, they may be tholins. It is believed that tholins on the surface of Nix could have arisen as a result of the reaction of methane with ultraviolet radiation from the Sun. According to crater counting data on images obtained by the New Horizons space probe, the age of the surface of Nix is estimated to be at least four billion years [246]. To explain the

resonances between the rotation periods of all Pluto's moons, it has been proposed to consider the influence of the gravitational field strength of the Pluto-Charon system. Of the smaller Pluto moons, only Nix and Hydra have been imaged with a resolution sufficient to clearly see details (Figs. 63, 64) on their surfaces.

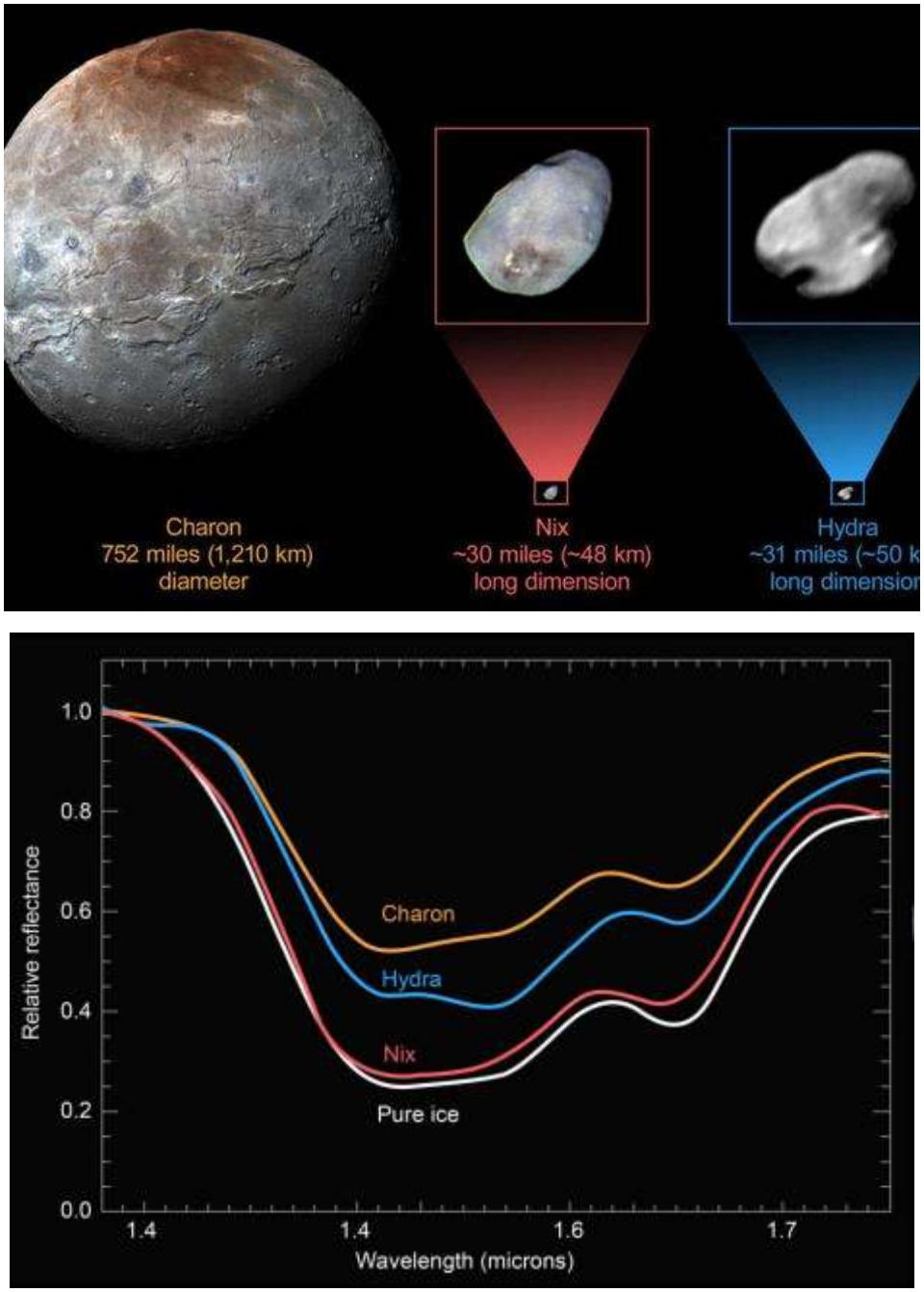

Fig. 64. Surface appearance (https://zn.ua/img/article/3496/59_main-v1591860776.jpg) and spectra (https://zn.ua/img/forall/u/0/-1/users/Jun2016/150964.jpg) of Pluto’s moons Charon, Nix, and Hydra.

20. Cerberus is a satellite of Pluto

On 28.06.2011, researchers from the Pluto Companion Search Group, using images obtained by the Wide Field Camera on the Hubble Space Telescope with exposures of about 8 minutes, discovered another satellite of the dwarf planet [199, 200, 203, 208] Pluto, S/2011 (134340) 1 (S/2011 P 1) [213, 224]. It received the temporary designation P4. According to preliminary estimates, its diameter could be in the range from 13 to 34 km. On 20.07.2011, the discovery of the fourth satellite was officially announced. At that time, it was proposed to give it the name Kerberos.

The convention for naming Pluto's satellites is to use names associated with the god Pluto in classical mythology. To decide on a name for the moon, Mark Showalter and the SETI Institute conducted an online poll on behalf of the research team in 2013, asking the general public to vote for their favorite names. The public could choose from a selection of Greek mythological names related to the god Pluto, or they could suggest their own names. After the initial announcement, actor William Shatner suggested the names Vulcan and Romulus, referring to Pluto's nephew, the fire god Vulcan, and the founder of Rome, Romulus. [250] The suggestion "Romulus" was rejected because an asteroid moon with the same name already existed. However, the name "Vulcan" won the poll after Shatner tweeted about it.

Second place went to "Cerberus," the dog that guards Pluto's underworld. Third place went to "Styx," the goddess of the river of the underworld. The names of these winners were submitted to the International Astronomical Union (IAU) [250]. However, the name "Vulcan" was not acceptable to the IAU, as it was not the name of an underworld deity and was already used for a hypothetical planet inside the orbit of Mercury, and had also given its name to hypothetical vulcanoids. The name "Cerberus" was already used for the name of an asteroid, 1865 Cerberus. However, the Greek form of the same name, "Kerberos", was accepted by the IAU. And on 2 July 2013, the IAU announced that it had officially approved the Kerberos name for Pluto's moon P4. Names of elements on the surface of bodies in the Pluto system should be related to mythology, literature, and the history of exploration of this dwarf planet. In particular,

names of objects on Kerberos should be related to dogs from literature, mythology, and history. The previous designation of a moon depends on the source used. The International Astronomical Union announced the name of the moon as S/2011 (134340) 1, while the New Horizons website announced it as S/2011 P 1. Thus, the moon Kerberos was discovered during an attempt to find any rings [239] that Pluto might have. The search for rings similar to those of the giant planets [172, 193, 197, 198] was motivated by the desire to avoid possible damage to the New Horizons space probe during its July 2015 flyby of the Pluto system.

Observations of the Pluto system were also conducted on July 3 and 18, 2011. And on July 20, 2011, Kerberos was confirmed as a newly discovered moon of Pluto based on all the data received. It was later found and identified in earlier archival images taken with shorter exposures with the Hubble Space Telescope on February 15, 2006, and June 25, 2010. At that time, Kerberos was obscured by diffraction flares in those images. Kerberos is only about 10% as bright as its satellite Nix.

Kerberos, like all other Pluto moons [178, 226], is thought to have formed from the coalescence of debris from a massive collision between Pluto and another object in the Kuiper Belt [242]. Kerberos is bilobed and measures about 19 km in its longest dimension and 10×9 km in its shortest dimension. It is believed that the two-bladed shape of Kerberos is likely formed by two smaller objects that merged many years ago. Kerberos has a fairly high albedo, up to 0.6. This reflectivity is similar to other small moons of Pluto [148, 173, 175]. This indicates a high probability of the presence of water ice, rather than nitrogen [211, 212] or methane [201] ice on its surface. Before the flyby of the New Horizons space probe, Kerberos was believed to have a darker surface and therefore a slightly larger size.

Like other small moons of Pluto, the surface of Kerberos is not the result of the action of a tidal mechanism. In addition, its rotation is quite chaotic, and changes relatively quickly on geological time scales. The varying gravitational effects of Pluto and Charon, as they rotate around their common barycenter, cause chaotic changes in the tilt of the axis of rotation of all of Pluto's small moons, including Kerberos. At the time of the New Horizons flyby (Fig. 65), Kerberos had a rotational period of about

5.33 Earth days; its axis of rotation was then tilted about 96 degrees to the plane of its orbit.

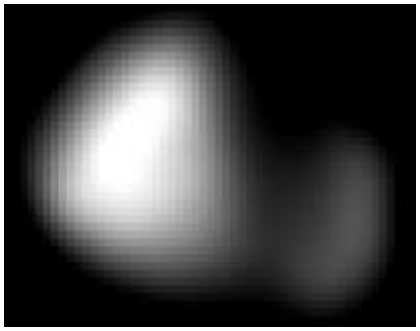

Fig. 65. Image of Kerberos obtained by the New Horizons spacecraft on July 14, 2015 from a distance of 396,100 km (https://thesolarsystem.fandom.com/wiki/Kerberos?file=KerberosPaint.NET.pn).

Remote sensing of Kerberos indicates a nearly circular equatorial orbit around the Pluto-Charon barycenter at a distance of 57,783 km [157]. All of Pluto's moons have such highly circular orbits (the eccentricity of Kerberos' orbit is only 0.00328±0.00020) with a very low inclination to Pluto's equator.

Kerberos orbits between the moons Nix and Hydra [226, 246], and completes one complete orbit around Pluto approximately every 32.167 Earth days. Its orbital period is close to the 1:5 orbital resonance with Charon, with a time difference of about 0.7%. As with the close resonances between Nix or Hydra with Charon (1:4 and 1:6, respectively), determining how close this relationship is to a true resonance requires more precise knowledge of Kerberos' orbit.

On July 14, 2015, during a flyby of the Pluto system, the New Horizons spacecraft acquired images of Kerberos. However, the first images were not released until three months later, on October 22. It was the last Pluto moon to have surface images released. They showed Kerberos to be quite small and have a fairly bright surface. This contradicted the original idea that the moon's surface was covered with some kind of dark material.

21. Styx – Pluto's smallest moon

On 11.06.2012 M.R. Showalter discovered a fifth moon (Fig. 66) around the dwarf planet Pluto [203, 208]. It was found in several images obtained on 26, 27 and 29 June and 7 and 9 July 2012 by the Wide Field Camera on the Hubble Space Telescope [158]. It was discovered while searching for possible potentially hazardous objects to plot a possible trajectory for the New Horizons space probe.

Fig. 66. Hubble image at 07.07.2015 of Styx (circled), with the outer moons' orbits shown (https://upload.wikimedia.org/wikipedia/commons/1/1a/Pluto_moon_P5_discovery_with_moons%27_orbits.jpg).

During the rather intensive search, it was concluded that there are no other satellites, about 15 times dimmer than the newly discovered satellite, beyond the orbit of Charon [173, 225]. Also, it was not possible to detect the ring system around Pluto, which exists around all giant planets [172, 193]. According to the observational data obtained, the diameter of the satellite could be in the range from 10 to 25 km. These values were calculated based on the apparent magnitude of the discovered satellite and using the albedo value of 0.35 in the calculations. This satellite turned out to be the

smallest of the five satellites [228] of Pluto known at that time. Its dimensions were refined to 16×9×8 km according to the single, albeit not very successful image (Fig. 67), taken by the New Horizons space probe in July 2015. It orbits between the satellites Charon and Nix with a period of about 20.16 Earth days [158] at a distance of about 42,656 km from the barycenter of the Pluto-Charon system [148, 212]. This satellite completes a complete rotation around its axis in a rather chaotic manner in 3.24±0.07 Earth days.

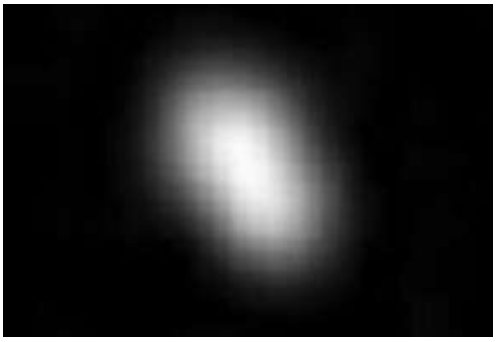

Fig. 67. Pluto's moon Styx, as seen by the New Horizons spacecraft on July 13, 2015, from a distance of 632,000 km (https://upload.wikimedia.org/wikipedia/commons/3/38/Styx_%28moon%29.jpg).

The discovery of this moon was announced on July 11, 2012. It was named Styx. The convention for naming Pluto's moons is to use names associated with the god Pluto in classical mythology. Styx is the name of a goddess and a river in the underworld. This name was approved by the International Astronomical Union [250].

Styx is about a hundred thousand times dimmer than Pluto and has a mass of about 7.5×10^{15} kg. The discovery of yet another small moon of Pluto has raised concerns that there may be more bodies in this region of space that are too small to detect, and that the spacecraft could have been damaged by an unknown body, or by a ring around the dwarf planet, as it passed through the Pluto system at speeds of over 13 km/s. Such tiny moons are also usually associated with thin rings or arcs, because their gravity is unable to hold back material ejected by meteoroid impacts [242]. Such diffuse material therefore poses a major navigational hazard. Fortunately, however, the New Horizons

spacecraft did not detect any smaller moons [246] or rings [239] and passed safely through the Pluto system.

All of Pluto's moons have been found to be in orbits that are very close to circular and coplanar with Pluto's orbit. All the satellites found around this dwarf [199, 200, 211] planet are in orbital resonance with each other [1, 250]. In contrast to orbital rotation, rotation around its own axis is quite chaotic [224, 226]. After all, as with other small satellites of Pluto, the surface of the satellite Styx is not regulated by the tidal mechanism [227]. Therefore, its rotation changes at very short time intervals.

22. On the search for rings around Pluto

Initially, the presence of rings around Pluto, due to its considerable distance from Earth, was predicted by some indirect signs [171]. In 1991, Robert Bless proposed using the equipment on the Hubble telescope for such a search [31]. In 1994, the magazine "Spaceflight" reported on NASA's plans to fly a spacecraft to Pluto. The plans for research with such devices also reported on the search for rings around Pluto. At that time, it was reported that if rings around Pluto exist, they may be located at a distance of about 1200 km from the planet; and if rings exist around its satellite Charon [225], they may be located at a distance of up to 4200 km from Charon.

A group of American scientists led by Alan Stern of the Southwest Research Institute [171, 174] also suggested in 2006 that Pluto had a ring system. They suggested that the sources of material for such rings could be Pluto's moons Nyx and Hydra [226, 227], as well as the later discovered Styx and Kerberos [228, 230]. A group of Brazilian astronomers in 2011 presented their calculations of the existence of a ring system around the then dwarf planet Pluto [147]. According to their calculations, Pluto's moons are constantly bombarded by micrometeorites. For this reason, a rather dark ring of dust particles with sizes from 1 to 10 μm should form around the dwarf planet. The width of these rings could reach 16,000 km. Due to the influence of the solar wind, half of these particles should have settled back on the satellites within one year.

In preparation for the launch of the space probe "New Horizons" to study the then ninth planet of the Solar System, Pluto, a group of astronomers Pluto Companion Search Team began a special program to search for possible potentially dangerous objects when plotting a possible trajectory of the space probe. For this purpose, it was planned to use astronomical images of the starry sky near Pluto, specially obtained by the Hubble telescope. This search program was dedicated to the search for a possible system of rings and other celestial bodies around Pluto [174]. And already on 15.05.2005 in these images, in addition to the satellite Charon [183], it was possible to detect two more small satellites around Pluto. They were then given the temporary designations S/2005 P 1 and S/2005 P 2. A little more than a year later, on July 21,

2006, the International Astronomical Union officially assigned them the proper names Nix, or Pluto II (P 2) and Hydra, or Pluto III (P 1). On July 20, 2011, the discovery of Kerberos, the fourth moon around Pluto, was officially announced. It was also discovered using images obtained with the Hubble telescope.

Using the same images, an attempt was made to search for a possible ring system around Pluto, or at least the arcs that were found around one of the giant planets. A year later, on July 7, 2012, a fifth moon, which was named Styx, was discovered. During the rather intensive searches, it was concluded that there are no satellites about 15 times dimmer than Styx beyond Charon's orbit. No ring systems were found either. In July 2015, the Pluto system was visited by the New Horizons space probe. The spacecraft's close approach to the planet provided the best opportunity to see them. If rings exist, they must be so sparse that their geometric albedo is less than $1 \cdot 10^{-7}$. According to various estimates, the optical thickness of possible hypothetical dust clouds can vary from $4 \cdot 10^{-10}$ to $5 \cdot 10^{-6}$.

In [108], the results of studies on the search for possible dust particles in the Pluto-Charon system before, during, and after their encounter with the New Horizons space probe in July 2015 are presented. The methodology of the studies performed included attempts to detect backscatter of solar radiation from possible dust rings at a phase angle of $\alpha \sim 15°$ during the approach of the space probe to Pluto, detection of the scattering particles themselves, observation of stellar eclipses by Pluto at the moments of the closest approach of the space probe to Pluto, and observation of scattering of solar radiation by dust particles at a phase angle of $\alpha \sim 165°$ during the distance of the space probe from the Pluto system. The search for rings in backscattered sunlight covered a range of distances from 35,000 to 250,000 km from the BaryCenter of the Pluto-Charon system [147]. Such distances covered a zone that began from the inner part of the orbit of the satellite Styx and extended four times the radius of the orbit of the most distant known satellite Hydra. All previous observational studies have shown no discernible rings, debris, or dust. However, these new ring detection limits provide a significantly improved picture of the surrounding space throughout the Pluto-Charon

system. Beyond a distance of 100,000 km from Pluto, observations with the Hubble Space Telescope have shown a complete absence of dust particles.

Scattered light searches for dust ejected from micrometeorite bombardment [242] from Pluto's surface have also failed to reveal evidence of a ring or dust cloud within 10,000 km. Several observations of the star coverage of Hydra have also indicated the absence of dust or debris around this moon. The dust counter on the New Horizons spacecraft detected a single particle impact at a distance of 3.6×106 km from Pluto. This value is consistent with the interplanetary space environment. The results support recent studies indicating that small dust particles are rapidly lost from the Pluto system [203, 208, 211, 212, 213, 224] due to solar radiation pressure. And particles of somewhat larger size are orbitally unstable due to constant perturbations by the currently known satellites in the Pluto–Charon system. Thus, a long search for rings from 2005 to 2015 using the Hubble Space Telescope contributed to the conclusion that there were no rings around Pluto. And after the flyby of the New Horizons space probe, the hypothesis of the existence of a supposed ring system around the dwarf planet [199, 200] Pluto was completely refuted.

23. Changes in temperature and pressure in Pluto's atmosphere

The dwarf planet Pluto is nearly spherical in shape with an equatorial diameter of 2374 km. Pluto orbits the Sun at 29.657 AU at perihelion and 48.87 AU at aphelion [233]. For almost 20 years, from 1979 to 1999, it was closer to the Sun than the giant planet Neptune. In 1999, Pluto crossed Neptune's orbit again and became the most distant planet. Pluto rotates in the opposite direction with a day length of 6.387 Earth days and an inclination of its axis to the plane of its orbit of more than 120°. Therefore, the seasons [250] should be more pronounced there than on Earth. As of 2025, its north pole is tilted toward the Sun, and spring is in full swing in its northern hemisphere.

At the same time, the temperature on its surface can vary seasonally [203, 208, 211, 212] from 33 K at aphelion to about 60 K at perihelion. Under such conditions, water and all liquids and gases that can exist on Pluto's surface freeze [161, 222]. These also include nitrogen N_2, methane CH_4, carbon monoxide CO and their derivatives. All of these compounds have freezing points much lower than even water. Pluto's rather thin atmosphere also consists mainly of nitrogen, as well as methane [10] and carbon monoxide. All of them are often in equilibrium with their frozen forms on the surface. Therefore, as Pluto moves away from the Sun, most of its atmosphere freezes in the winter and remains frozen for over a hundred years. And at perihelion in the summer, the surface heats up again and releases nitrogen, methane, and carbon monoxide.

Data from the New Horizons space probe on the atmosphere on Pluto showed that the atmospheric pressure in 2015 was almost 2 times lower than that measured just a few years earlier [216]. Most likely, the surface pressure varies seasonally in the range from 0.6 to 2.4 Pa [218, 221]. It is under such physical conditions in the upper part of Pluto's atmosphere that molecular nitrogen N_2 begins to absorb sunlight already when the spacecraft is just beginning to approach the planet's shadow during the observed solar eclipse. As the eclipse progresses, atmospheric methane and other hydrocarbon components also begin to absorb sunlight. When the space probe left Pluto's shadow, the reverse process was observed. That is, the analysis of the obtained observational data showed that the characteristics of the atmosphere on opposite sides of Pluto were

practically the same. This made it possible to follow the changes in thickness and partially measure the composition of Pluto's atmosphere. The obtained data showed that Pluto's atmosphere is actually much thicker than previously thought. However, such facts can only be a seasonal phenomenon. After all, frozen nitrogen on the surface of the dwarf planet [74, 199, 200] could be exposed to direct sunlight, and this could cause its sharp increase in evaporation.

Such a phenomenon, similar to other planets [67, 132, 134, 193, 194], can be associated with seasonal changes [238, 240], and last on Pluto for several decades. While Pluto is closer to the Sun, it may have a noticeable atmosphere. In addition, Pluto's troposphere [261] is only a very thin and discontinuous boundary layer. And the temperature within it is relatively constant [85]. This tropospheric layer was discovered by radio scanning of the atmosphere with equipment on the New Horizons probe. It was detected when the spacecraft passed Pluto.

The thickness of this layer was about 4 km, and the temperature when measured was 37 ± 3 K. After all, the value of the saturated vapor pressure of molecular nitrogen is equal to the observed value of the atmospheric pressure at this temperature. It is believed that this boundary layer consists of gas that has only recently been able to evaporate from the planet's surface and has not yet had time to mix with the rest of the atmosphere. This scenario is supported by the fact that this layer was observed over the Sputnik Planitia plain (Fig. 68), which is currently a large reservoir of such volatile ices. Their evaporation could have occurred either at the time of observations from the space probe or shortly before. Calculations have shown that without constant renewal this tropospheric layer could exist for no more than a couple of Earth years [85]. Above this boundary layer, the stratosphere region begins. In it, the temperature increases quite rapidly with height; that is, the so-called temperature inversion is observed there. The rate of such increase varies significantly in different places above the surface of Pluto. For example, when the space probe set behind Pluto, its measured value was 6.4±0.9 K/km, and when the device left the planet's shadow, it was already equal to 3.4±0.9 K/km.

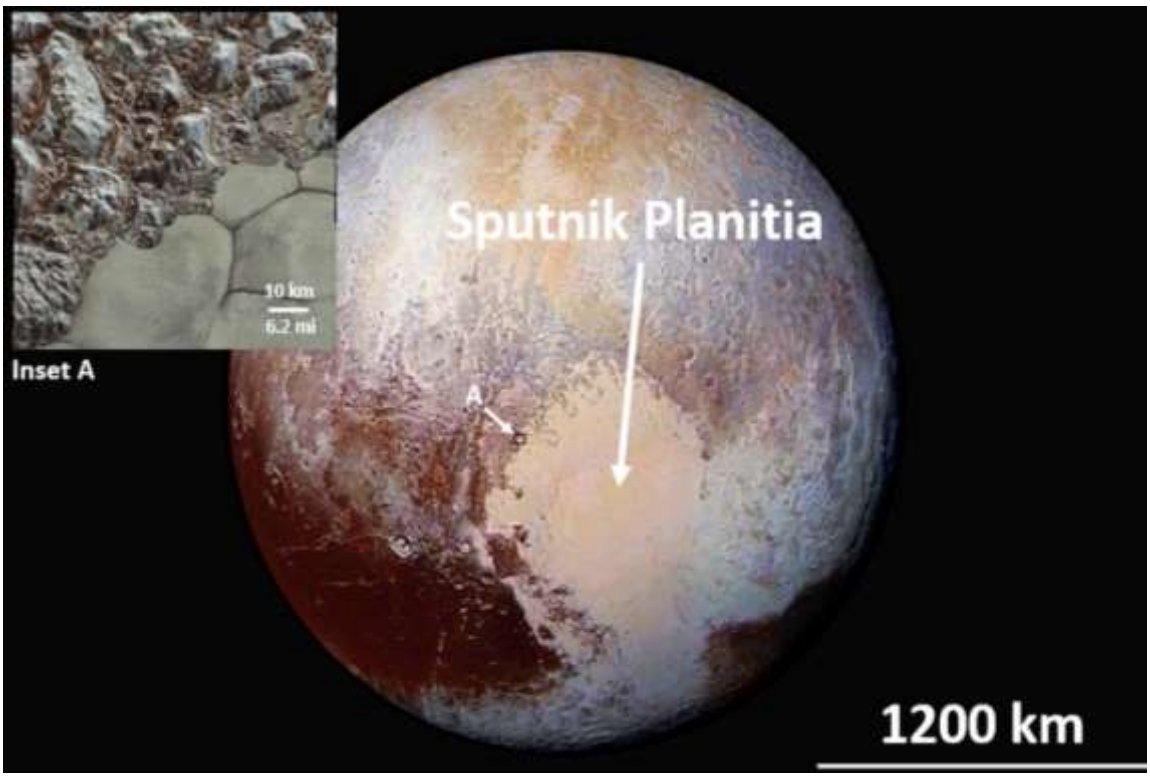

Fig. 68. Features of the Sputnic Planitia region on the surface of Pluto (https://www.labroots.com/trending/space/21937/pluto-s-landscape-formation-mysteries-revealed).

These results were obtained for the lower ten kilometers in the stratosphere [85]. According to the results of ground-based observations, this value was already estimated at 2.2 K/km [75], 3÷15 K/km [114] and 5.5 K/km [113]. It is believed that such an increase in temperature may be the result of the methane-induced greenhouse effect. At the same time, the average surface temperature, according to observations in 2005 [89], was 42±4 K. While the average temperature in the atmosphere was 90 (+25 −18) K according to observations in 2008 [112, 113]. The maximum temperature was reached in the stratopause at altitudes of 20-40 km (100÷110 K). And further, in the mesosphere, the temperature slowly decreased at a rate of about 0.2 K/km [75, 112]. The reason for this decrease is probably the cooling effect of acetylene, hydrogen cyanide [85] and (or) carbon monoxide [112]. At an altitude of more than 500 km from the surface, the temperature reached 70 K, and then practically did not change [74].

According to the results of observations of Pluto's coverage of stars in 1988, 2002 and 2006, it turned out that the temperature changes over time in the upper and middle

layers of the dwarf planet's atmosphere, the temperature was practically the same within the measurement error and was about 100 K with an uncertainty of □10 K. At the same time, the value of the atmospheric pressure itself increased almost twice [73, 75]. According to the same observational data, no significant dependence of the temperature on the time of day and on the latitude of the area was found. After all, the temperature value was almost the same over the entire surface. This is in good agreement with theoretical data that predicted fairly rapid atmospheric mixing [112].

However, according to data obtained by the New Horizons probe, in 2015, a noticeable difference was observed between the temperature-height curves on different sides of Pluto [85]. Also, according to the results of star coverages in Pluto's atmosphere, small vertical inhomogeneities of temperature changes were found. They manifested themselves during the coverages of stars by Pluto in rather sharp and very short bursts of brightness [161].

The magnitude of such inhomogeneities at altitudes of several kilometers was estimated at 0.5÷0.8 K. It is believed that they could be the result of, for example, gravitational waves or manifestations of turbulence caused by convection or winds [162]. The interaction of surface layers with the atmosphere can affect the temperature near the surface layer of Pluto. The calculations showed that the atmosphere, despite the relatively small pressure near the surface of Pluto, is still able to significantly smooth out the changes in this temperature during the day [258]. Although observations have shown that there are still temperature changes with an amplitude of up to 20 K.

The reason for this may be the existence of areas on the surface from which nitrogen ice is “right now” evaporating. This leads to significant cooling in such areas. Although the pressure of Pluto’s atmosphere is very small, it changes significantly over time. Observations of Pluto’s coverage of stars have shown that from 1988 to 2015 the pressure value gradually increased almost threefold. And this is despite the fact that after 1989 Pluto began to move away from the central star [161, 258]. It is possible that this could be a consequence of the fact that in 1987 a polar day occurred at Pluto’s north pole, which contributed to the evaporation of nitrogen from this polar region

[162]. While the southern hemisphere was still warm enough for its condensation [258].

The first detailed and direct studies of the lower layers of Pluto's atmosphere were carried out by the New Horizons space probe in 2015. By scanning the atmosphere with radio waves, it was possible to determine that the pressure at that time near the surface was 1 Pa. At the moment of the device's entry into the disk of the dwarf planet, its value was measured as 1.1 ± 0.1, and during its exit – as 1.0 ± 0.1 Pa [85]. These values are in good agreement with observations of the coatings a few years earlier [85]. However, it should be noted that some of the published calculations also indicated that the results obtained with some coatings corresponded to a pressure with twice the value.

The results of the calculations also showed that the value of the so-called pressure scale in the atmosphere of Pluto varies significantly with altitude. That is, the dependence of pressure on altitude deviated from a purely exponential law. This could be due to the fact that at different altitudes in the atmosphere the temperature values are very different. For atmospheric layers near the surface, the value of the height scale was estimated at 17÷19 [32] km, while for altitudes of 30–100 km – already at 50÷70 km [74, 75, 85].

24. Seasonal changes on Pluto

Due to the elongated orbit, Pluto receives 2.8 times more heat at perihelion than at aphelion [85, 218]. This should cause strong changes in its atmosphere [67, 131, 132, 134, 232] (Fig. 69). It was previously believed that at aphelion the entire atmosphere should freeze and fall to the surface layer. This was indicated by the significant dependence of the sublimation pressure of all its components on temperature. However, refinement of the initial models suggests that a noticeable atmosphere should persist on Pluto throughout the year [141].

Fig. 69. Part of the image obtained from the space probe "New Horizons": sunlight scattered through the atmosphere of Pluto has a blue color (https://www.reddit.com/r/spaceporn/comments/oksi29/6_years_1_day_ago_new_horizons_flew_by_pluto/#lightbox).

Pluto's last passage through the perihelion point occurred on September 5, 1989 [213]. And now this dwarf planet [199, 200] has begun to move away from the Sun. Therefore, the illumination of its surface has begun to decrease. It is clear that the significant inclination of its axis of rotation to the plane of the orbit, which is more than 122°, significantly complicates the resulting picture. After all, such a large inclination indicates that very long polar nights and days last on a significant part of Pluto's surface. According to the data obtained, almost before the moment of passing the perihelion point – 16.12.1987 – the moment of equinox came for Pluto [60]. It was at

this moment that its northern (or rather, positive) pole began to emerge from the polar night, which lasted about 124 Earth years.

Based on the results of existing observational data, one of the models of seasonal changes existing in the atmosphere of Pluto was built [193, 194, 208, 211, 212]. When passing the aphelion point of the orbit in 1865, a significant amount of gases was in a frozen state in both the southern and northern hemispheres. Shortly before this moment, the moment of the next equinox came on Pluto. And after that, Pluto began to return to the Sun through the southern hemisphere. The frozen components of volatile chemical compounds began to heat up, evaporate and gradually migrate to the warmer [233] at that time northern hemisphere. Calculations showed that by 1900 a significant part of them had "moved" from the southern hemisphere to the northern one. After the moment of the next equinox (16.12.1987) the southern hemisphere began to move away from the Sun. However, its surface, depleted by this time of volatile ices, was already quite well warmed up. And the significant thermal inertia provided by non-volatile water ice still does not allow it to cool down quickly. Therefore, those gases that began to evaporate intensively from the northern hemisphere will not be able to condense relatively quickly in the southern hemisphere. Therefore, the newly formed gas components replenish the atmosphere illuminated by the Sun. This effect leads to an increase in its pressure.

Thus, due to seasonal changes in surface illumination, ice [26] of the volatile components will migrate around the planet [143, 161, 203, 240, 261]; these ices will evaporate in some regions and condense in others. According to some estimates, seasonal variations in the thickness of their layer reach values of about one meter [141, 238]. This fact should lead to noticeable changes in the color and brightness (Fig. 70) of Pluto [113]. It is believed that in 2035-2050 the surface in the southern hemisphere will be able to cool down so much that significant condensation of gaseous components will become possible. This will lead to the beginning of their migration to the cold south from the northern hemisphere, where at that time the polar day will prevail.

Fig. 70. Image of Pluto obtained by the New Horizons space probe (https://newatlas.com/new-horizons-xray-red-charon/45437/).

This situation will occur until the next equinox near the aphelion point in about 2113. However, again, the northern hemisphere will never be able to completely get rid of volatile ices. After all, as a result of their evaporation from the warmer part of Pluto's surface, a small atmosphere can persist even near the aphelion point. Estimates show that in such a model, seasonal changes in atmospheric pressure values can reach up to 4 times. The minimum pressure values should have been in the 1970-1980s; and Pluto should reach its maximum atmospheric pressure around 2030. During the same time, the temperature value will vary within a few degrees [141]. According to estimates based on the results of the New Horizons spacecraft, Pluto's atmosphere will dissipate into space at rates per second for nitrogen of 1×10^{23} molecules and for methane of 5×10^{25} molecules. These values correspond to the loss of a layer several centimeters thick for nitrogen ice and a layer several tens of meters thick for methane

ice over the entire time since the formation of planetary bodies in the Solar System [85]. Before the measurements made by the New Horizons spacecraft, the temperature values in the upper layer of Pluto's atmosphere were considered somewhat higher. These values gave a fairly high rate of dissipation of atmospheric components [188]. The rates of its loss were previously estimated at 4÷5 orders of magnitude higher; and they reached up to 50÷500 kg of nitrogen per second. At such speeds, a layer hundreds or even thousands of meters thick could evaporate from Pluto's surface during the existence of the planetary system [164]. Under such conditions, the relative rate of atmospheric loss from Pluto would be greater than for all the large planets [188].

Pluto has no way to replenish its nitrogen reserves: calculations have shown that meteorite bodies falling onto its surface are insufficient for this [164]. Those molecules that have sufficient speed to overcome Pluto's gravitational pull escape into outer space and there must be ionized by solar ultraviolet radiation. When the solar wind collides with the ions it receives, it will slow down, deflect slightly, pick up the ions, and carry them with it, forming an elongated tail behind Pluto. Therefore, behind Pluto, a kind of cavity with a length of more than 100 thousand km remains in the solar wind flow; however, it is filled with relatively cold nitrogen ions.

This was detected using the solar wind particle parameter meter installed on the New Horizons spacecraft during its flight through this cavity. The region of interaction of Pluto's atmosphere with the solar wind on the sunward side is located at a distance of almost 6 Pluto radii (about 7 thousand km), and on the opposite side the interaction region exceeds 400 Pluto radii (more than 500 thousand km). The obtained estimates refer to the zone in which the speed of the solar wind has slowed down by about 20% [17].

25. Dwarf planet 136199 Eris and its satellite

According to the Minor Planet Center catalog, the dwarf planet Eris (136199 Eris, previously designated 2003 UB313) is the second largest dwarf planet in the Solar System after Pluto [160] and the most massive and farthest from the Sun to date. It was previously called Xena. It belongs to the so-called trans-Neptunian objects, or plutoids. And until the XXVI Assembly of the International Astronomical Union, this object claimed the status of the tenth planet of the Solar System [132, 193]. However, on August 24, 2006, the International Astronomical Union approved a new definition for classical planets. And after that, both Eris and Pluto ceased to correspond to this updated status. The dwarf planet Eris was long considered to be much larger than Pluto [160]. According to the results of observational data in 2010, their sizes were almost equal. And only data obtained in July 2015 by the New Horizons space probe showed that Pluto was slightly larger than Eris and is the largest of the known trans-Neptunian objects [234].

Eris was discovered by a group of American astronomers consisting of M. Brown, D. Rabinowitz and C. Trujillo. The group used for their observations a 122-cm telescope with CCD arrays, located at the Palomar Observatory. To search for moving objects in the obtained images, they used a special program. Conducting systematic searches for trans-Neptunian objects for several years allowed to discover during this time such rather large celestial bodies as (50000) Quavar and (90377) Sedna [199, 239]. Eris was first spotted on 5/01/2005 during a reanalysis of an image obtained on 21/10/2003. The same object was also found in several other previously obtained images. A few days after the discovery, Brown's group managed to detect the same object again using the 1.3-meter SMARTS telescope at the Cerro Tololo Observatory. Several more months of careful research were spent to determine the parameters of the orbit and the approximate size of the object. The claim for the discovery of Eris was published on 29/07/2005.

Usually, when registering the discovery of a celestial object, it is given a temporary designation. This celestial body was named 2003 UB313. Due to uncertainty

about the classification of the object as a minor or major planet, the proposal for its name was postponed until the IAU meeting on 24/08/2006.

The group of discoverers reserved the name Xena for this trans-Neptunian object. This unofficial name for the object was given in honor of the heroine of the TV series "Xena: Warrior Princess". The discoverers chose this name because it begins with the letter "x" (Planet X) and sounds mythological. Since 2003 UB313 was long considered a major planet, it was proposed to give it a name using Greco-Roman mythology, within the framework of which other major planets are named. The name of the Greek goddess of discord, Eris, was not yet taken.

Therefore, this name was sent to the IAU commission. It was approved on September 13, 2006 (IAU Circular No. 8747). And on September 7, Pluto and 2003 UB313 were included in the catalog of minor planets. And 2003 UB313 was listed under the number 136199. Although the orbit of Eris was tracked from archival images until 1954, its very slow movement still does not allow for reliable determination of orbital characteristics (Fig. 71) with good accuracy. The average value of the distance of Eris from the Sun is about 68.05 AU. However, its orbit is highly elongated, having an eccentricity of as much as 0.435. With this value of eccentricity, the orbit of Eris is significantly superior to all classical objects in the Kuiper belt. Celestial bodies with such characteristics are referred to as objects in the scattered disk, or even to isolated trans-Neptunian objects. Such a large value of eccentricity leads to the fact that the maximum distance of Eris from the Sun is 97.63 AU. e., minimum – 38.46 AU. e. Therefore, at perihelion, Eris appears closer to the Sun than Pluto at aphelion [61, 199, 208, 211]. Eris passed the aphelion point close to March-April 1977 and has now begun to approach the Sun. Such data place it in third place on the list of the most distant bodies of the Solar System known to date, after the recently discovered 2020 FA31 (97.4 AU) and 2020 FY30 (98.9 AU). In addition, its orbit is also highly inclined to the ecliptic plane: at an angle of 43.82°. The value of the period of rotation of Eris around the Sun is about 561 years, so it will reach the closest point of its orbit to the Sun only in 2258.

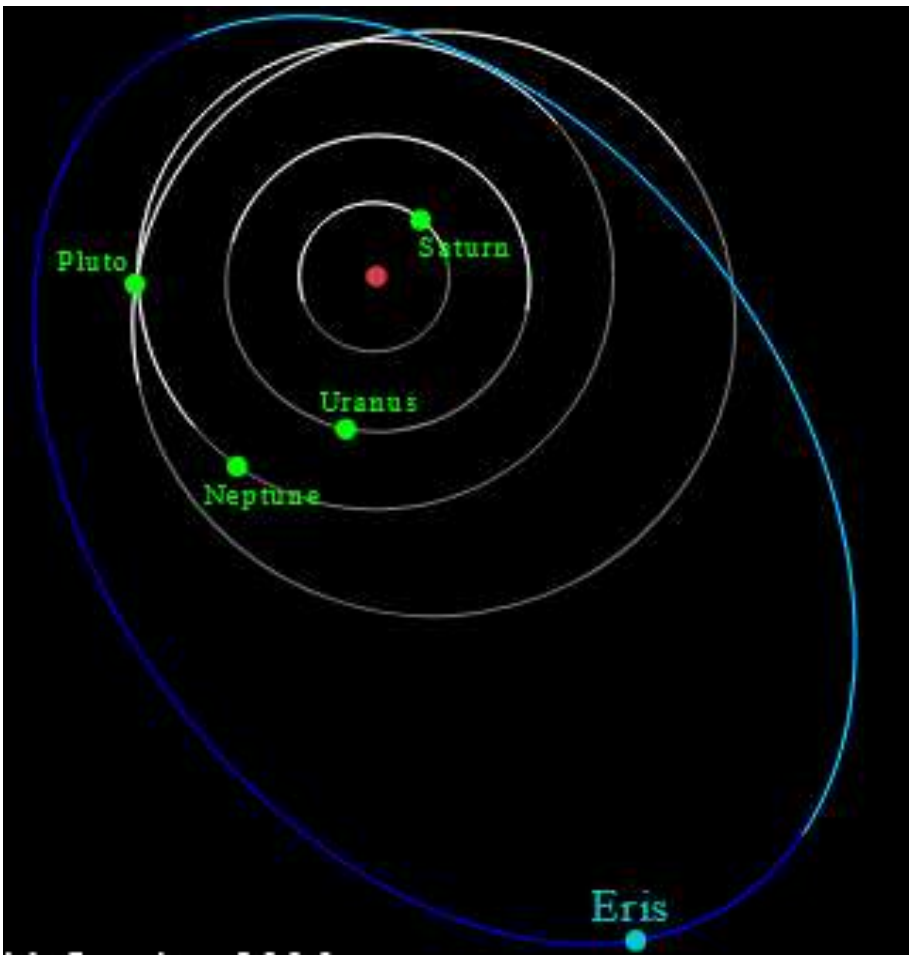

Fig. 71. View of the orbit of the dwarf planet 136199 Eris (https://upload.wikimedia.org/wikipedia/commons/d/dc/Eris_Orbit.svg).

Determining the size of such a distant celestial body with good accuracy is quite difficult. After all, the brightness of the observed object is proportional to its surface area multiplied by the albedo value (the fraction of reflected sunlight that is reflected by this object). Therefore, in order to calculate the value of its diameter, it is necessary to know the value of the absolute magnitude (which is easy to determine) and the albedo (which is unknown). However, Eris is quite bright, and if its albedo is taken to be 1, then its diameter can be at least 2300 km.

According to measurements made in April 2006 with the Hubble Space Telescope, the diameter of Eris should be 2400±100 km, and the albedo – 0.86±0.07 [127]. Measurements made in 2007 with the infrared Spitzer Space Telescope allowed us to estimate the diameter of Eris at 2600 (+400−200) km. The most precise measurements were made in November 2010, when in Chile three groups of

astronomers observed the eclipse of the dwarf planet Eris by the very faint star USNO-A2 0825-00375767 [166] in the constellation Cetus with an apparent magnitude of 17.1^{m}.

The data obtained at that time allowed us to determine its diameter to within 12 km (IAU Circular No. 8596). According to those measurements, the diameter of Eris does not exceed 2326±12 km, and the albedo should be 0.96 (+0.09−0.04) [51]. The data obtained in this way allowed us to state that Eris is slightly smaller than Pluto in size. Recall that the diameter of Pluto, measured during the flyby of the New Horizons space probe in July 2015, is 2376.6 km [234, 239]. The mass of Eris was determined by the presence of a satellite. It turned out to be almost a quarter larger than the mass of Pluto and is equal to $(1.67\pm0.02)\cdot10^{22}$ kg. Such data gave an average density of Eris of 2.52±0.05 g/cm³ [51]. Observations with the Hubble Space Telescope (Fig. 72) in early 2018 of the Eris-Dysnomia system allowed us to determine an orbital period of 15.78590±0.00005 Earth days and an eccentricity of 0.0062. This allowed us to refine the density to 2.43±0.05 g/cm³ and the mass to $1.6466\cdot10^{22}$ kg [132]. For distant celestial bodies, the value of the period of rotation around its axis is determined from the analysis of the light curve. However, determining the period of rotation of Eris is difficult due to the homogeneity of its surface and fairly regular shape. Measurements made in 2008 using the Swift orbital telescope gave a period of 25.9 hours [166]. The tilt of the axis of rotation of Eris still remains unknown. However, if we assume that the plane of Dysnomia's orbit coincides with the equatorial plane of the planet itself, we find that the axis of rotation of Eris is inclined to the plane of the ecliptic at an angle of 78° [43]. Measurements of the heat flux from Eris allow us to calculate that at the present time the average temperature of its surface is close to 20 K. While at the closest point of its orbit to the Sun the temperature should reach 43 K [127]. Spectroscopic observations made on 25.01.2005 at the Gemini Observatory indicated the presence of methane snow on the surface of this dwarf planet.

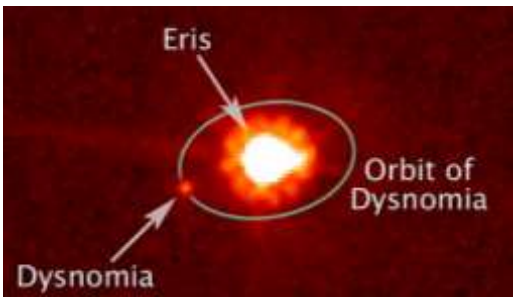

Fig. 72. Image of the dwarf planet Eris with its satellite Dysnomia, obtained using the Hubble telescope (https://commons.wikimedia.org/wiki/File:Hubble_Dysnomia_orbit_overlay.jpg?uselang).

This explains the high albedo of this object. Its snows also contain nitrogen ice, the proportion of which should increase with increasing depth. It is also known that Pluto is somewhat reddish, while Eris turned out to be gray. This may indicate the presence of ethane and ethylene ices on the surface of Eris. It is assumed that with increasing temperature near perihelion, a thin layer of various frozen gases can evaporate and even form a temporary atmosphere. Such an atmosphere on Eris may appear in the middle of the 23rd century. Based on the analysis of data on the isotopic composition of methane present on the surface of Eris, it was concluded that it has signs of hydrothermal origin. Therefore, there must still be some thermal activity in the interior of this planet. At the Keck Observatory on September 10, 2005, using an adaptive optics telescope, a satellite was discovered around the object 2003 UB313, which was designated S/2005 (2003 UB313) 1. Its discoverers named the satellite Gabrielle in honor of the satellite Xena. The official name Dysnomia (with the designation (136199) Eris I Dysnomia) was given to the satellite on September 13, 2006, simultaneously with the naming of the dwarf planet Eris. This name was given in honor of the daughter of Eris – Dysnomia – in Greek mythology, the goddess of lawlessness. Dysnomia rotates at a distance of about 37,000 km from Eris, making a complete rotation in about 16 Earth days. The inclination of Dysnomia's orbit relative to the plane of Eris' heliocentric orbit has been calculated to be 78.29±0.65°. Dysnomia's mass is about $(8.2\pm5.7)\times10^{19}$ kg) [41].

References

1. Abramenko A.N, Avramchuk V.V., Kucherov V.A. (1981) Reflective properties of Pluto's surface. Phys. planetary atmospheres. Kyiv. P. 148-158. (In Ukrainian).
2. Avramchuk V.V., Rakhimov V.Yu., Chernova G.P., Shavlovsky V.I. (1992) Photometry and polarimetry of Pluto near perihelion. I. Kinematics and physics of celestial bodies. 8(4). P. 37-45. (In Ukrainian).
3. Golitsyn G.S. (1975) On a possible atmosphere of Pluto. Letters to the Astron. J. 1(1), p. 38-42. (In Ukrainian).
4. Lupishko D.F. (1998) Photometry and polarimetry of asteroids: observation results and data analysis: Diss. ... Doctor of Physical and Mathematical Sciences. Kharkov. 259 p. (In Ukrainian).
5. Lyuty V.M., Tarashchuk V.P. (1982) Photometric studies of Pluto near perihelion. I. UBV photometry. Letters to the Astron. J. 8(2), P. 109-114. (In Ukrainian).
6. Morozhenko O.V. (2004) Methods and results of remote sensing of planetary atmospheres. Naukova dumka. K.: – 647 p. (In Ukrainian).
7. Alfvén H., Arrhenius G. (1976) Resonance Structure in the Solar System. NASA Special Paper 345.
8. Allen D.A. (1970) Infrared diameter of Vesta. Nature. 227(5254), p. 158-159.
9. Allen R.L., Gladmanand B., Kavelaars J.J., et al. (2006) Discovery of low-eccentriciti, high-inclination Kuiper belt object at 58 AU. Astrophys. J. 640(1), Pt. 2, p. L83-L86.
10. Altenhoff W.J., Chini R., Hein H., et al. (1988) First radio astronomical estimate of the temperature of Pluto. First radio astronomical estimate of the temperature of Pluto. Astron. Astrophys. 190(1-2). P. L15-L17.
11. Anderson L.E., Fix J.D. (1973) Pluto: new photometry and a determination of the axis of rotation. Icarus. 20(3), p. 279-283.
12. Anderson D.L., Miller W.F., Duennebier F.K., et al. (1976) The Viking seismic experiment. Science. 194(4271), p. 1318-1321.

13. Apt J., Carleton N.P., Mackay C.D. (1983) Methane on Titan and Pluto: new CCD spectra. Astrophys. J. 270(1), Pt. 1, p. 342-350.

14. Archinal B.A., A'Hearn M.F., Bowell E. et al. (2011) Report of the IAU Working Group on Cartographic Coordinates and Rotational Elements. Celestial Mechanics and Dynamical Astronomy. 109(2), p. 101-135.

15. Aumann H.H., Walker R.G. (1987) IRAS observations of the Pluto-Charon system. Astron. J. 94(4), p. 1088-1091.

16. Avramchuk V.V., Rakhimov V.Yu., Chernova G.P., Shavlovskij V.I (1992) Photometry and polarimetry of Pluto near its perihelion position. I. Kinematics Phys. Celest. Bodies, 8(4), p. 30-37.

17. Bagenal F., Horányi M., McComas D.J., et al. (2016) Pluto' interaction with its space environment: Solar wind, energetic particles, and dust. Science. 351(6279), id.aad9045.

18. Bagheri A., Khan A., Deschamps F., et al. (2022) The tidal–thermal evolution of the Pluto–Charon system. Icarus. 376, article id. 114871.

19. Bagnulo S., Belskaya I., Muinonen K., et al. (2009) Discovery of two distinct polarimetric behaviours of trans-Neptunian objects. Astron. Astrophys. 491(2), p. L33–L36.

20. Barkume K.M, Brown M.E., Water E.L. (2006) Ice on the Satellite of Kuiper Belt Object 2003 EL61. Astrophys. J. 640(1), Pt. 2, p. L87–L89.

21. Barr A.C., Collins G.C. (2015) Tectonic activity on Pluto after the Charon-forming impact. Icarus. 246, p. 146-155.

22. Barucci M.A., Cruikshank D.P., Dotto E., et al. (2005) Is Sedna another Triton? Astron. Astrophys. 439(2), p. L1-L4.

23. Belskaya I., Bagnulo S., Muinonen K., et al. (2008) Polarimetry of the dwarf planet (136199) Eris. Astron. Astrophys. 479(1), p. 265-269.

24. Belskaya I.N., Levasseur-Regourd A.-Ch., Cellino A., et al. (2009) Polarimetry of main belt asteroids: Wavelength dependence. Icarus. 199(1), p. 97-105.

25. Benner D.Ch., Fink U., Cromwell R.H. (1978) Image tube spectra of Pluto and Triton from 6800 to 9000A. Icarus. 36(1), p. 82-91.

26. Bernstein G., Khushalani B. (2000) Orbit Fitting and Uncertainties for Kuiper Belt Objects. Astron. J. 120(6), p. 3323-3332.

27. Bierson C., Nimmo F., Stern S.A. (2020) Evidence for a hot start and early ocean formation on Pluto. Nature Geoscience. 769(7), p. 468-472.

28. Binzel R.P. (1988) Hemispherical color differences on Pluto and Charon. Science. 201(4869), p. 1070-1072.

29. Binzel R.P., Mulholland J.D. (1983) Photometry of Pluto during the 1982 opposition. Astron. J. 88(2), p. 222-225.

30. Binzel R.P., Mulholland J.D. (1984) Photometry of Pluto during the 1983 opposition: a new determination of the phase coefficient. Astron. J. 89(11), p. 1759-1761.

31. Bless R. (1991) Do Neptune and Pluto have Rings? Part 2. Proposal ID 4198. Cycle 2.

32. Boehnhardt H., Tozzi G.P., Birkle K., et al. (2001) The FORS instrument team. Visible and near IR observations of transneptunian objects. Results from ESO and Calar Alto telescopes. Astron. Astrophys. 378(2), p. 653-667.

33. Bohn R.B., Sandford S.A., Allamandola L.J., Cruikshank D.P. (1974) Infrared spectroscopy of Triton and Pluto ice analogs: The case for saturated hydrocarbons. Icarus. 111(1), p. 151-173.

34. Bosh A.S., Person M.J., Levine S.E., et al. (2013) The state of Pluto's atmosphere in 2012-2013. Icarus, 246, p. 237-246.

35. Breger M., Cochran W.D. (1982) Polarimetry of Pluto. Icarus. 49(1), p. 120-124.

36. Briggs F.H. Radio emission from Ceres. Astrophys. J. 184(2), Pt. 1. P. 637-639.

37. Brosch N. (1995) The 1985 stellar occultation by Pluto. Monthly Notices of the Royal Astronomical Society. 276(2), p. 551-578.

38. Brosch N., Mendelson H. (1985) Occultation by Pluto on 1985 August 19. International Astronomical Union, p. Circular 4097, p. 2.

39. Brown M.E. (2008) The Largest Kuiper Belt Objects. In.: The Solar System Beyond Neptune (Eds. Barucci M.A., Boehnhardt H., Cruikshank D.P., Morbidelli A.) University of Arizona Press, Tucson. P. 335-344.

40. Brown M.E., Bouchez A.H., Rabinowitz D., et al. (2005) Keck Observatory Laser Guide Star Adaptive Optics Discovery and Characterization of a Satellite to the Large Kuiper Belt Object 2003 EL61. Astrophys. J. Lett. 632(1), p. L45–L48.
41. Brown M.E., Butler B.J. (2023) Masses and Densities of Dwarf Planet Satellites Measured with ALMA. The Planetary Science Journal. 4(10), p. 193.
42. Brown M.E., Trujillo C., Rabinowitz D. (2004) Discovery of a Candidate Inner Oort Cloud Planetoid. Astrophys. J. 617(1), Pt. 1, p. 645-649.
43. Brown M.E., van Dam M.A., Bouchez A.H., et al. (2006) Satellites of the Largest Kuiper Belt Objects. The Astronomical Journal Letters. 639(1), p. L43-L46.
44. Brucker M.J., Grundy W.M., Stansberry J.A., et al. (2009) High albedos of low inclination classical Kuiper belt objects. Icarus. 201(1), p. 284-294.
45. Buie M.W., Fink U. (1987) Methane absorption in the spectrum of Pluto. Icarus. 70(3), p. 483–498.
46. Buie M.W., Grundy W. M., Young E.F., et al. (2006) Orbits and Photometry of Pluto's Satellites: Charon, S/2005 P1, and S/2005 P2. Astron. J. 132(1), Pt. 1, p. 290-298.
47. Buie M.W., Grundy W.M., Young E.F., et al. (2010) Pluto and Charon with the Hubble Space Telescope. II. Resolving Changes on Pluto's Surface and a Map for Charon. Astron. J. 139(3), p. 1128-1143.
48. Buie M.W., Tholen E.F. (1989) The surface albedo distribution of Pluto. Icarus. 79(1), p. 23-37.
49. Buie M.W., Tholen D.J., Horne K. (1992) Albedo maps of Pluto and Charon: initial mutual event results. Icarus.97(2), p. 211-27.
50. Buratti B.J., Hillier M.D., Heunze A., et al. (2003) Photometry of Pluto in the last decade and before: evidence for volatile transport. Icarus. 162(1), p. 171-182.
51. Carraro G., Maris M., Bertin D., Parisi M.G. (2006) Time series photometry of the dwarf planet ERIS (2003 UB313). Astronomy and Astrophysics. 460(2), p. L39-L42.
52. Carry B., Dumas C., Fulchignoni M., et al. (2008) Near-infrared mapping and physical properties of the dwarf-planet Ceres. Astron. Astroph. 478(1), p. 235-244.

53. Castillo-Rogez J.C., Conrad P.G. (2010) Habitability Potential of Ceres, a Warm Icy Body in the Asteroid Belt. Astrobiology Science Conference 2010: Evolution and Life: Surviving Catastrophes and Extremes on Earth and Beyond, held April 26-20, 2010, in League City, Texas. LPI Contribution No. 1538. P.5302.

54. Chamberlain M.A., Sykes M.V., Esquerdo G.A. (2007) Ceres lightcurve analysis — Period determination. Icarus. 188(2), p. 451-456.

55. Chant C.A. (1930). A New Major Planet. Journal of the Royal Astronomical Society of Canada. 24, p. 193-195.

56. Cheng A.F., Summers M.E., Gladstone G.R. et al. (2017) Haze in Pluto's atmosphere. Icarus. 290, p. 112-133.

57. Christy J.S., Harrington R.S. (1978).The Satellite of Pluto. Astronomical Journal, 83(8), p. 1005-1008.

58. Cook J.C., Desch S.J., Roush T.L., et al. (2007) Near-Infrared Spectroscopy of Charon: Possible Evidence for Cryovolcanism on Kuiper Belt Objects. The Astrophysical Journal. 663(2), p. 1406-1419.

59. Croswell K. (1999) Planet Quest: The Epic Discovery of Alien Solar Systems. Oxford University Press. P. 48–71.

60. Cruikshank D.P., Grundy W.M., DeMeo F.E. et al. (2015) The surface compositions of Pluto and Charon. Icarus. 246, p. 82-92.

61. Cruikshank D.P., Mason R.E., Dalle Ore C.M., et al. (2006) Ethane on Pluto and Triton. American Astronomical Society, DPS meeting #38, #21.03.

62. Cruikshank D.P., Pilcher C.B., Morrison D. (1976) Pluto: Evidence for methane frost. Science. 194, p. 835-837.

63. Cruikshank D.P., Silvaggio P.M. (1980) The surface and atmosphere of Pluto. Icarus. 41(1), p. 96-102.

64. De Bergh C., Delsanti A., Tozzi G.P., et al. (2005) The surface of the transneptunian object 90482 Orcus. Astron. Astrophys. 437(3), p. 1115-1120.

65. Desch S.J., Neveu M. (2017) Differentiation and cryovolcanism on Charon: A view before and after New Horizons. Icarus. 287, p. 175-186.

66. Dias-Oliveira A., Sicardy B., Lellouch E. (2015) Pluto's Atmosphere from Stellar Occultations in 2012 and 2013. The Astrophysical Journal, 811(1), 53, p. 1-20.
67. Dlugach J.M., Morozhenko A.V., Vid'Machenko A.P., Yanovitskij E.G. (1983) Investigations of the optical properties of Saturn's atmosphere carried out at the main astronomical observatory of the Ukrainian Academy of Sciences. Icarus, 54 (May 1983), p. 319-336.
68. Dobar W.I., Tiffany O.L., Gnaedinger J.P. (1964) Simulated extrusive magma solidification in vacuum. Icarus. 3(4), p. 323-331.
69. Dollfus A. (1971) Diameter of asteroids. In: Physical studies of minor planets. Ed. T.Gehrels (NASA SP-267), Washington, D.C.: U.S. Government Printing Officce. P. 25-31.
70. Doute S., Schmitt B., Quirico E., et al. (1999) Evidence for methane segregation at the surface of Pluto. Icarus. 142(3), p. 421–444.
71. Duncombe R.L., Seidelmann P.K. (1980) A history of the determination of Pluto's mass. Icarus, 44(1), p. 12-18.
72. Edgeworth K.E. (1943) The evolution of our planetary system. J. Brirish. Astron. Association. 53(2). P. 181-188.
73. Elliot J.L., Ates A., Babcock B.A., et al. (2003) The recent expansion of Pluto's atmosphere. Nature. 424(6945), p. 165-168.
74. Elliot J.L., Dunham E.W., Bosh A.S. et al. (1989) Pluto's atmosphere. Icarus, 77, p. 148-170.
75. Elliot J.L., Person M.J., Gulbis A.A.S., et al. (2007) Changes in Pluto's Atmosphere: 1988-2006. The Astronomical Journal. 134(1), p. 1-13.
76. Elliot J.L., Young L.A. (1991) Does Charon have an Atmosphere? Abstracts of the Lunar and Planetary Science Conference, 22, p. 347.
77. Elliot J.L., Young L.A. (1992) Analysis of stellar occultation data for planetary atmospheres. I - Model fitting, with application to Pluto. Astron. J. 103, p. 991-1015.
78. Edgeworth K.E. (1943) The evolution of our planetary system. J. Brirish. Astron. Association. 53(2), p. 181-188.

79. Fink U.F., DiSanti M.A. (1988) The separate spectra of Pluto and its satellite Charon. Astron. J. 95(1), p. 229-236.

80. Fix J.D., Neff J.S., Kelsey L.A. (1970) Spectrophotometry of Pluto. Astron. J. 75(8), p. 895-896.

81. Fray N., Schmitt B. (2009) Sublimation of ices of astrophysical interest: A bibliographic review. Planetary and Space Science. 57(14–15), p. 2053-2080.

82. Galad A., Kornos L., Gajdos S., et al. (2004) Relative photometry of numbered asteroids (3712), (4197), (5587), (28753) and (66063). Contrib. Astron. Obs. Skalnate Pleso.34(3), p. 157-166.

83. Gaslac Gallardo D.M., Giuliatti Winter S.M., Pires P. (2019) Pluto system: external stable regions. Monthly Notices of the Royal Astronomical Society. 484(4), p. 4574–4590.

84. Gehrels T. (1967) Minor planets. I. The rotation of Vesta. Astron. J. 72(8), p. 929-938.

85. Gladstone G.R., Stern S.A., Ennico K., et al. (2016) The atmosphere of Pluto as observed by New Horizons. Science, 351(6279), id.aad8866.

86. Grundy W.M., Binzel R.P., Buratti B.J. et al. (2016) Surface compositions across Pluto and Charon. Science. 351(6279). P. 9189-1 – 1989-8.

87. Grundy W.M., Buie M.W. (2001) Distribution and evolution of CH4, N2, and CO ices on Pluto's surface 1995 to 1998. Icarus. 153(2), p. 248–263.

88. Grundy W.M., Olkin C.B., Young L.A., et al. (2013) Near-infrared spectral monitoring of Pluto's ices: Spatial distribution and secular evolution. Icarus. 223(2) p. 710-721.

89. Gurwell M.A., Butler B.J. (2005) Sub-Arcsecond Scale Imaging of the Pluto/Charon Binary System at 1.4 mm. American Astronomical Society, DPS meeting #37, id.#55.01; Bulletin of the American Astronomical Society, 37, p.743.

90. Gurwell M., Lellouch E., Butler B., et al. (2015) Detection of Atmospheric CO on Pluto with ALMA. American Astronomical Society, DPS meeting #47, #105.06.

91. Hand E. (2015) Late harvest from Pluto reveals a complex world. Science, 350(6258), p. 260-261.

92. Harris A.W., Young J.W., Bowell E., et al. (1989) Photoelectric observation of asteroids 3, 24, 60, 261, 863. Icarus. 77(1), p. 171-186.
93. Hart M.H. (1974) A possible atmosphere for Pluto. Icarus. 21(3), p. 242-247.
94. Hartig K., Barry T., Carriazo C.Y., et al. (2015) Constraints on Pluto's Hazes from 2-Color Occultation Lightcurves. American Astronomical Society, DPS meeting #47, #210.14.
95. Holler B.J., Young L.A., Buie M.W., et al. (2017) Measuring temperature and ammonia hydrate ice on Charon in 2015 from Keck/OSIRIS spectra. Icarus. 284, p. 394-406.
96. Holler B.J., Young L.A., Grundy W.M., et al. (2014) Evidence for longitudinal variability of ethane ice on the surface of Pluto. Icarus. 243, p. 104-110.
97. Hoyt W.G. (1976) W.H. Pickering's Planetary Predictions and the Discovery of Pluto. Isis. 67(4), p. 551-564.
98. Hubbard W.B., Hunten D.M., Dieters S.W., et al. (1989) Occultation evidence for an atmosphere on Pluto. Nature. 336(6198), p. 452–454.
99. Jewitt, D., Luu J. (1993) Discovery of the candidate Kuiper belt object 1992 QB1. Nature. 362(6422), p. 730–732.
100. Jewitt D.C., Luu J. (2004) Crystalline water ice is on Kuiper belt object (50000) of Quaoar. Nature. 432(7018), p. 731-733.
101. Johnson K.J., Seidelmann P.K., Wade C.M. (1982) Observations of 1 Ceres and 2 Pallas at centimeter wavelengths. Astron.J. 87(11). P. 1593-1599.
102. Kaeufl H.-U., Ballester P., Biereichel P., et al. (2004) CRIRES: a high-resolution infrared spectrograph for ESO's VLT. Ground-based Instrumentation for Astronomy. Edited by Alan F.M. Moorwood and Iye Masanori. Proceedings of the SPIE. 5492, p. 1218-1227.
103. Kelsey L.A., Fix J.D. (1973) Polarimetry of Pluto. Astropohys. J. 184(2), Pt. 1, p. 633-636.
104. Kenyon S.J., Bromley B.C. (2004) The Size Distribution of Kuiper Belt Objects. Astron. J. 128(4), p. 1916-1926.

105. Krushevska V.M., Benedichuk T.B., Vid'machenco A.P. (2003) Variations of brightness temperatures of Uranus and Neptune. Astronomical School's Report. 4(2), p. 77-82.

106. Labeyrie A. (1970) Attainment of difraction limited resolution in large telescopes by Fouerier analyzing specle patterns in star images. Astron.Astrophys. 6(1), p. 85-87.

107. Larson H.P., Feierberg M.A., Fink U., Smith H.A. (1979) Remote spectroscopic identification of carbonaceous chondrite mineanalogies: applications to Ceres and Pallas. Icarus. 39(2), p. 257-271.

108. Lauer T.R., Throop H.B., Showalter M.R., et al. (2018) The New Horizons and Hubble Space Telescope search for rings, dust, and debris in the Pluto-Charon system. Icarus. 301, p. 155-172.

109. Lebofsky L.A., Rieke G.H., Lebofsky M.J. (1979) Surface composition of Pluto. Icarus. 37(3), p. 554-558.

110. Lellouch E. (1994) The thermal structure of Pluto's atmosphere: Clear VS hazy models. Icarus. 108(2), p. 255-264.

111. Lellouch E., de Bergh C., Sicardy B., et al. (2011) High resolution spectroscopy of Pluto's atmosphere: detection of the 2.3 μm CH4 bands and evidence for carbon monoxide. Astronomy and Astrophysics. 530, id. L4, 4 p.

112. Lellouch E., de Bergh C., Sicardy B., et al (2011) The Tenuous Atmospheres of Pluto and Triton Explored by CRIRES on the VLT. The Messenger. 145, p. 20-23.

113. Lellouch E., de Bergh C., Sicardy B., et al (2015) Exploring the spatial, temporal, and vertical distribution of methane in Pluto's atmosphere. Icarus. 246, p. 268-278.

114. Lellouch E., Sicardy B., de Bergh C., et al. (2009) Pluto's lower atmosphere structure and methane abundance from high-resolution spectroscopy and stellar occultations. Astronomy and Astrophysics, 495(3), p. L17-L21.

115. Leonard F.C. (1930) The new planet Pluto. Astron. Soc. Pacific Leaflets. 1(2), p. 121.

116. Lim L.F., McConnochie T.H., Bell III J.F., Hayward T.L. (2005) Thermal infrared (8–13 μm) spectra of 29 asteroids: the Cornell Mid-Infrared Asteroid Spectroscopy (MIDAS) Survey. Icarus. 173(2). P. 385-408.

117. Lisse C.M., McNutt R.L., Wolk S.J., et al. (2017) The puzzling detection of x-rays from Pluto by Chandra. Icarus, 287, p. 103-109.

118. Listing J.B. (1873) Uber unsere jetzige Kenntnis der Gestalt und Grosse der Erde // Nachr. d. Kgl., Gesellsch. d. Wiss. und der Georg-August-Univ., Gottingen. P. 33-98

119. Lithwick Y., Wu Y. (2018) On the Origin of Pluto's Minor Moons, Nix and Hydra. Draft version. Preprint typeset. -10 p.

120. Lupishko D. F., Mohamed R.A. (1996) A New Calibration of the Polarimetric Albedo Scale of Asteroids. Icarus.119(1), p. 209-213.

121. Malamud U., Perets H.B., Schubert G. (2017) The contraction/expansion history of Charon with implications for its planetary-scale tectonic belt. Monthly Notices of the Royal Astronomical Society. 468(1), p. 1056-1069.

122. Malhotra R., Williams J.G. (1997) Pluto's heliocentric orbit. Pluto and Charon. University of Arizona Press. P. 127–158.

123. Marchi S., Lazzarin M., Magrin S., Barbieri C. (2003) Visible spectroscopy of the two largest known trans-Neptunian objects: Ixion and Quaoar. Astronomy Astrophysics. 408(1), p. L17-L19.

124. Marcialis R.L. (1988) A two-spot albedo model for the surface of Pluto. Astron. J. 95(3), p. 941-948.

125. Marcialis R.L., Lebofsky L.A. (1991) CVF spectrophotometry of Pluto: Correlation of composition with albedo. Icarus. 89(2), p. 255-263.

126. McCord T.B., McFadden L.A., Russell C.T., et al. (2006) Ceres, Vesta, and Pallas: Protoplanets, Not Asteroids // Eos. Transactions American Geophysical Union. 87(10), N1, p. 105-109.

127. Merlin F., Alvarez-Candal A., Delsanti A., et al. (2009) Stratification of methane ice on Eris' surface. The Astronomical Journal. 137(1), p. 315-328.

128. Michalowski T. (1988) Photometric astrometry applied to asteroids: 6, 15, 43. and 624. Acta Astron. 38(4), p. 455-468.1

129. Moore M.H., Hudson R.L., Ferrante R.F. (2003) Radiation Products in Processed Ices Relevant to Edgeworth-Kuiper-Belt Objects. Earth, Moon and Planets. 92(1), p. 291-306.

130. Moore J.M., McKinnon W.B., Spencer J.R., et al. (2016) The geology of Pluto and Charon through the eyes of New Horizons. Science. 351(6279), p. 1284-1293.

131. Morozhenko A.V., Ovsak A.S., Vid'machenko A.P., Teifel V.G., Lysenko P.G. (2016) Imaginary part of the refractive index of aerosol in latitudinal belts of Jupiter's disc. Kinematics and Physics of Celestial Bodies. 32, p. 30-37.

132. Morozhenko A.V., Vid'machenko A.P. (2004) Polarimetry and Physics of Solar System Bodies Photopolarimetry in Remote Sensing: Proceedings of the NATO Advanced Study Institute. Yalta, Ukraine. 20 September - 4 October 2003. -503 p. P. 369-384.

133. Morozhenko A.V., Vidmachenko A.P., Nevodovskiy P.V. (2013) Aerosol in the upper layer of earth's atmosphere. Kinematics and Physics of Celestial Bodies, 29(5), p. 243-246.

134. Morozhenko A.V., Vidmachenko A.P., Nevodovskiy P.V. Kostogryz N.M. (2014) On the Efficiency of Polarization Measurements while Studying Aerosols in the Terrestrial Atmosphere. Kinematics and Physics of Celestial Bodies. 30(1), p. 11-21.

135. Morrison D. (1973) Determination of radii of satellites and asteroids from radiometry and photometry. Icarus. 19(1), p. 1-14.

136. Morrison D. (1977) Asteroids size and diameters. Icarus. 31(2), p. 185-220.

137. Morrison D., Lebofsky L. (1979) Radiometry of asteroids. Asteroids, Ed.T.Gehrels. The university of Arizona press, Tucson, Arizona. P. 184-205.

138. Muinonen K., Piironen J., Kaasalainen S., Cellino A. (2002) Asteroid photometric and polarimetric phase curves: empirical modeling. Memorie della Societa Astronomica Italiana. 73(3), p. 716-721.

139. Nimmo F., Umurhan O., Lisse C.M., et al. (2017) Mean radius and shape of Pluto and Charon from New Horizons images. Icarus. 287, p. 12-29.

140. O'Leary B., Marsden B.C., Dragon D., et al. (1976) The occultation of k Geminorum be Eros. Icarus. 28(1), p. 133-146.

141. Olkin C.B., Young L.A., Borncamp D., et al. (2015) Evidence that Pluto's atmosphere does not collapse from occultations including the 2013 May 04 event. Icarus. 246, p. 220-225.

142. Ostro S.J., Pettengill G.H., Shapiro I.I., et al. (1979) Radar observations of asteroid 1 Ceres. Icarus. 40(3), p. 355-358.

143. Owen T.C., Roush T.L., Cruikshank D.P. et al. (1993) Surface Ices and the Atmospheric Composition of Pluto. Science. 261(5122), p. 745–748.

144. Palluconi F.D., Kieffer H.H. (1981) Thermal inertia mapping of Mars from 60oS to 60oN. Icarus. 45(2), p. 415-426.

145. Parker J.W., McFadden L.A., Russell C.T., et al. (2006) Ceres: High-resolution imaging with HST and the determination of physical properties. Adv. Space Res. 38(9), p. 2039-2042.

146. Person M.J., Dunham E.W., Bosh A., et al. (2013) The 2011 June 23 Stellar Occultation by Pluto: Airborne and Ground Observations. The Astronomical Journal, 146(4), id. 83, p. 1-15.

147. Pires dos Santos P.M., Giuliatti Winter S.M., Sfair R., Mourão D.C. (2013) Small particles in Pluto's environment: effects of the solar radiation pressure. Earth and Planetary Astrophysics. Monthly Notices of the Royal Astronomical Society. 430(4), p. 2761–2767.

148. Quillen A.C., Nichols-Fleming F., Chen Y.-Y. Noyelles B. (2017) Obliquity evolution of the minor satellites of Pluto and Charon. Icarus. 293, p. 94-113.

149. Quirico E., Schmitt B. (1977) Near-Infrared Spectroscopy of Simple Hydrocarbons and Carbon Oxides Diluted in Solid N_2 and as Pure Ices: Implications for Triton and Pluto. Icarus. 127(2), p. 354-378.

150. Ragozzine D., Brown, M.E. (2009) Orbits and Masses of the Satellites of the Dwarf Planet Haumea, 2003 EL61. Astron. J. 127(6), p. 4766—4776.

151. Resnick A.C., Barry T., Buie M.W., et al. (2015) The State of Pluto's Bulk Atmosphere at the Time of the New Horizons Encounter. American Astronomical Society, DPS meeting #47, #210.15.

152. Rivkin A.S., Volquardes E.L. (2010) Rotationaly-resolved spectra of Ceres in the 3-μm region. Icarus. 206(1), p. 327-333.

153. Sato K., Miyamoto M., Zolensky M.E. (1997) Absorption bands near three micrometers in diffuse reflectance spectra of carbonaceous chondrites: Comparison with asteroids. Meteoritics & Planetary Sci. 32(4), p. 503-507.

154. Scaltriti F., Zappala V. (1976) Photometric lightucurves and pole determination of 433 Eros. Icarus. 28(1), p. 29-35.

155. Schaller E.L., Brown M.E. (2007) Detection of Methane on Kuiper Belt Object (50000) Quaoar. Astrophys. J. 670(1), Pt. 2, p. L49-L51.

156. Sheppard S.S. (2010) The Colors of Extreme Outer Solar System Objects. Astron. J. 139(4), p. 1394-1405.

157. Showalter M.R., Hamilton D.P. (2015) Resonant interactions and chaotic rotation of Pluto's small moons. Nature. 522(7554), p. 45-49.

158. Showalter M.R., Weaver H.A., Stern S.A., et al. (2012) New Satellite of (134340) Pluto: S/2012 (134340) 1. IAU Circular. 9253, p. 1.

159. Sicardy B., 8 Ortiz J.L., Assafin M., et al. (2011) A Pluto-like radius and a high albedo for the dwarf planet Eris from an occultation. Nature. 478, p. 493–496.

160. Sicardy B., Ortiz J.L., Assafin M., et al. (2011) Size, density, albedo and atmosphere limit of dwarf planet Eris from a stellar occultation. European Planetary Science Congress Abstracts: journal. EPSC-DPS Joint Meeting. 6. -2 p.

161. Sicardy B., Talbot J., Meza E., et al. (2016) Pluto's Atmosphere from the 2015 June 29 Ground-based Stellar Occultation at the Time of the New Horizons Flyby. The Astrophysical Journal Letters. 819(2), p. L38.

162. Sicardy B., Widemann T., Lellouch E. Et al. (2003) Large changes in Pluto’s atmosphere as revealed by recent stellar occultations. Nature, 424(6945), p. 168-170.

163. Singer K.N. (2022) Large-scale cryovolcanic resurfacing on Pluto. Nature Communications. 13(1), p. 1542.

164. Singer K.N., Stern S.A. (2015) On the Provenance of Pluto's Nitrogen (N2). The Astrophysical Journal Letters. 808(2).

165. Slipher V.M. (1930) Planet X-Lowell Observatory Observation Circular. Journal of the Royal Astronomical Society of Canada, 24, p. 282.

166. Soter S. (2006) What is a Planet? The Astronomical Journal. 132(6), p. 2513-2519.

167. Spencer J.R., Stansberry J.A., Trafton L.M., et al. (1997) Volatile Transport, Seasonal Cycles, and Atmospheric Dynamics on Pluto. Pluto and Charon. Edited by S. Alan Stern, David J. Tholen; with the editorial assistance of A.S. Ruskin, M.L. Guerrieri, M. S. Matthews. Tucson: University of Arizona Press. P. 435-445.

168. Spudis P.D., Reisse R.A., Gillis J.J. (1994) Ancient multiring basins on the Moon revealed by Clementine lasar altimetry. Science. 266(5192), p. 1848-1851.

169. Standish E.M. (1993) Planet X: No dynamical evidence in the optical observations. Astronomical Journal. 105 (5): 2000-2006.

170. Steffl A.J.,Mutchler M.J., Weaver H.A., et al. (2006) New Constraints on Additional Satellites of the Pluto System. The Astronomical Journal. 132(2), p. 614-619.

171. Steffl A.J., Stern S.A. (2007) First Constraints on Rings in the Pluto System. The Astronomical Journal. 133(4), p. 1485-1489.

172. Steklov A.F., Vidmachenko A.P., Miniailo N.F. (1983) Seasonal variations in the atmosphere of Saturn. Soviet Astronomy Letters 9 (Mar.-Apr. 1983), p. 135, 136.

173. Stern S.A., Bagenal F., Ennico K., et al. (2015) The Pluto system: Initial results from its exploration by New Horizons. Science, 350 (6258), id.aad1815.

174. Stern S.A., Grundy W., McKinnon W.B., et al. (2017) The Pluto System After New Horizons. Annual Review of Astronomy and Astrophysics. Annual Reviews, 2018, p. 357-392.

175. Stern S.A., Mutchler M.J., Weaver H.A., Steffl A.J. (2006) The Positions, Colors, and Photometric Variability of Pluto's Small Satellites from HST Observations 2005–2006. Astronomical Journal. 132(3), p. 1405-1414.

176. Stern S.A., Skinner T.E., Brosch N., et al. (1989) The UV spectrum of Pluto-Charon - IUE observations from 2600 to 3100 A. Astrophys. J. 343(1, Pt 1, p. 533-538.

177. Stern, S.A., Trafton, L. (1984) Constraints on bulk composition, seasonal variation, and global dynamics of Pluto's atmosphere. Icarus. 57(2), p. 231–240.

178. Stern S.A., Weaver H.A., Steff A.J., et al. (2006) A giant impact origin for Pluto's small moons and satellite multiplicity in the Kuiper belt. Nature. 439(7079), p. 946-948.

179. Sussman G.J., Wisdom J. (1988) Numerical evidence that the motion of Pluto is chaotic. Science. 241. P. 433–437.

180. Taylor R.C., Gehrels T., Capen R.C. (1976) Minor planets and related objects.XXI. Photometry of eight asteroids. Astron. J. 81(9), p. 778-786.

181. Tegler S.C., Cornelison D.M., Grundy W.M., et al. (2010) Methane and Nitrogen Abundances on Eris and Pluto. American Astronomical Society, DPS meeting #42, #20.06; Bulletin of the American Astronomical Society, 42, p. 984.

182. Telfer M.W., Parteli E.J.R., Radebaugh J., et al. (2018) Dunes on Pluto Science, 360, p. 992-997.

183. Teolis B., Raut U., Kammer J.A. (2022) Extreme Exospheric Dynamics at Charon: Implications for the Red Spot. Geophysical Research Letters. 49(8), article id. e97580.

184. Tholen D.J., Buie M.W., Binzel R.P., Frueh M.L. (1987) Improved Orbital and Physical Parameters for the Pluto-Charon System. Science, 4814, p. 512-514.

185. Thomas P.C., Parker J.W., McFadden L.A., et al. (2005) Differentiation of the asteroid Ceres as revealed by its shape. Nature. 437(7056), p. 224-226.

186. Tombaugh C.W. (1946). The Search for the Ninth Planet, Pluto. Astronomical Society of the Pacific Leaflets. 5(209), p. 73-80.

187. Tombaugh C.W. (1996). Struggles to Find the Ninth Planet. Completing the Inventory of the Solar System, Astronomical Society of the Pacific Conference Proceedings. 107, p. 157-162.

188. Trafton L.M., Hunten D.M., Zahnle K.J., et al. (1997) Escape Processes at Pluto and Charon. Pluto and Charon / A. Stern, D. J. Tholen. University of Arizona Press, p. 475–522.

189. Trujillo C.A., Brown M.E., Rabinowitz D.L., Geballe T.R. (2005) Near-Infrared Surface Properties of the Two Intrinsically Brightest Minor Planets: (90377) Sedna and (90482) Orcus. Astrophys. J. 627(2), Pt.1, p. 1057-1065.

190. Urey H.C. The Structure and Chemical Composition of Mars // Physical Review. – 1950.- V. 80, No 2.- P. 295-295.

191. Vanyo J., Wilde P., Cardin P., Olson P. (1995) Experiments on precessing flows in the Earth's liquid core. Geophys. J. International. 121(1), p. 136-142.

192. Verbiscer A.J., Porter S.B., Buratti B.J., et al. (2018) Phase Curves of Nix and Hydra from the New Horizons Imaging Cameras. The Astrophysical Journal. 852(2), p. L35-1-L35-4.

193. Vid'Machenko A.P. (1991) Giant planets – Theoretical and observational aspects. Astronomicheskii Vestnik. May-June 1991, 25(3), p. 277-292.

194. Vid'Machenko A.P. (1997) Temporal changes in methane absorption in Jupiter's atmosphere. Kinematics and Physics of Celestial Bodies. 13(6), p. 21-25.

195. Vidmachenko A.P. (1985) Reflectivity of Saturn's south equatorial region from 1977 through 1981. Solar System Research. 18(3), p. 123-128.

196. Vidmachenko A.P. (1987) Manifestations of seasonal variations in the atmosphere of Saturn. Kinematics and Physics of Celestial Bodies. 3(6), p. 9-12.

197. Vidmachenko A.P. (1999) Seasonal variations in the optical characteristics of Saturn's atmosphere. Kinematics and Physics of Celestial Bodies, 15(5), p. 320-331.

198. Vidmachenko A.P. (2000) Variations of the reflective characteristics of Jupiter's atmosphere. 31st Lunar and Planetary Science Conference. March 13-17, 2000, Houston, Texas, abstract no. 1060.

199. Vidmachenko A.P. (2005) Sedna: the history of the discovery and its features. Astronomical almanac, 52, p. 201-212.

200. Vidmachenko A.P. (2015) Dwarf planets (to the 10th anniversary of the introduction of the new class of planets). Astronomical almanac, 62, p. 228-249.

201. Vidmachenko A.P. (2015) Influence of solar activity on seasonal variations of methane absorption in the atmosphere of Saturn. Kinematics and Physics of Celestial Bodies. 31(3), p. 131-140.

202. Vidmachenko A.P. (2016) Could it be the ninth planet in the Solar system? International Conference Astronomy and Space Physics in Kyiv University. May 24-27, 2016. Kyiv, Ukraine. P. 67-68.

203. Vidmachenko A.P. (2016) Features of surface topography and the geological activity of Pluto. 18 International scientific conference Astronomical School of Young Scientists. National Aviation University, Kyiv, Ukraine, May 26-27, 2016. P. 12-14.

204. Vidmachenko A.P. (2016) Is there 9-th planet in our solar system? Odessa astronomical publications, p. 224-225.

205. Vidmachenko A.P. (2016) Periodic changes in the activity of Jupiter's hemispheres. 47th Lunar and Planetary Science Conference, March 21-25, 2016, Woodlands, Texas. LPI Contribution No. 1903, 1091.

206. Vidmachenko A.P. (2016) Seasonal changes on Jupiter. I. Factor of activity of hemispheres. Kinematics and Physics of Celestial Bodies, 32(4), p. 189-195.

207. Vidmachenko A.P. (2016) So is there any 9-th planet in the Solar system? 18th International scientific conference Astronomical School of Young Scientists. P. 108-110.

208. Vidmachenko A.P. (2016) The floating ices on the surface of Pluto. 18 International scientific conference Astronomical School of Young Scientists. National Aviation University, Kyiv, Ukraine, May 26-27, 2016, p. 10-12.

209. Vidmachenko A.P. (2018) Modern volcanic activity on the Moon. 20 International scientific conference Astronomical School of Young Scientists. May 23-24, 2018. Uman, Ukraine. P. 5-7.

210. Vidmachenko A.P. (2018) Water in Solar system. 20 ISCo Astronomical School of Young Scientists, May 23-24 2018, Uman, Ukraine, p. 91-93.

211. Vidmachenko A.P. (2019) Pluto (to the 90th anniversary of the discovery of the planet). Astronomical almanac, 66, p. 217-229.

212. Vidmachenko A.P. (2022) Features of seasonal changes on Pluto. Proceedings of the 8th International scientific and practical conference. Science, innovations and education: problems and prospects. (March 9-11, 2022). Chapter 17. CPN Publishing Group. Tokyo, Japan. P. 108-116.

213. Vidmachenko A.P. (2024) About discovering and getting of all new information about the now dwarf planet Pluto. Proceedings of the XIII International Scientific and Prhctical Conference «Modern science: fundamental and applied aspects», December 30-31, 2024, Beijing. China. P. 20-26.

214. Vidmachenko A.P. (2025) Features of Pluto's rotation around its axis and around the Sun. Sciences of Europe. Editorial office: Křižíkova 384/101 Karlín, 186 00 Praha. 156, p. 24-28.

215. Vidmachenko A.P. (2025) Physical parameters of Pluto according to the results of remote observations and the earliest data from the flyby trajectory. Proceedings of the 6th International scientific and practical conference "Scientific achievements of contemporary society" (January 10-12, 2025). Chapter 60. Cognum Publishing House, London, United Kingdom. 898 p. P. 312-320.

216. Vidmachenko A.P. (2025) The history of the discovery and study of Pluto's atmosphere. Proceedings of the XV International Scientific and Practical Conference «Innovative scientific research», January 02-03, 2025, Toronto. Canada. 32 p. P. 4-8.

217. Vidmachenko A.P. (2025) Updating data on the physical characteristics of the dwarf planet Pluto thanks to research from the "New Horizons" spacecraft. Proceedings of the 6th International scientific and practical conference "Current trends in scientific research development". Chapter 52. 16-18 January 2025. BoScience Publisher. Boston, USA. P. 323-332.

218. Vidmachenko A.P. (2025) Physical parameters of Pluto according to the results of remote observations and the earliest data from the flyby trajectory. Proceedings of the 6th International scientific and practical conference "Scientific achievements of contemporary society" (January 10-12, 2025). Chapter 60. Cognum Publishing House, London, United Kingdom. 898 p. P. 312-320.

219. Vidmachenko A.P. (2025) The chemical composition of Pluto's atmosphere. The Proceedings of the 1st International Scientific and Practical Conference «Modern problems of science and technology» (January 20-22, 2025). Section: Physical and mathematical sciences. Tallinn, Estonia. European Open Science Space, 2025. 92 p. P. 62-68.

220. Vidmachenko A.P. (2025) Gaseous and aerosol components in Pluto's atmosphere. Proceedings of the XIII International Scientific and Practical Conference «Modern science: fundamental and applied aspects», January 07-08, 2025, Rome. Italy. Publisher: «SC. Scientific conferences». 61 p. P. 10-14.
221. Vidmachenko A.P. (2025) Vertical structure of Pluto's atmosphere. Proceedings of the 1st International Scientific and Practical Conference «Scientific Innovation: Theoretical Insights and Practical Impacts». Section: Physical and mathematical sciences. January 13-15, 2025. Naples, Italy. European Open Science Space. 255 p. P. 214-220.
222. Vidmachenko A.P. (2025) The earliest data on the general characteristics of Pluto's topography. Proceedings of the 5th International scientific and practical conference "Science in the modern world: innovations and challenges". (January 23-25, 2025). Chapter 35. Perfect Publishing. Toronto, Canada. 624 p. P. 202-211. 10
223. Vidmachenko A.P. (2025) Data update on the characteristics of the topography of Pluto. Proceedings of the 3rd International Scientific and Practical Conference «Global Directions in Scientific Research and Technological Development» (January 27-29, 2025). Section: Physical and mathematical sciences. Valencia, Spain. European Open Science Space. 131 p. P. 101-108. 11
224. Vidmachenko A.P. (2025) Features of the satellite system around Pluto. Scientific collection "InterConf+", No 54(236). February 2025. Proceedings of the 4th International Scientific and Practical Conference «Modern Knowledge: Research and Discoveries» (February 19-20, 2025). Vancouver, Canada) / comp. by LLC SPC «InterConf». Vancouver: A.T. International. 601 p. P. 388-396. 13
225. Vidmachenko A.P. (2025) The history of the discovery of Pluto's satellite Charon and its main characteristics. Proceedings of the 3rd International Scientific and Practical Conference «Evolving Science: Theories, Discoveries and Practical Outcomes» (February 3-5, 2025). Zurich, Switzerland. European Open Science Space. 252 p. P. 175-181. 14
226. Vidmachenko A.P. (2025) Pluto's satellite Hydra. Collection of scientific papers «ΛΌΓΟΣ». Proceedings of the VII International Scientific and Practical Conference

"Scientific practice: modern and classical research methods". (February 14, 2025). Section 17. Physics and Mathematics. Boston. Boston-Vinnytsia: Primedia eLaunch & UKRLOGOS Group LLC. 405 p. P. 220-225. 15

227. Vidmachenko A.P. (2025) Pluto's satellite – Nix. Scientific collection "InterConf", No 235. February 2025. Proceedings of the 5th International Scientific and Practical Conference «Society and Science: Interconnection» (February 16-18, 2025; Porto, Portugal) / comp. by LLC SPC «InterConf». Porto: Kramer. 251 p. P. 154-160. 16

228. Vidmachenko A.P. (2025) Pluto's satellite – Kerberos. Collection of Scientific Papers "International Scientific Unity". Proceedings of the 2nd International Scientific and Practical Conference. "Modern Science, Economy and Digital Innovation". Section Physics and Astronomy. (March 12-14, 2025). Bucharest, Romania. 274 p. P. 214-217. 17

229. Vidmachenko A.P. (2019) Pluto (to the 90th anniversary of the discovery of the planet). Astronomical almanac, 66, p. 217-229.

230. Vidmachenko A.P. (2025) Styx is the smallest satellite of Pluto. Proceedings of the 7th International scientific and practical conference "Scientific achievements of contemporary society" (February 6-8, 2025). Chapter 32. Cognum Publishing House, London, United Kingdom. 551 p. P. 193-197. 18

231. Vidmachenko A.P. (2025) The history of the discovery and study of Pluto's atmosphere. Proceedings of the XV International Scientific and Practical Conference «Innovative scientific research», January 02-03, 2025, Toronto. Canada. 32 p. P. 4-8.

232. Vidmachenko A.P. (2025) Gaseous and aerosol components in Pluto's atmosphere. Proceedings of the XIII International Scientific and Practical Conference «Modern science: fundamental and applied aspects», January 07-08, 2025, Rome. Italy. Publisher: «SC. Scientific conferences». 61 p. P. 10-14.

233. Vidmachenko A.P. (2025) Physical parameters of Pluto according to the results of remote observations and the earliest data from the flyby trajectory. Proceedings of the 6th International scientific and practical conference "Scientific achievements of

contemporary society" (January 10-12, 2025). Chapter 60. Cognum Publishing House, London, United Kingdom. 898 p. P. 312-320.

234. Vidmachenko A.P. (2025) Vertical structure of Pluto's atmosphere. Proceedings of the 1st International Scientific and Practical Conference «Scientific Innovation: Theoretical Insights and Practical Impacts». Section: Physical and mathematical sciences. January 13-15, 2025. Naples, Italy. European Open Science Space. 255 p. P. 214-220.

235. Vidmachenko A.P., Dlugach Z.M., Morozhenko O.V. (1984) Nature of the optical nonuniformity in Saturn's disk. Solar System Research 17(4), p. 164-171.

236. Vidmachenko A.P., Klimenko V.M., Morozhenko A.V. (1980) Multicolor photometry of features on the disk of Jupiter. I - Relative spectrophotometry in the 1977-1978 observing period. Solar System Research, 14(2), p. 62-67.

237. Vidmachenko A.P., Morozhenko O.V. (2012) The study of the satellites surfaces and the rings of the giant planets. Main Astronomical Observatory NAS of Ukraine Press, Kyiv, Ltd. Dia. -255 p.

237a. Vidmachenko A.P., Morozhenko O.V. (2014) The physical characteristics of surface Earth-like planets, dwarf and small (asteroids) planets, and their companions, according to distance studies // Main Astronomical Observatory NAS of Ukraine, National University of Life and Environmental Sciences of Ukraine. Kyiv, Publishing House "Profi". -388 p.

238. Vidmachenko A.P., Morozhenko O.V. (2014) The study Earth-like planets using spacecraft. Astronomical School's Report, 10(1), p. 6-19.

239. Vidmachenko A.P., Morozhenko O.V. (2017) Physical characteristics of the surface of satellites and rings of giant planets. Kyiv. Editorial and publishing department of NUBiP of Ukraine. -412 p.

240. Vidmachenko A.P., Morozhenko O.V. (2019) Physical parameters of terrestrial planets and their satellites. Kyiv, Editorial and Publishing Department of NULES of Ukraine. -468 p.

241. Vidmachenko A.P., Steklov A.F. (2022) Features of volcanic structures on Venus. Proceedings of the 9th International scientific and practical conference. Modern directions of scientific research development. P. 195-204.

242. Vidmachenko A.P., 19 23 30 Vidmachenko H.A. (2007) Is it dangerous asteroids? Astronomical almanac, 53, p. 195-207.

243. Wan X.-S., Huang T.-Y., Innanen K.A. (2001) 1:1 Superresonance in Pluto's Motion. The Astronomical Journal. 121(2). P. 1155–1162.

244. Ward W.R., Canup R.M. (2006) Forced Resonant Migration of Pluto's Outer Satellites by Charon. Science. 313(5790), p. 1107-1109.

245. Ward D.B., Gull G.E., Harwit M. (1977) Far-infrared spectral observations of Venus, Mars, and Jupiter. Icarus. 30(2), p. 295-300.

246. Weaver H.A., Buie M.W., Showalter M.R., et al. (2016) The Small Satellites of Pluto as Observed by New Horizons. Science. 351(6279): aae0030-1-26.

247. Webster W.J., Johnston K.J., Hobbs R.W., et al. (1988) The microwave spectrum of asteroid Ceres. Astron. J. 95(4), p. 1263-1268.

248. Williams J.G., Benson G.S. (1971) Resonances in the Neptune-Pluto System. Astronomical Journal. P. 167–177.

249. Wisdom J., Holman M. (1991) Symplicit maps for the n-body problem. Astronomical Journal. P. 1528–1538.

250. Witze A. (2013) Moon and planet names spark battle: Nature News & Comment. Nature. 496(7446), p. 407.

251. Yamaguchi A., Taylor G.J., Keil K. (1997) Metamorphic history of the eucritic crust of 4 Vesta. J. Geophys. Res. 102(E6), p. 13381-13386.

252. Yelle R.V., Elliot J.L. (1997) Atmospheric Structure and Composition: Pluto and Charon. University of Arizona Press. P. 347–390.

253. Young L.A. (2013) Pluto's Seasons: New Predictions for New Horizons (PDF). The Astrophysical Journal Letters. 766(2), p. 1-6.

254. Young E.F., Binzel R.P., Crane K.A. (2001) Two-Color Map of Pluto's Sub-Charon Hemisphere. The Astronomical Journal. 121(1), p. 552–561.

255. Young L.A., Elliot J.L., Tokunaga A., Owen T. (1997) Detection of Gaseous Methane on Pluto. Icarus. 127(1), p. 258-262.

256. Young E.F., Young L.A., Buie M. (2007) Pluto's Radius. Bulletin of the American Astronomical Society. DPS meeting #39, id.62.05, p. 541.

257. Young L.A. (2013) Pluto's Seasons: New Predictions for New Horizons (PDF). The Astrophysical Journal Letters. 766(2), p. 1-6.

258. Young L.A., Elliot J.L., Tokunaga A., et al. (1997) Detection of Gaseous Methane on Pluto. Icarus. 127(1), p. 258-262.

259. Young E.F., French R.G., Young L.A., et al. (2008) Vertical Structure in Pluto's Atmosphere from the 2006 June 12 Stellar Occultation. Astron. J. 1369, p. 1757-1769.

260. Zalucha A.M. 29 31 (2016). An atmospheric general circulation model for Pluto with predictions for New Horizons temperature profiles. Monthly Notices of the Royal Astronomical Society. 459(1), p. 902-923.

261. Zalucha A.M., Zhu X., Gulbis A.A.S., et al. (2011) An investigation of Pluto's troposphere using stellar occultation lig, p.t curves and an atmospheric radiative-conductive-convective model. Icarus. 214(2), p. 685-700.

262. Zappala V., Di Martino M., Kneźević Z., Djurasević G. (1984) New evidence for the effect of phase angle on asteroid lightcurve shape: 21 Lutetia. Astron. Astrophys. 130(1), p. 208-210.

263. Zellner B., Gradie J. (1976) Polarization of the reflected light of asteroid 433 Eros. Icarus. 28(1), p. 117-123.